ALMA MATER STUDIORUM
UNIVERSITÀ DI BOLOGNA

DOTTORATO DI RICERCA IN

ONCOLOGIA, EMATOLOGIA E PATOLOGIA

Ciclo 37

Settore Concorsuale: 06/A2 - PATOLOGIA GENERALE E PATOLOGIA CLINICA

Settore Scientifico Disciplinare: MED/04 - PATOLOGIA GENERALE

USE OF IN VITRO ALTERNATIVE METHODS IN THE STUDY OF EMERGING CONTAMINANTS FOR IDENTIFYING MECHANISMS OF ACTION IN NON-GENOTOXIC CARCINOGENESIS

Presentata da: Gelsomina Pillo

Coordinatore Dottorato

Manuela Ferracin

Supervisore

Fabio Dall'Olio

Co-supervisore

Annamaria Colacci

Esame finale anno 2025

CONTENTS

Summary

Chemical carcinogenesis, particularly induced by non-genotoxic compounds, remains a complex and evolving field. Unlike genotoxic carcinogens that directly damage DNA, non-genotoxic carcinogens such as Di-(2-ethylhexyl) phthalate (DEHP) and Perfluorooctane sulfonic acid (PFOS) are known to induce cancer through various indirect mechanisms. Understanding these mechanisms is essential for improving chemical risk assessments and developing reliable *in vitro* models.

This thesis aimed to explore the carcinogenic potential of DEHP and PFOS in the BALB/c 3T3 A31-1-1 cell model using the Cell Transformation Assay (CTA) and to elucidate molecular events, particularly those associated with receptor-mediated carcinogenesis. Particularly, given that peroxisome proliferator-activated receptor alpha (PPARα) activation has been associated with tumorigenesis in rodents iduced by both PFOS and DEHP, the relevance of this pathway in human carcinogenesis was critically assessed.

The first part of the study involved the evaluation of the *in vitro* carcinogenic potential of DEHP using CTA combined with transcriptomics. Three concentrations of DEHP were tested to assess their ability to induce cell transformation. CTA was further integrated with transcriptomic analysis to identify key molecular changes following DEHP exposure. This integrative approach provides insights into the gene expression profiles and signaling pathways affected by DEHP, allowing a comprehensive

understanding of its mechanism of action at the cellular level. Additionally, a comparison was made with the results obtained from other studies that employed CTAs using different models. Understanding this aspect is important to improve both the application of CTA within the Integrated Approaches to Testing and Assessment (IATA) for non-genotoxic compounds and the selection of an appropriate model when evaluating potentially non-carcinogenic chemicals.

In the second phase, the study focused on the effects of PFOS, which is known for its receptor-mediated activities, particularly through PPARα activation. Co-treatment with GW6471, a specific PPARα antagonist, was employed to evaluate the influence of PPARα on PFOS-induced cell transformation. The results revealed that although PFOS induced a significant transformation in the BALB/c 3T3 A31-1-1 model, co-treatment with GW6471 did not markedly alter the transforming potential. This finding suggests that PPARα activation alone may not fully explain the carcinogenicity of PFOS, indicating the involvement of other pathways in the BALB c/ 3T3 A31-1-1 cell model.

Key findings from this research demonstrated that DEHP did not induce cellular transformation *in vitro* in BALB/c 3T3 A31-1-1, whereas PFOS did. Although both compounds activate PPARα, they exhibited different mechanisms of action. This study underscored the complexity of non-genotoxic carcinogenesis, where receptor-mediated events, metabolic alterations, and disruptions in signaling pathways interact to promote tumorigenesis. The integration of CTA with additional mechanistic

approaches, such as transcriptomics for DEHP and the use of a PPARα inhibitor for PFOS, has allowed for a deeper investigation into the mechanisms of action underlying the cellular effects observed. This integrative model provides a more detailed perspective on the multifaceted nature of non-genotoxic carcinogens and highlights the utility of *in vitro* assays for chemical carcinogenicity testing.

In conclusion, this thesis contributes to the growing body of knowledge on non-genotoxic carcinogens by investigating the transforming potential of DEHP and PFOS using an *in vitro* model and exploring the mechanisms underlying their actions. These results indicate that PPARα activation, while significant, may not be the sole driver of carcinogenesis, emphasizing the need for further research into alternative pathways. These findings support the advancement of *in vitro* methodologies, such as CTA, combined with omics technologies, to understand chemical carcinogenesis. The insights gained from this study have implications for chemical risk assessment and underscore the importance of refining *in vitro* models to better mimic human responses, ultimately contributing to improved public health.

CHAPTER 1

Chemical Carcinogenesis

1.0 – Global Cancer Trends and the Evolving Challenge of Cancer Risk Assessment

Cancer is one of the leading causes of mortality worldwide, with approximately 20 million new cases and 9.7 million deaths by 2022 (Bray et al., 2024). Studies and statistics have suggested that these numbers are expected to increase over the next decade (Madia et al., 2019). Recent estimates from the International Agency for Research on Cancer (IARC) and Global Cancer Observatory show that 10 types of cancer account for roughly two-thirds of new cases and deaths globally, spanning 185 countries and 36 cancer types. Lung cancer remains the most common, with 2.5 million new cases, representing 12.4% of the total. Breast cancer in women follows with 2.3 million cases (11.6%), colon-rectal cancer with 1.9 million cases (9.6%), prostate cancer (1.5 million cases, 7.3%), and stomach cancer (970,000 cases, 4.9%) (Bray et al., 2024).

Moreover, according to the European Environment Agency, exposure to carcinogenic agents such as air pollution, chemicals, residential radon, UV radiation, and secondhand smoke accounts for over 10% of new cancer cases and approximately 9% of all cancer deaths in Europe (GBD, 2019). These estimates have heightened attention toward studying environmental pollutants and implementing prevention strategies,

as highlighted in the European Union Chemicals Strategy for Sustainability Towards a Toxic-Free Environment and the European Cancer Plan (EC, 2020; OECD, 2024).

Assessment of carcinogenicity, plays a crucial role in health risk assessment. Competent authorities are tasked with setting appropriate environmental standards and classifying the carcinogens to which populations may be exposed. A carcinogen is any agent whose exposure increases the incidence of malignant tumors either by inducing tumor development in humans or animals, increasing tumor incidence or malignancy, or accelerating ongoing carcinogenesis. Chemical carcinogenesis is the process by which a chemical agent induces the transformation of normal cells into cancerous cells.

Carcinogenesis is conventionally described as a multistep process that comprises initiation, promotion, and progression. In chemical carcinogenesis, initiation is often linked to genotoxic mechanisms that are characterized by direct DNA damage. According to this model, initiation can occur with a single treatment or exposure, which results in a rapid and irreversible process. Promotion follows initiation and acts on already-altered cells by exerting additional stress, such as proliferative stimuli, placing cells and their DNA in a more vulnerable state.

Since the 1950s, studies on the initiation and promotion of mouse skin carcinogenesis by Berenblum and Shubik have led to a widespread distinction between initiating and promoting carcinogens, based on their primary role in either the first or second phase of carcinogenesis

(Berenblum and Shubik, 1947). In risk assessment, within the traditional concept of multistep carcinogenesis and the centrality of mutagenic initiating events in the mutational theory of cancer, the risk posed by non-genotoxic carcinogens has been historically underestimated, partly because of difficulties in identifying these agents.

Currently, assessing the risk associated with non-genotoxic carcinogens is of paramount importance, and the creation of new testing strategies, known as New Approach Methodologies (NAMs), has emerged as an urgent requirement (Louekari and Jacobs, 2024; Zuang et al., 2024). Increasingly, studies are highlighting the fundamental role that non-genotoxic mechanisms play in carcinogenesis, with the majority of human environmental carcinogens acting through non-mutational mechanisms, often termed "promoting" mechanisms (Balmain, 2020; Zuang et al., 2024).

Even well-known cancer risk factors such as smoking and ultraviolet light, traditionally characterized as mutagens that cause direct DNA damage, are now recognized to promote various phases of carcinogenesis through multiple mechanisms. At the individual substance level, polycyclic aromatic hydrocarbons such as benzo(a)pyrene and 3-Methylcholanthrene, typically classified as indirect genotoxic chemicals, have demonstrated a wide array of non-genotoxic mechanisms through transcriptomic analyses (Mascolo et al., 2018; Pillo et al., 2022).

All of these considerations point to the need to revise the initiation-promotion-progression model, historically defined based on *in vivo* tests,

and replace it with a more holistic but substance-specific approach, integrating the Hallmarks of Cancer and Key Characteristics of Carcinogens (KCCs) frameworks into the chemical evaluation process (Smith et al., 2020; Madia et al., 2021; Hanahan, 2022; Colacci et al., 2023; Senga et al., 2024).

In the past decade, with significant advances in sampling and sequencing technologies, many somatic mutations have been identified in normal tissues. These mutations are highly consistent with driver mutations that play key roles in cancer progression. This finding, coupled with the relatively low annual tumor incidence rate, suggests that the presence of mutations alone is insufficient to explain cancer development. In this context, environmental stressors and aging are considered critical factors capable of disrupting balance and increasing the risk of malignant transformation in mutated cells (Zhang et al., 2024).

Numerous studies have demonstrated that "promotion" is a critical process for acquiring a fully malignant phenotype, and that its effects can occur at very early stages, intertwining with and overlapping the so-called initiation phase. Promotion can act by altering both intrinsic cellular factors, such as the cell cycle, and extrinsic factors related to the microenvironment and neighboring cells (Iversen and Iversen, 1982; Zhang et al., 2024). As our understanding of cancer has deepened, promotion can be seen as an ongoing dynamic involving complex interactions between cells and their environment rather than a discrete phase. This includes signals from surrounding stromal cells, immune cells,

cytokines, and various growth factors that modulate cellular behavior and contribute to clonal selection. These elements are not restricted to a specific phase, but play a continuous role in cancer development, influencing growth, resistance, and plasticity (Hanahan and Weinberg, 2011; Zhang et al., 2024).

1.1 – Chemical Carcinogens: Classification, Mode of Action and Advances in Testing Methodologies

The classification of carcinogenic substances provides a practical framework to support their identification, characterization, and regulation. Depending on the context, several classification schemes have been proposed (Stewart, 2019). In regulatory contexts and risk assessment, a mechanistic classification based on the *mode of action* is commonly used.

A mode of action refers to a biologically plausible series of key events (KEs) that lead to an adverse outcome, whereas a *mechanism of action* offers more detailed insights into how a substance exerts its specific effects at the biochemical level (Sonich-Mullin et al., 2001; Jacobs et al., 2020).

Carcinogens are typically categorized into genotoxic and non-genotoxic categories based on their mechanisms of action, specifically whether they directly induce damage to cellular DNA.

Historically, genotoxic carcinogens have been more easily identified through widely available *in vitro* and *in vivo* tests, such as the Ames test, which remains the standard screening method for genotoxicity (Mccann et al., 1975; Ames, 1979).

For many years, the focus on DNA damage and the ability of some chemicals to form DNA adducts has led to the prioritization of genotoxic carcinogens in research and regulatory settings. However, growing evidence has highlighted the significant role of non-genotoxic carcinogens, which can induce cancer through alternative mechanisms without directly interacting with DNA or genome integrity machinery (Jacobs et al., 2020). These mechanisms include altering the cellular microenvironment, promoting chronic inflammation, and influencing cellular signaling pathways that regulate proliferation. Recognizing and evaluating these non-genotoxic mechanisms has become an urgent challenge, especially given the limitations of the existing tests for identifying non-genotoxic carcinogens (Audebert et al., 2023; Louekari and Jacobs, 2024).

To address these challenges, the development of NAMs and IATA have become essential. These frameworks aim to combine multiple experimental strategies, advancing our ability to identify non-genotoxic carcinogens by integrating mechanistic insights from various *in vitro*, *in vivo*, and computational models (Jacobs et al., 2016). A key aspect of NAMs is their potential to utilize the Adverse Outcome Pathway (AOP) framework, which organizes existing knowledge of toxicity mechanisms into a series of KEs that can predict adverse effects at higher biological levels.

An example of an NAM-targeting genotoxic mechanism is the ToxTracker assay, a reporter-based system derived from transcriptomics, which uses mouse embryonic stem cells to identify multiple genotoxic

pathways. Although primarily focused on genotoxicity, this method represents evolving efforts to characterize the mode of action through mechanistic testing. ToxTracker has undergone successful inter-laboratory validation and has shown high precision in distinguishing genotoxic and non-genotoxic compounds (Hendriks et al., 2024). While ToxTracker focuses on genotoxicity, the broader application of transcriptomics could be instrumental in developing similar mechanistic insights for non-genotoxic carcinogens. This will help to bridge the gap in our ability to understand and evaluate non-genotoxic mechanisms, ultimately leading to the development of reliable testing methods tailored to these substances (Jacobs et al., 2020).

1.2 – Genotoxic Carcinogens

Genotoxic carcinogens include chemical compounds or their metabolites that can cause direct DNA damage. Some notable genotoxic compounds include benzo(a)pyrene, aflatoxin B1, nitrosamines, cisplatin, and vinyl chloride.

These substances, owing to their specific structure and reactivity, typically show mutagenic results *in vitro* and are not species-, tissue-, or organ-specific. Genotoxic damage manifests in various forms, including reversible and irreversible DNA lesions (heritable by daughter cells). Key markers of genotoxicity include gene mutations (point mutations, insertions, deletions, gene amplifications), structural chromosomal aberrations, and numerical chromosomal changes (Corvi and Madia, 2017). The primary mechanism driving genetic mutations is DNA adduct

formation, which serves as a marker of exposure to carcinogens and can be detected through techniques such as immunocytochemistry and mass spectrometry (Poirier, 2016).

From a regulatory perspective, genotoxic carcinogens are generally assumed to have no threshold dose, implying that even minimal exposure could theoretically pose a risk (Schrenk, 2019; Jacobs et al., 2020). This assumption stems from the idea that a single point mutation can trigger cancer. However, studies suggest that at low doses, DNA repair and detoxification mechanisms can prevent or reverse damage, indicating that additional events beyond mutations are needed for full transformation (Mascolo et al., 2018; Schrenk, 2019; Zhang et al., 2024).

Despite this, the absence of a clear threshold for most genotoxic carcinogens remains the default assumption unless unequivocally proven otherwise. In recent years, the need for advanced methodologies for assessing genotoxic risk has been highlighted, moving beyond classic genotoxicity endpoints. Integrating multiple testing approaches and identifying mechanistic pathways is essential for providing a qualitative and quantitative evaluation of genotoxic modes of action while also supporting the development of AOPs (ECHA, 2024). The ToxTracker assay has shown strong potential for mechanistic insights and for optimizing test batteries for risk assessment (Hendriks et al., 2024).

1.3 – Non Genotoxic Carcinogens

Non-genotoxic carcinogens do not directly interact with DNA, do not form adducts, and show negative results in mutagenicity tests conducted

in vivo and *in vitro*. These compounds induce cancer through alternative, often multiple, interacting mechanisms. The term *non-genotoxic* was introduced in the late 1980s, following the evaluation of 222 chemicals by the United States National Toxicology Program (NTP). This assessment uses three approaches: analysis of chemical structure and DNA reactivity, Ames mutagenicity testing, and rodent carcinogenicity testing (Ashby and Tennant, 1988). Of the 115 chemicals found to be carcinogenic, 62% were correlated with positive Ames test results, while the remaining 38% were carcinogenic *in vivo* but tested negative in mutagenicity assays. This distinction highlights the complexity of non-genotoxic carcinogens, which often display species- or tissue-specific effects, particularly in single organs, such as the liver.

The term *promoter* has traditionally been associated with non-genotoxic agents, reflecting their ability to support tumor development by creating a favorable microenvironment. However, this concept, rooted in a two-stage animal model, may inadequately capture the multifaceted modes of action of these substances. Non-genotoxic carcinogens often disrupt key cellular processes such as cell signaling, immune responses, or metabolic pathways, leading to chronic inflammation, oxidative stress, and hyperproliferation. These disturbances, although not directly genotoxic, indirectly contribute to tumorigenesis by fostering conditions in which cancer can thrive.

Modern approaches emphasize the diverse mechanisms through which non-genotoxic carcinogens act, including epigenetic modifications,

endocrine disruption, receptor-mediated effects, and immunomodulation (Oliveira and Faustino-Rocha, 2022). These mechanisms often function together, making it challenging to predict the carcinogenic potential of these substances.

In contrast to genotoxic agents, non-genotoxic carcinogens to exhibit a threshold (safe dose), below which they do not induce carcinogenic effects (Corvi and Madia, 2017; Schrenk, 2019). Additionally, it has been hypothesized that non-genotoxic substances induce tumorigenesis through repeated or prolonged exposure, causing lasting disturbances to physiological processes (Veltman et al., 2023).

Non-genotoxic carcinogens are not detected by standard genotoxicity tests and there are currently no validated *in vitro* tests specifically designed for their identification (Jacobs et al., 2020). The 2-year rodent bioassay (RCB) remains the only regulatory method for assessing these substances. However, efforts have been underway, guided by the OECD since 2016, to develop IATA, which combines *in vitro*, *in vivo*, and computational models to bridge the gap in regulatory testing (Jacobs et al., 2020). Research in this area is critical not only for advancing public health protection but also for promoting 3Rs principles (Reduction, Refinement, and Replacement of animal testing in scientific research).

1.3.1 – Receptor-mediated mechanism of action

Many non-genotoxic carcinogens function through receptor binding and interact with various cellular receptors, such as estrogen and/or

androgen receptors (ERs/ARs), progesterone receptor (PR), aryl hydrocarbon receptor (AhR), PPARs, thyroid hormone receptors (TRs), and glucocorticoid receptors (GR) (Senga et al., 2024). The biological responses induced by these interactions depend on receptor type and generally follow two main pathways: (i) membrane-bound or intracellular receptors that initiate signal transduction, affecting cytoplasmic processes and gene transcription, and (ii) nuclear receptors that act as transcription factors upon ligand binding (Hernández et al., 2009). These pathways are central to carcinogenesis mechanisms, with receptor activation usually acting as a primary molecular event that drives subsequent mechanisms supported by other KCCs, such as electrophilicity, immune response disruption, oxidative stress, and inflammation (Senga et al., 2024).

For instance, estrogenic hormones, such as 17β-estradiol, bind to ERs, resulting in mitogenic effects through gene expression modulation and functional changes in the cell membrane and cytoplasm. In the genomic pathway, estrogens form homo- or heterodimers with ERα and ERβ, binding to estrogen-responsive elements in DNA or interacting with other transcription factors (Yaşar et al., 2017). Non-genomic pathways involve membrane-bound ERs that trigger cellular responses, including phosphorylation cascades through direct interactions with proteins, such as Src tyrosine kinases and PI3K, influencing cellular proliferation, differentiation, motility, apoptosis, and DNA repair (Thiebaut et al., 2021).

The interaction of Seveso dioxin (TCDD) with AhR provides another example of receptor-mediated mechanism. TCDD binds to AhR in the

cytoplasm, forming a complex that translocates to the nucleus and modulates gene expression. This process is linked to the upregulation of genes such as RAS, ErbA, c-FOS, and c-JUN and enzymes such as cytochrome P450 CYP1A1 and glutathione-S-transferase (Knerr and Schrenk, 2006; Yamaguchi and Hankinson, 2018; Grishanova et al., 2023).

Notably, several compounds exhibit complex receptor interactions, as binding can vary in specificity and can be reversible or irreversible. A ligand may either activate or inhibit the function of a receptor, and each ligand can interact with multiple receptor subtypes. For example, DDT acts as both an estrogenic agent and an androgen antagonist, influencing multiple hormonal pathways and inducing enzymes such as CYP2B and CYP3A (Hernández et al., 2009).

Phthalates, such as DEHP, and perfluorinated chemicals, such as PFOS, can activate the PPARα signaling pathway, exerting transcriptional control over various physiological processes. Additionally, DEHP and PFOS can influence the activity of various other receptors through different mechanisms, including both receptor-binding and indirect activation pathways. These chemicals have been shown to modulate receptors, such as ERs, AhR, pregnane X receptor (PXR) and hepatocyte nuclear factor 4 alpha (HNF4α), leading to changes in cellular metabolism, immune responses, and oxidative stress. The ability of these compounds to interact with multiple receptor pathways further complicates their role in

carcinogenesis, and underscores the need for in-depth mechanistic studies.

PPARα is a ligand-activated transcription factor of the nuclear receptor superfamily which primarily regulates lipid metabolism, inflammation, and glucose homeostasis (Huang et al., 2020; Takada and Makishima, 2020; Asgharzadeh et al., 2024). Among its isoforms, PPARα, PPARβ/δ, and PPARγ, PPARα are the most abundantly expressed in the liver (Umemoto and Fujiki, 2012; Wahli and Michalik, 2012). Upon ligand binding, PPARα translocates to the nucleus, forms a heterodimer with retinoid X receptors (RXR), and binds to peroxisome proliferator response elements on DNA, thereby initiating target gene transcription (Wahli and Michalik, 2012; Corton et al., 2014; Evans and Mangelsdorf, 2014; Asgharzadeh et al., 2024).

In the absence of ligands, PPARα associates with co-repressors, such as G-protein suppressor 2, SMRT, NCoR and Recruiting histone deacetylase 3, to inhibit gene expression. However, binding to lipophilic ligands, including eicosanoids, fatty acids, or synthetic compounds such as fibrates, converts PPARα into a transcriptional activator (Pan et al., 2024). PPARα has a higher affinity for very long-chain fatty acids (C20-C24) and their branched CoA thioesters as well as bioactive molecules such as leukotriene B4, highlighting its involvement in immune regulation and inflammation (Pan et al., 2024).

PPARα receptor-binding and activation, as seen with others, can initiate other KCCs, including metabolism disruption, oxidative stress,

inflammation and proliferation. Research with several ligands, such as WY-14643, has shown that PPARα activation increases peroxisome number and size in the rodent liver, enhancing β-oxidation and metabolic enzyme activity. This process increases catalase activity, resulting in higher hydrogen peroxide levels and potential DNA damage. This evidence suggests that PPARα activation contributes to carcinogenic processes through non-genotoxic mechanisms (Ito et al., 2007; Corton et al., 2014; Pan et al., 2024).

Emerging evidence also suggests that PPARγ may influence cancer progression by modulating key cellular processes, such as glucose metabolism, lipid metabolism, and inflammatory signaling pathways (Hartley and Ahmad, 2023; Asgharzadeh et al., 2024). However, further research is required to explore the role of PPARs in human cancer (Corton et al., 2018; Foreman et al., 2021; Pan et al., 2024).

The role of PPARα activation in human carcinogenesis is limited because of significant interspecies differences between rodents and humans. In rodents, particularly mice and rats, PPARα is highly expressed in the liver, and its ligand activation triggers pronounced physiological responses. Although human PPARα expression is similar to that in rodents, its activation does not elicit comparable physiological effects (Ito et al., 2019). Activation of PPARα in rodents results in increased peroxisome numbers, induction of peroxisomal and mitochondrial fatty acid oxidation enzymes, and sustained oxidative stress, all of which contribute to liver tumor development (Foreman et al., 2021). In contrast,

human hepatocytes do not display the same proliferative response to PPARα agonists, nor do they undergo peroxisomal proliferation or exhibit elevated oxidative stress to the same extent.

Moreover, studies using humanized PPARα transgenic mice, in which the mouse receptor was replaced by the human counterpart, showed an increased expression of target genes involved in lipid metabolism in response to PPARα ligand activation, but a marked reduction in the carcinogenic responses which were typically observed in wild-type rodents (Corton et al., 2014, 2018; Ito et al., 2019; Foreman et al., 2021; Zhu et al., 2023).

In contrast, other studies using PPARα-null mice pointed out a background increase in the development of steatosis and liver cancer, highlighting the “protective role” of PPARα, probably related to metabolic regulation (Régnier et al., 2020; Foreman et al., 2021).

It is hypothesized that differences in human PPARα regulation, potentially attributable to variations in DNA response element binding and target gene sets, result in metabolic discrepancies and distinct metabolite profiles, which may, on the one hand, reduce the levels of reactive and potentially deleterious metabolites, and on the other, lead to an attenuated inflammatory and proliferative response in the liver. Nevertheless, due to the incomplete understanding of the mechanisms that differentiate PPARα functions between humans and rodents, along with certain evidence linking PPARα activation to pro-inflammatory pathways and the promotion of oxidative stress in humans, it is not possible to entirely dismiss the

relevance of this mechanism of action in humans. Furthermore, the role of PPARα in the tumor microenvironment remains ambiguous, with conflicting data suggesting both tumor-promoting and tumor-suppressive activities in human cancers, raising questions about its potential impact on organs beyond the liver.

CHAPTER 2

Carcinogenicity Assessment and *in vitro* tests

2.0 – Overview of Carcinogenicity Assessment and Alternative Strategies

Carcinogenicity assessment is an essential component for evaluating the safety of all types of substances across various industrial sectors, as mandated by international regulations, including the European Commission's Regulation on the Registration, Evaluation, Authorization, and Restriction of Chemicals (REACH). Regulatory strategies and requirements for carcinogenicity assessment can vary significantly depending on the type of substance and industry involved. However, standard tests for genotoxicity, both *in vitro* and *in vivo*, and classical RCB remain the standard methods in use today. Differences in sectoral regulations are primarily due to the varying health risks posed by specific product use, differences in human and environmental exposure levels, and economic and ethical concerns related to animal welfare (Madia et al., 2020a). For industrial chemicals, requirements depend on the production volume and associated exposure levels, with carcinogenicity testing mandated mainly for high-tonnage substances or mutagenic agents (GHS category 3). For agrochemicals, the current standard involves genotoxicity testing and two RCB, with cancer tests required for all new non-genotoxic biocides. For pharmaceuticals, carcinogenicity testing is primarily required for chronically administered drugs, whereas cosmetic ingredients have

been exempt from *in vivo* testing since 2013, relying instead on *in vitro* genotoxicity assays (Corvi et al., 2017; Luijten et al., 2020; Madia et al., 2020a).

Despite the implementation of the REACH regulation, which has helped reduce the overall risks of chemicals in the environment and decrease the production of highly toxic Carcinogenic, Mutagenic, and Reprotoxic (CMR) substances, there is still a significant gap in the assessment of the carcinogenicity of new substances. This requirement is contingent upon specific conditions being met, such as the European Chemicals Agency (ECHA) (2024):

1) Significant exposure, as:
    a) The substance has widespread dispersive use (or)
    b) There is evidence of frequent or long-term human exposure
2) This substance is hazardous as follows:
    a) classified as a category 2 mutagen for germ cells (or)
    b) Associated with hyperplasia and/or preneoplastic lesions in repeated-dose studies.

As a result of these restrictions, carcinogenicity testing is rarely conducted, creating a vulnerability in protection and prevention strategies, particularly for non-genotoxic carcinogens. If not classified for other hazardous properties and not identified in limited repeated-dose toxicity studies, these carcinogen risks will not be detected (Jacobs et al., 2020; Luijten et al., 2020; Louekari and Jacobs, 2024).

Another recognized limitation of the current strategy for carcinogenicity assessment lies in the type of tests used: genotoxicity tests are limited to detecting genotoxic carcinogens, whereas *in vivo* tests such as the RCB have limitations in applicability and scientific relevance, such as uncertainties related to extrapolating data from animals to humans (Paparella et al., 2017; Felter et al., 2020).

Moreover, RCB and chronic toxicity studies do not specifically address the four most common human cancers (lung, breast, colorectal, and prostate) discussed in Chapter 1, as they were originally designed to cover a wide range of possible health effects and tumor types. In particular, RCB has proven inadequate for studying hormone-dependent cancers (Madia et al., 2019).

Along with these concerns about the scientific relevance of animal testing for carcinogenicity, there is a strong demand within the EU to reduce the use of animals in scientific research and to implement new alternative approaches (Madia et al., 2019; ECHA, 2024).

To support the development of alternative testing strategies, the OECD has promoted a project to evaluate and identify new methodological approaches for identifying non-genotoxic carcinogens based on the hallmarks of cancer since 2016 (Jacobs et al., 2016). In the same year, the OECD issued guidelines for the development and use of IATA based on the AOP concept.

Preliminary research has shown some critical processes and KEs in cancer development (hallmarks), such as genotoxicity, metabolic

activation, oxidative stress, immunosuppression and immune evasion, transcriptional and signaling pathways alterations, and increased resistance to apoptosis. However, there is a need to develop methods for assessing neo-/pathogenic angiogenesis and genetic instability, as well as a deeper understanding of the critical process leading from inflammation and hyperplasia to tumor formation (ECHA, 2024).

An important outcome of this working group was the detailed description of a modular strategy for assessing non-genotoxic carcinogens, in which each module represents a different level of complexity and specificity in the evaluation process (Louekari and Jacobs, 2024).

The first level of investigation (Module A) focused on evaluating available information and using existing *in silico* tools to help formulate a mechanistic hypothesis and guide the selection of the most appropriate tests. Four additional modules (B, C, D, and E) correspond to KEs in cancer development. For example, Module B involves studying the Molecular Initiating Event (MIE), while Module C focuses on downstream KEs, such as inflammation and the modulation of specific signaling pathways. Finally, Module F evaluates all gathered information using a weight of evidence approach (Louekari and Jacobs, 2024).

These new methodological approaches prioritize the use of AOP, mechanistic information, and an increasingly detailed characterization of substances and molecular mechanisms. An AOP refers to a substance-specific action framework that describes a chain of causally linked events

at different biological levels that interact to produce adverse effects. More specifically, the AOP approach uses current knowledge to reconstruct the dynamics and causal links between molecular perturbations and the final effect, starting from an MIE, through a series of KEs, culminating in an adverse outcome (OECD, 2016a).

Applying the AOP concept to cancer endpoints is a complex task that requires significant methodological and knowledge-based effort. Currently, work is underway to develop AOPs that describe various specific modes of genotoxicity or mutagenic action (ECHA, 2024).

2.1 – Cell Transformation Assay

The Cell Transformation Assay (CTA) is one of the few existing *in vitro* tests for evaluating the carcinogenic potential of substances, including non-genotoxic carcinogens. Recently, a categorization of genotoxic and non-genotoxic chemicals based on the results from CTA studies has been published (Colacci et al., 2023).

Although this test has been used and known for many years, it is not considered a stand-alone test for regulatory carcinogenicity evaluation. However, its potential has been re-evaluated in discussions on designing new IATA, which include multiple types of tests and various levels of investigation (Jacobs et al., 2016; Colacci et al., 2023; Louekari and Jacobs, 2024).

CTAs can mimic certain stages of *in vivo* chemical carcinogenesis *in vitro*. When combined with other molecular and mechanistic investigation methods, they are considered an important tool both for

studying carcinogenesis mechanisms and as potential *in vitro* tests within cancer risk assessment frameworks (Pillo et al., 2022; Colacci et al., 2023; Louekari and Jacobs, 2024). The assay itself aims to induce cell transformation by exposing cells to chemicals or physical agents whose carcinogenic potential is currently being investigated.

In animal cells, "transformation" refers to the process of significant morphological and behavioral alterations caused by permanent, heritable genetic changes. Phenotypic changes progressively emerge from the primary state of the cell to the acquisition of a fully malignant phenotype, including: cellular differentiation arrest, immortality and genetic instability, substrate-independent growth, loss of cell-cell contact inhibition and production of autocrine growth factors (Heidelberger et al., 1983).
Malignancy and invasiveness are associated with metastasis *in vivo*.

The endpoint of the assay is represented by transformed cells with an aberrant phenotype and altered growth patterns, known as *foci*, from which the transforming potential of the substance is calculated (Sakai, 2007).

The first carcinogenicity study using CTA was attributed to Berwald and Sachs, who observed a correlation between morphological transformation and exposure to polycyclic aromatic hydrocarbons in Syrian Hamster Embryo (SHE) cell cultures (Berwald and Sachs, 1963). Over the years, various modifications have been made to CTA protocols and to the types of cellular models used to enhance the sensitivity and specificity of the method.

Currently, the three most widely used CTA models are primary fibroblasts (SHE), stabilized mouse embryonic fibroblasts (BALB/c 3T3), and fibroblasts transfected with oncogenes (Bhas 42). Protocols for these models have been standardized for regulatory purposes and coordinated by the European Center for the Validation of Alternative Methods (ECVAM) since 1998.

Recent reports have suggested that the three cell models currently used for CTA may represent different stages of carcinogenesis. Specifically, the SHE model, which consists of primary cells with a normal karyotype, is typically used to investigate the early stages of the carcinogenic process, such as the initial transformation steps and arrest of cellular differentiation (Creton et al., 2012; Colacci et al., 2023). In contrast, mouse cell lines, which are already immortalized and aneuploid (advanced transformation stages), have been used to study the later steps of carcinogenesis, including full malignancy and invasiveness.

An additional key advantage of these assays is their ability to generate dose-response curves at very low concentrations, which are difficult to test *in vivo,* but more accurately reflect real exposure levels.

2.1.1 – BALB/c 3T3 Cell Transformation Assay

BALB/c 3T3 CTA demonstrated a high predictive value and concordance with *in vivo* carcinogenicity tests. It has shown strong discriminatory power for substances acting at different stages of the carcinogenesis process with diverse modes of action.

The BALB/c 3T3 model was originally developed in 1968 to study virus-induced cell transformation (Aaronson and Todaro, 1968). Since then, this assay has been extensively used for various purposes, such as clarifying uncertain results from other biological tests, supporting positive findings from *in vitro* genotoxicity studies, comparing the effects of substances from the same chemical class, and evaluating the efficacy of chemopreventive agents (ECVAM, 2010).

BALB/c 3T3 cells are a stabilized hypotetraploid cell line derived from immortalized murine embryonic fibroblasts that have already undergone some stages of transformation. Nevertheless, these cells retain a relatively low rate of spontaneous mutations, substrate-dependent growth, and contact inhibition.

Among the various clones derived from this line, A31 clone gave rise to several subclones, including A31-714, A31-1, and A31-13. The A31-1-1 clone, created in 1980, was selected for its sensitivity to various transforming agents, and is recommended as a good model for CTA because of its high efficiency *in vitro* and low saturation density (ECVAM, 2010; Colacci et al., 2023). Subsequent genotyping revealed that the BALB/c 3T3 A31-1-1 cell line was derived from a Swiss mouse strain (Kakunaga and Crow, 1980; Uchio-Yamada et al., 2017).

This misidentification explains the observed differences in transformation sensitivity and metabolic competence compared to other subclones (Kakunaga and Crow, 1980; Colacci et al., 2011). Nevertheless, after several studies, it was concluded that the A31-1-1 clone is suitable

for CTA application as it exhibits intrinsic physiological characteristics, such as high sensitivity to contact inhibition and susceptibility to chemically induced transformation, and that these functional traits are independent of the origin of the cell line (OECD, 2016b).

The key feature of BALB/c 3T3 cells is their distinct morphological changes upon transformation. These changes include spindle-shaped morphology, intense basophilia, uncontrolled over-confluent proliferation, chaotic, multilayered growth patterns, and the formation of *foci*. These phenotypic markers of transformation were most pronounced in type III *foci* as opposed to types I and II. The photo catalogue published by Sasaki and colleagues in 2012 greatly improved result consistency and method transferability, specifically defining the characteristics of type III *foci*, which are the only foci associated with a positive test outcome (Sasaki et al., 2012b; Steinberg, 2016).

2.2 – Transcriptomics in BALB c/ 3T3 A31-1-1

Transcriptomics has become a widely used technique in contemporary toxicological research as it provides large-scale mechanistic and quantitative information through gene expression profiling.

Typically, toxicogenomic experiments using transcriptomics aim to characterize transcriptional changes in response to specific exposures, whether *in vitro* or *in vivo*, across various concentrations and durations. The core aim of this analysis is to identify differentially expressed genes (DEGs) between exposed samples and solvent or vehicle controls. To further understand the toxicological effects, the next step involved linking

the DEGs to biological functions by integrating gene lists with higher-order biological categories, such as molecular pathways or gene sets. Enrichment analyses, for example, assess the likelihood that DEGs are co-regulated within the same pathway, thereby providing additional insight into the significance of the identified perturbations. Notably, the results depend heavily on the content of the databases used for gene set analysis (Meier et al., 2024).

Pathway and gene network analyses have proven to be powerful tools for analyzing large transcriptomic datasets, enabling the identification of toxicological mechanisms and potential health effects. However, the relationship between gene expression changes, either adaptive or adverse, and toxicity outcomes remains an active area of research. The complexity of interpreting transcriptomic profiles currently limits their systematic use in regulatory decision making. Emerging goals in predictive toxicology include building and continuously updating databases to support pattern-matching approaches and developing transcriptomic biomarkers that can reliably link molecular changes to modes of action and toxicological risks, thereby ensuring objectivity, efficiency, and reproducibility.

Through these studies, the use of omics techniques in risk assessment has become more tangible, as highlighted in recent reports from the ECVAM and OECD, which also emphasizes the need for further standardization (OECD, 2024; Zuang et al., 2024). Available transcriptomic studies applied to CTA assays have identified key biological

processes in the *in vitro* transformation process, alongside potential biomarkers. In the 3T3 model, immune-mediated signaling pathways appear to play a crucial role in oncogenic transformation (Mascolo et al., 2018; Pillo et al., 2022; Colacci et al., 2023). In the BALB/c 3T3 A31-1-1 model, a series of molecular events linked to carcinogen exposure have been identified, including i) the activation of metabolic processes, often involving the AhR; ii) activation of pathways related to innate immune response; iii) regulation of cell cycle and apoptosis-proliferation pathways; and iv) modulation of stress and damage-related pathways (Colacci et al., 2023). Transcriptomic profiles from different exposure concentrations suggest that detoxification processes lose efficiency at transforming concentrations, leading to the breakdown of cellular homeostasis. This imbalance is marked by the modulation of molecular pathways related to differentiation, tissue homeostasis, and the epithelial-mesenchymal transition (EMT). These molecular responses create a microenvironment that favors genetic instability, proliferation, and cytoskeletal remodeling, thereby setting the stage for oncogenic transformation (Colacci et al., 2023).

Receptor-mediated activation of metabolic pathways that support the bioactivation and detoxification of xenobiotics is certainly a key early event, detectable through the modulation of enzymes such as cytochrome oxidases Cyp1A1 and Cyp1B1 and detoxification-related enzymes such as glucuronosyltransferases. Immune-mediated KEs, such as inflammation, mitogenic signaling, and cellular damage, are indicated by the modulation

of pathways such as classical and alternative complement, interferon (IFN), interleukin signaling (IL-1, IL-4, IL-6, IL-9, IL-17, IL-18), and TNFR2 (Tumor Necrosis Factor Receptor 2). These markers, which are also linked to cell proliferation, play a role in altering the tumor microenvironment, cell adhesion, and cytoskeleton (Colacci et al., 2023).

EMT is a morphogenetic process integral to many cellular functions, especially in response to external stimuli, such as embryogenesis and tissue repair. However, EMT is also observed in pathological conditions, notably in fibrosis and cancer. In human tumors, EMT is recognized as a key step in tumor progression and acquisition of dysplasia and invasive properties. Moreover, transcription factors associated with EMT, such as Twist, Snail, Slug, and Zeb, have a prognostic value (Imani et al., 2016; Colacci et al., 2023). At the cellular level, EMT is characterized by changes in cell morphology, including a transition to a more elongated shape, loss of cell-cell junctions, basement membrane disruption, and acquisition of migratory and invasive capabilities. These events are detected in CTA as *foci* formation and can be described at the molecular level through gene expression profiles.

These data support the use of CTA in identifying KEs underlying morphological and functional alterations in transformed cells, known as hallmarks. In particular, there is the potential to deepen our understanding of the early stages of homeostatic disruption and to distinguish between adaptive and adverse responses, thus reconstructing the steps leading to malignant transformation in chemical carcinogenesis.

CHAPTER 3

Test Chemicals:

3.1 – Diethylhexyl Phthalate and the Phthalate Class

Phthalates are synthetic chemical compounds that are primarily used in plastic production, particularly polyvinyl chloride (PVC), to modify their mechanical properties. Despite concerns about their potential health risks, they remain widely used because of their cost-effectiveness and efficiency compared with alternative compounds. In 2014, the annual global production of phthalates reached 5 million tons, with an upward trend (Ranucci, 2022). Phthalates are diesters of phthalic acid and are classified as either high-molecular-weight (HMW) or low-molecular-weight (LMW) based on their carbon chain length. LMW phthalates with 3–7 carbon atoms are commonly found in personal care products, solvents, lacquers, and some pharmaceuticals. In contrast, HMW phthalates, including DEHP (8–13 carbon atoms), are primarily used in flexible vinyl products, such as flooring, wall coverings, food packaging, and medical devices (Hunt et al., 2024).

Phthalates have a strong electrostatic affinity for PVC, but are not chemically bound, allowing them to be easily released into the environment, especially through degradation, oxidation, or mechanical stress. This leads to their widespread presence in air, water, soil, and contact matrices, such as food and biological tissues (Jeon et al., 2016; ATSDR, 2022; Bajagain et al., 2023).

Their extensive use and persistence in the environment have made phthalates a major focus of international regulation (SCENIHR, 2016; Silano et al., 2019; Monti et al., 2022; Bajagain et al., 2023).

DEHP, a commonly used HMW phthalate, served as the reference compound for this chemical class for the calculation of the group tolerable daily intake (TDI).

Its global consumption is estimated to exceed 3.07 million tons, with a market value of approximately $20 million in 2020 (Benjamin et al., 2017). DEHP is found in various products, toys, medical devices, blood storage bags, and personal care items. Owing to its low biodegradability and partial degradation in standard wastewater treatments, DEHP poses a risk of bioaccumulation (Kanaujiya et al., 2022).

Exposure to DEHP and other phthalates can occur via various routes, including diet, direct contact, and inhalation (Chen et al., 2018; Silano et al., 2019; Bajagain et al., 2023).

Biomonitoring studies have detected phthalate metabolites in the urine, serum, and other body fluids, confirming their ubiquitous presence (Wang et al., 2019; Tait et al., 2020). Although diet is considered the primary exposure route for the general population, the highest exposure levels are often associated with the use of medical devices (SCENIHR, 2016; Silano et al., 2019; Den Braver-Sewradj et al., 2020).

The daily intake of the four most commonly used phthalates, including DEHP, ranges between 0.9–7.2 µg/kg body weight for average consumers and 1.6–11.7 µg/kg for high consumers. This intake can

contribute up to 23% of the TDI group (50 μg/kg body weight/day) in the worst-case scenarios (Silano et al., 2019). Children are at greater risk owing to their higher intake of food relative to body weight, and phthalates can cross the placental barrier, leading to prenatal exposure.

The toxicity of phthalates has been a subject of debate for several years. Some phthalates are recognized as reproductive toxins, endocrine disruptors, and metabolic disruptors with possible neurodevelopmental effects. Moreover, some phthalates have been identified as possible nongenotoxic carcinogens.

3.1.1 – Chemical-Physical Properties of DEHP

DEHP (CAS No. 117-81-7), IUPAC name bis(2-ethylhexyl) benzene-1,2-dicarboxylate (Fig. 3.1), has been identified as the reference compound for the phthalate class mainly because it is among the most widely used and studied compounds, thus having the most robust toxicological data set.

DEHP is an organic ester containing an eight-carbon alcohol moiety. The substance appears as an oily liquid, ranging from colorless to pale yellow, and is almost odorless.

DEHP is an organic compound that barely dissolves in water, a characteristic that must be considered, particularly in toxicological studies. The solubility of DEHP in water is 0.00003% (23.8 °C) (PubChem, 2024).

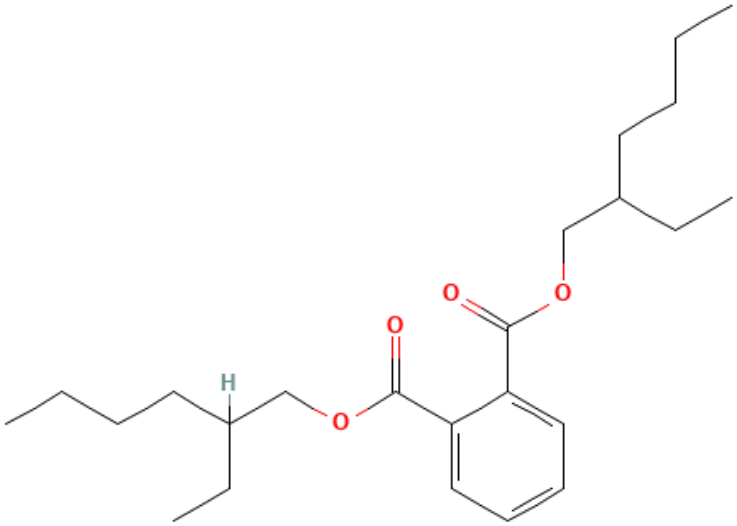

Fig. 3.1 – Chemical Structure of DEHP $C_{24}H_{38}O_4$

3.1.2 – Absorption and Metabolism of DEHP

The toxicity of phthalates is primarily attributable to their metabolites. Diesters of o-phthalic acid, including DEHP, are rapidly metabolized *in vivo* by esterolytic enzymes, transforming them into primary metabolites (monoesters), primarily in the gastrointestinal tract (Wang et al., 2019; Ranucci, 2022). Specific data on DEHP toxicokinetics in humans, mostly includes qualitative information on absorption and distribution, with fewer quantitative details on metabolites and urinary excretion kinetics.

DEHP metabolism has been extensively studied in various animal models, such as cynomolgus monkeys, marmosets, dogs, rabbits, rats, mice, and hamsters. Notably, there is significant interspecies variability in absorption rates linked to differences in metabolism. For instance, male

rats absorb approximately 98% of inhaled DEHP compared to less than 30% in other models. Oral absorption in humans is estimated to be approximately 70%, whereas dermal absorption is approximately 2% (Andersen et al., 2018; Krais et al., 2018).

Following its absorption, DEHP and its metabolites are rapidly distributed across various tissues. In animals, they are predominantly localized in the blood, liver, intestine, muscles, kidneys, and adipose tissues (Tanaka et al., 1975; Ikeda et al., 1980; Rhodes et al., 1986). Transplacental transfer to the fetus during gestation has also been confirmed in rodents and humans (Clewell et al., 2013; Arbuckle et al., 2016). However, in humans, specific information regarding DEHP distribution beyond the blood remains limited.

A recent human physiologically based pharmacokinetic model suggests that chronic dermal exposure could be a significant route of exposure (Li et al., 2022). Furthermore, it has been proposed that direct dermal absorption into the bloodstream, bypassing the first-pass metabolism observed in oral exposure, could potentially increase accumulation (Zhao et al., 2022).

In both rodents and humans, DEHP metabolism primarily involves hydrolysis to mono(2-ethylhexyl) phthalate (MEHP) and 2-ethylhexanol (2-EH) by various hydrolases, including carboxylesterases and lipases, which are found in tissues such as the pancreas, intestines, liver, kidneys, and lungs (Choi et al., 2012; Hopf et al., 2014; Ozaki et al., 2017).

Interspecies differences in DEHP hydrolytic activity are notable, with mice exhibiting the highest hepatic microsomal activity. Human liver microsomes exhibit hydrolytic activity up to five times lower than that in mice (Ito et al., 2005).

After hydrolysis, MEHP undergoes oxidation of its aliphatic side chain, occurring either terminally (ω-oxidation) or subterminally (ω-1 oxidation). This process is catalyzed by cytochrome P450 enzymes, particularly CYP2C9 and CYP2C19 in humans and CYP2C6 in rats (Choi et al., 2012; Tait et al., 2020). Oxidized metabolites may further undergo α- or β-oxidation, resulting in carboxylated and ketonic side-chain products (Ito et al., 2005). These metabolites are then conjugated with glucuronic acid to form acyl glucuronides, which facilitate their excretion (Silva et al., 2003; ATSDR, 2022).

The 2-EH product of DEHP hydrolysis is metabolized separately through β-oxidation (Albro and Corbett, 1978).

The elimination of DEHP and its metabolites mainly occurs through urinary and fecal excretion. Although excretion profiles in humans resemble those observed in animal models, significant interspecies differences exist in the relative abundance of metabolites and glucuronide conjugates. For instance, glucuronides are predominantly found in human excretions, but are absent in rats (ATSDR, 2022).

3.1.3 – Toxicity and Health Effects

Numerous studies have linked DEHP exposure to various toxicological endpoints in rodents, including reproductive and

developmental disorders, disruptions in the nervous, immune, and endocrine systems, and carcinogenesis (Rowdhwal and Chen, 2018). Eleven phthalates, including benzyl butyl phthalate (BBP), dibutyl phthalate (DBP), and DEHP, are classified as Category 1B reproductive toxins (suspected of being toxic to reproduction) according CMR classification (Silano et al., 2019; SCHEER, 2024).

Liver and Kidney Toxicity: Human data on liver and kidney effects from DEHP exposure remain limited, with epidemiological studies showing inconsistent associations between urinary DEHP metabolites and serum levels of triglycerides or cholesterol. In rodents, high doses of DEHP cause degenerative and necrotic liver changes, while lower doses lead to liver enlargement, linked to peroxisome proliferation and PPARα activation. Given the interspecies differences in PPARα function and expression, these rodent-specific effects are generally considered less relevant to human health (Foreman et al., 2021). However, studies on PPARα-null mice have indicated potential PPARα-independent toxicity mechanisms, as kidney and testicular lesions have been observed even in the absence of liver toxicity (ATSDR, 2022).

Immune System Effects: Data on the immunological effects of DEHP in humans are extremely limited. Animal studies have shown that DEHP acts as an immunological adjuvant in sensitized animals at low exposure levels, with variable effects depending on the exposure route. There is no consistent evidence that DEHP exposure at levels relevant to human health increases allergic sensitization (ECHA, 2023).

Reproductive Effects: Epidemiological studies suggest a potential association between DEHP exposure and reduced serum testosterone levels and altered sperm parameters in males. Animal studies have consistently shown male reproductive system susceptibility to DEHP toxicity, especially in the testes, as well as reduced fertility in both sexes at high oral doses (ATSDR, 2022).

Developmental Effects: Prenatal exposure studies in humans point to potential associations between DEHP exposure, reduced anogenital distance, and testicular dysfunction in male infants. In rodents, prenatal exposure affects glucose and lipid homeostasis as well as reproductive system development, highlighting these as key toxicological endpoints (ATSDR, 2022; ECHA, 2023).

Endocrine Disruption: DEHP is an endocrine disruptor that affects various hormones, including thyroid hormones, steroids (e.g., progesterone and estrogen), and corticotropin-releasing hormones (Rowdhwal and Chen, 2018; Wu et al., 2021; Barrett et al., 2022; Zhang et al., 2022; Li et al., 2024). Prenatal DEHP exposure in rodents alters mineralocorticoid receptor expression in Leydig cells, affecting aldosterone-induced androgen formation and reducing testosterone levels, potentially by interfering with the renin-angiotensin-aldosterone system (Rowdhwal and Chen, 2018). Additionally, DEHP exposure has been linked to the disruption of the hypothalamic-pituitary-thyroid axis and alteration of thyroid hormone metabolism (Wu et al., 2021). Oral exposure studies in rats have indicated that thyroid hyperactivity is associated with

cellular hypertrophy and endoplasmic reticulum stress (Rowdhwal and Chen, 2018). The pathways involved in thyroid toxicity include JAK/STAT, PI3K/Akt, and Nuclear factor-kB (NF-kB) signaling (Zhang et al., 2022).

3.1.4 – Carcinogenicity of DEHP

Numerous studies have suggested that DEHP is not genotoxic, but can induce liver tumors in mice and rats, with inconclusive evidence for testicular and pancreatic cancer (Madia et al., 2020b; ATSDR, 2022; ECHA, 2023). However, extrapolation of these results to humans has not yet been established.

DEHP and other phthalates, particularly its main metabolite, MEHP, are associated with several KCCs, including oxidative stress, inflammation, epigenetic alterations, immunomodulation, activation of various cellular receptors, endocrine disruption, and altered cellular energy balance (Senga et al., 2024).

The primary mechanism involved in DEHP-induced hepatocarcinogenicity in rodents is the transactivation of the PPARα signaling pathway, which plays a physiological role in regulating lipid metabolism and glucose homeostasis. The relevance of this pathway in humans remains debatable (Isenberg et al., 2000; Corton et al., 2014; Corton et al., 2018; Foreman et al., 2021). Other studies have suggested additional PPARα-independent carcinogenic mechanisms, such as those involving NF-kB, the constitutive androstane receptor (CAR), and the PXR, which may have greater relevance for humans (Ito et al., 2019).

In vivo studies on PPARα-null mice and transgenic mice expressing human PPARα have produced contrasting results, with some evidence of DEHP-related hepatocarcinogenesis in both genotypes. However, these findings have been strongly criticized (Ito and Nakajima, 2008; Corton et al., 2018; Foreman et al., 2021).

Based on the available data, the IARC and the US-EPA have classified DEHP as a possible carcinogen (Group 2B), indicating a non-genotoxic mode of action involving multiple mechanisms and signaling pathways. In contrast, the ECHA does not propose a carcinogenicity classification for DEHP.

DEHP has also been studied for its weak agonistic activity towards the AhR in various human cell lines, supported by the induction of the enzyme CYP1A1, a known AhR target gene (Sérée et al., 2004; Krüger et al., 2008; Rusyn and Corton, 2012; Wójtowicz et al., 2019; Neff et al., 2024). However, the downstream effects of AhR activation are complex and not fully understood. Intracellular interactions of the AhR complex with other transcription factors, such as retinoblastoma protein, NF-kB, ERs, and sphingosine-1-phosphate, along with different co-activators and repressors, can modify its transcriptional activity, adding further complexity. To date, the involvement of AhR in mediating adverse effects of DEHP has not been clearly demonstrated.

3.2 – Perfluorooctanesulfonic Acid and the Class of Per- and Polyfluoroalkyl Substances

Per- and polyfluoroalkyl substances (PFASs) represent a vast group of synthetic molecules with carbon chain lengths varying from C4 to C16, where hydrogen atoms are entirely (perfluorinated) or partially (polyfluorinated) replaced by fluorine atoms and have a terminal hydrophilic group, $F(CF_2)_n$-R.

Perfluorinated substances can form polyfluorinated substances through progressive hydrogen substitution via metabolic processes or abiotic degradation in the environment, leading to highly persistent molecules (Thapa et al., 2024).

The carbon-fluorine (C-F) bond grants these substances exceptional thermal and chemical stability. Furthermore, as amphipathic molecules, PFASs exhibit both hydrophobic and lipophobic properties, making them highly versatile for producing water-repellent and flame-resistant materials such as food packaging, textiles, paints, firefighting equipment, non-stick cookware, and cosmetics. Their widespread use has resulted in global PFAS distribution in the environment.

In the European Union, PFASs are classified as substances of "very high concern" under Regulation (EC) No. 1907/2006 (REACH) and are categorized as Persistent, Bioaccumulative, and Toxic or very Persistent and very Bioaccumulative. The Directive (EU) 2020/2184, effective from December 2020, sets a concentration limit of 0.5 µg/L for total PFASs in

drinking water and 0.1 µg/L for concerning PFASs, with a stricter application by some countries.

PFOS, perfluorooctanoic acid (PFOA), and perfluorononanoic acid (PFNA) are among the most common PFASs in air, water, sediments, animal tissues (Giesy and Kannan, 2001), and humans (Pérez et al., 2013; Jian et al., 2018; Uhl et al., 2023). Owing to their strong C-F bonds, these compounds are poorly biodegradable, have long half-lives, and tend to bioaccumulate by binding to proteins in organisms.

Over the past decade, PFAS research and monitoring has gained significant attention owing to the discovery of highly contaminated areas worldwide. In 2013, a large contaminated area was discovered in Veneto, Italy, which affected soil and drinking water across 30 municipalities and exposed approximately 150,000 inhabitants (the "Red Area"). In response, the Veneto Region implemented measures such as human water filters, a Health Surveillance Plan, and epidemiological investigations. A recent study by the University of Padua reported increased mortality in the Red Area population from 1985 (the onset of contamination) to 2018, with a higher incidence of cardiovascular diseases (notably heart disease and ischemic heart disease) and malignant neoplasms, including kidney and testicular cancers (Biggeri et al., 2024).

Recently, high PFAS levels were detected in several water bodies in Lombardy, Piedmont, and Tuscany, as reported by regional environmental protection agencies (ARPAs). On an international level, the potential ban on PFASs is under discussion, with five EU member states

(Denmark, Germany, Norway, the Netherlands, and Sweden) proposing a revision of the REACH Regulation.

3.2.1 – Chemical-Physical Properties of PFOS

PFOS (CAS No. 1763-23-1) IUPAC name 1,1,2,2,3,3,4,4,5,5,6,6,7,7,8,8,8-heptadecafluorooctane-1-sulfonic acid is a perfluoroalkane sulfonic acid, specifically an octane-1-sulfonic acid in which all 17 hydrogens attached to the carbon atoms were replaced by fluorine (Fig. 3.2).

Similar to most PFAS, under normal atmospheric conditions, they appear as crystalline solids or powders, although short-chain compounds (with 4-6 carbon atoms) can exist in liquid form.

As a long-chain PFAS, PFOS is relatively hydrophobic with a solubility of 519 mg/L at 20°C. Some studies have suggested that the solubility of PFOS in water decreases with increasing salinity (Olsen et al., 2008). In its acidic form, PFOS is a strong acid; however, it is often commercialized in its salt form, such as sodium or potassium salts

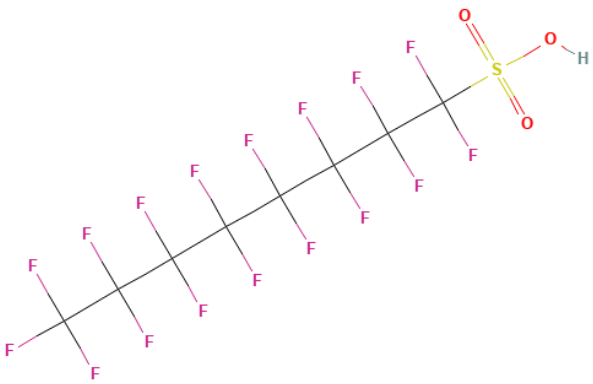

Fig. 3.2 – Chemical Structure of PFOS $C_8F_{17}SO_3H$

3.2.2 – Absorption and Metabolism of PFOS

After ingestion or inhalation, PFAS are rapidly absorbed and distributed in the body, mainly in the plasma and liver for ingestion and in the lungs for inhalation (Wee and Aris, 2023). These molecules are resistant to metabolism and are not easily eliminated, leading to long half-lives in both humans and animals.

Membrane transporters, such as organic anion transporters (OAT and OATP), multidrug resistance proteins (MDR), and urate transporters, are suggested to play key roles in the absorption, transport, and excretion of PFAS (Nigam and Granados, 2024; Shan et al., 2024; U.S. EPA, 2024).

Unlike other persistent organic pollutants that accumulate in fatty tissues, PFAS tend to bind to proteins, particularly albumin, low-density lipoproteins, and globulins, resulting in accumulation in the blood and liver (Chen and Guo, 2009; Zhang et al., 2009; Beesoon and Martin, 2015). The binding of PFOS and PFOA to serum albumin affects the natural transport function of the protein (Zhang et al., 2009; Salvalaglio et al., 2010). Moreover, PFOS can interact with cell membranes, mimic fatty acids, and potentially alter membrane function (Xie et al., 2010). Evidence suggests that PFOS, PFOA, and PFBS are primarily distributed in the serum and liver across species and can cross the placenta but not the blood-brain barrier (U.S. EPA, 2024). However, PFAS levels in the human body vary depending on factors, such as molecular type, tissue, life stage, and sex (Baumert et al., 2023; Wee and Aris, 2023). For instance, PFOS is the most frequently detected PFAS in the liver, likely due to its

accumulation in membrane lipids, unlike shorter-chain PFAS, which may rely on protein absorption mechanisms (Baumert et al., 2023).

Inter-species differences were noted, with lower liver accumulation in monkeys and humans than in rats, suggesting a lower susceptibility to liver-related effects of PFOS in humans (Pizzurro et al., 2019).

Higher doses usually show less tissue distribution, hinting at a saturation effect, possibly mediated by molecular transporters (Cheng and Ng, 2017; Pizzurro et al., 2019).

Urinary excretion is the primary elimination route, whereas fecal excretion is equally important in rats (U.S. EPA, 2024). Unlike PFOA, PFOS elimination half-lives are generally longer, with serum concentrations being three times higher in females than in males in rodents, a pattern not observed in humans. In humans, the half-life of PFOS is significantly longer, ranging from 2 to 5 years (Li et al., 2018; Pizzurro et al., 2019).

3.2.3 – Toxicity and Health Effects

Human exposure to PFAS is complex, typically involving chronic, aggregate exposure to various PFAS mixtures through multiple routes (EFSA Panel on Contaminants in Food Chain et al., 2020; U.S. EPA, 2024). Based on toxicity studies and their bioaccumulative and persistent nature, ECHA has classified PFOA and PFOS as reproductive toxins and suspected carcinogens.

Epidemiological and rodent studies have suggested that PFOS exposure can cause toxicity to the liver, immune, cardiovascular, and

reproductive systems, as well as developmental effects. These effects appear in humans at exposure levels between 0.57 and 5.0 ng/mL and in animals at doses ranging from 0.0017 to 0.4 mg/kg/day (U.S. EPA, 2024).

PFOS is also commonly considered an endocrine disruptor due to observed thyroid dysregulation and developmental neurotoxicity, although it is not formally classified for regulatory purposes (Wiklund et al., 2024).

Liver Effects: Evidence shows increased serum liver enzyme levels in humans and hepatotoxicity in animals, including increased liver weight and hepatocellular hypertrophy, sometimes accompanied by inflammation or necrosis. Initially, PPARα receptor activation was proposed as the main mechanism, but subsequent studies have indicated lipid accumulation in the liver of rodents exposed to PFOS, even without PPARα activation. This suggests that PFOS may exert its effects through the modulation of multiple nuclear receptors, including CAR, LXR, HNF4α, ERβ, and variants of PPARγ, β, and δ (Armstrong and Guo, 2019; U.S. EPA, 2024).

Immune System Effects: Immunotoxicity is considered a critical endpoint because some regulatory agencies use it to establish PFOS and PFOA toxicity levels. Animal studies have shown immunosuppressive effects, such as reduced spleen and thymus weights and altered immune cell populations (Qazi et al., 2009). In humans, the main studies have assessed antibody response variations to vaccinations, such as tetanus and diphtheria (Grandjean et al., 2012, 2017; Fenton et al., 2021). Although data limitations exist, reports suggest that PFAS-related

immunotoxicity may increase susceptibility to specific diseases and impair tumor immune surveillance (Garvey et al., 2023; Bline et al., 2024).

Cardiovascular Effects: Studies have shown increased serum lipid levels, especially total cholesterol and low-density lipoprotein (LDL), in humans (Steenland et al., 2009; Frisbee et al., 2010; Li et al., 2020; Fenton et al., 2021; Uhl et al., 2023). However, rodent studies often show opposite findings, such as decreased serum cholesterol and triglycerides but increased hepatic lipid concentrations. Interspecies variations in metabolism, lipid homeostasis, and PPARα have been proposed as the most likely contributing factors. For example, humans and primates have higher LDL levels, whereas rodents primarily exhibit high-density lipoprotein (HDL) associated cholesterol levels (Fragki et al., 2021). However, some rodent studies have demonstrated non-monotonic dose-response curves, with increased serum lipids at low exposure levels and decreased levels at higher doses, patterns that are more closely aligned with human observations. This suggests that differences in exposure duration and dietary fat content between humans and rodents may also contribute to these discrepancies (Fragki et al., 2021; U.S. EPA, 2024). Despite these factors, the observed differences in animal models compared to epidemiological data cannot be fully explained, warranting careful evaluation of the reliability of rodent models and the need for further mechanistic studies (Fragki et al., 2021; U.S. EPA, 2024).

Reproductive, Developmental Toxicity, and Endocrine Disruption: Epidemiological studies have linked prenatal PFAS exposure to reduced

fetal growth and preterm births, with results consistent with those of rodent studies (EFSA Panel on Contaminants in Food Chain et al., 2020; U.S. EPA, 2024). PFOS, PFOA, and perfluoroundecanoic acid have been associated with altered serum levels of sex hormone-binding globulin, follicle-stimulating hormone, and testosterone in males, and lower levels of estradiol and progesterone in nulliparous women (Uhl et al., 2023). PFAS also interfere with thyroid hormone signaling, potentially affecting pregnancy outcomes and fetal-neonatal development (Coperchini et al., 2021).

Hypothyroidism is the most common thyroid disorder, although differences in sex and age have been observed (Ballesteros et al., 2017; Uhl et al., 2023; Wiklund et al., 2024). Reduced antibody production against diphtheria and tetanus has been observed in children prenatally exposed to PFOS, perfluorohexanesulfonic acid, and PFOA (EFSA Panel on Food Contact Materials Enzymes and Processing Aids et al., 2019; Bline et al., 2024).

3.1.5 – PFOS Carcinogenicity

Recent studies have classified PFOS as a possible human carcinogen, based on *in vivo* studies showing a significant increase in the incidence of adenomas and carcinomas in the liver, thyroid, and mammary glands of rats. Epidemiological data in humans remain inconclusive, although recent studies have suggested a potential association between bladder and liver cancers (Cao et al., 2022; Goodrich et al., 2022; Alexander et al., 2024).

In December 2023, the IARC placed PFOS in Group 2 B and PFOA in Group 1, classifying the latter as “carcinogenic to humans” (Zahm et al., 2024).

Genotoxicity and mutagenicity tests have been negative for both PFOS and PFOA, *in vitro* and *in vivo* (EFSA Panel on Contaminants in Food Chain et al., 2020). Chronic toxicity and carcinogenicity studies in rats have shown hepatotoxicity and hepatocarcinogenesis, with a significant increase in hepatocellular adenomas in both males and females at the highest dose of 20 ppm. Thyroid follicular cell adenomas and mammary tumors were also observed, although the lack of dose-response relationships complicates the interpretation of these findings (Butenhoff et al., 2012; U.S. EPA, 2024).

Several epidemiological studies have reported associations between PFOS exposure and cancers, particularly hepatocellular carcinoma and testicular and kidney cancers (Steenland and Winquist, 2021; Cao et al., 2022; Goodrich et al., 2022).

PFOS exhibits multiple KCCs, including epigenetic alterations, oxidative stress, inflammation, and immunomodulation, with effects on immune suppression and receptor-mediated pathways. Recent evidence points to several mechanisms of action for PFOS-induced carcinogenesis, including widely studied ones like PPARα activation, CAR activation, cytotoxicity and oxidative stress, and others under investigation, such as HNF4α receptor suppression, alteration of cell membrane fluidity, potentially affecting calcium signaling and apoptosis response, and

interference with the immune system (Xie et al., 2010; Senga et al., 2024; U.S. EPA, 2024).

Several *in vitro* and *in vivo* studies have indicated that PFOS and PFOA activate gene regulation through PPARα activation, and that PFOA exhibits stronger PPARα agonism than PFOS (Wolf et al., 2012; Fragki et al., 2021). Conversely, studies using PPARα-null and humanized PPARα transgenic mice have suggested that additional signaling pathways might partly contribute to lipid metabolism deregulation caused by these chemicals (Fragki et al., 2021; U.S. EPA, 2024).

Metabolic disruption is a recognized hallmark of cancer, suggesting that alterations in metabolic regulators such as PPARs, CAR, and HNF4α could play a role in PFAS-mediated carcinogenesis. PFOS modifies hepatic metabolism through both PPARα-dependent and -independent mechanisms, affecting amino acid biogenesis, the Krebs cycle, and increasing β-oxidation enzyme activity (Tan et al., 2012; Yu et al., 2016).

CHAPTER 4

Objectives and Experimental Designs

4.1 – Immunofluorescence Experiment

In this study, the murine fibroblast cell line, BALB/c 3T3 (clone A31-1-1), was used. As both substances examined are agonists of the PPARα receptor and are carcinogenic in rodents partly because of this property, the initial objective was to characterize the cell line to verify the expression of the PPARα receptor. To achieve this, an indirect immunofluorescence experiment was conducted to identify and localize the protein in BALB/c 3T3 clone A31-1-1 cells.

Recent studies have highlighted that the expression of each PPAR isoform is tissue specific. PPARα is primarily expressed in the liver, kidneys, and tissues and is involved in lipid oxidation. Additionally, PPARα is mainly expressed in the nucleus at the subcellular level (Feige et al., 2005; Patel et al., 2005; Umemoto and Fujiki, 2012).

4.2 – Assessment of the Carcinogenic Potential of Diethylhexyl Phthalate and Transcriptomic Analysis

The main objective of this study was to evaluate the carcinogenic potential of DEHP using CTA in the BALB/c 3T3 A31-1-1 cell model. Following this, microarray transcriptomic analysis was performed to identify and explore molecular events, cellular responses, and potential mechanisms of action related to its toxicological profile and *in vitro* activity. The application of omics techniques to CTA models adds depth to the

analysis, supporting phenotypic data with mechanistic insights. This integrated approach aims to develop new alternative methods for assessing carcinogenic substances and deepen our understanding of the mechanisms of *carcinogenesis in vitro*. The results of this analysis could also be valuable for evaluating the robustness of the "Transformics Assay" as an integrated alternative strategy for assessing potentially carcinogenic chemicals (Mascolo et al., 2018; Pillo et al., 2022; Colacci et al., 2023).

The BALB/c 3T3 A31-1-1 model expresses AhR, a receptor extensively studied for its involvement in the metabolism and bioactivation of xenobiotics as well as its potential key role in chemical carcinogenesis.

The transcriptomic experiment focused on analyzing the effects of three different DEHP concentrations associated with varying levels of cytotoxicity. Additionally, cellular lysates were collected at three different time points: at the end of 24 h and 72 h treatments to examine early cellular responses and resilience, and 28 days post-72 h treatment to assess long-term effects.

It is important to note that although DEHP has been tested in many CTAs in the past, the results in the literature are often conflicting and confusing. Moreover, no previous study has used the A31-1-1 clone. Many previous studies have employed different experimental conditions, cell models, and solvents, often using concentrations that exceeded the solubility limits, thus complicating the interpretation of results. Furthermore, previous assays commonly used BALB/c 3T3 A31 or A31-1

clones, which differ significantly from the A31-1-1 clone in terms of both metabolism and ontogeny.

4.3 – Carcinogenic Potential of Perfluorooctane Sulfonic Acid with a PPARα Antagonist

The aim of this experiment was to explore the carcinogenic mechanism of PFOS, building on existing data from CTAs (Vaccari et al., 2024) and transcriptomic analyses conducted using the integrated Transformics Assay approach (Aldrovandi et al., in preparation).

PFOS is a PPARα receptor agonist; however, it is unknown whether this interaction is crucial in determining transforming effects in the CTA.

Given this context, a CTA using BALB/c 3T3 A31-1-1 cells was designed to test three PFOS concentrations known to induce cellular transformation in conjunction with PPARα receptor activity inhibition. To inhibit PPARα receptor activity, the cells were co-treated with the PPARα antagonist GW6471, a compound that binds to PPARα and induces a conformational change, enhancing its affinity for co-repressors. GW6471 is capable of fully blocking receptor activation by the agonist GW409544, with a half-maximal inhibitory concentration (IC50) of 0.24-0.25 μM (~ 0.15 μg/mL) (Xu et al., 2002).

In designing this experiment, attention was given to the documented antiproliferative activity of GW6471 in various tumor cell lines (Abu Aboud et al., 2015; Ammazzalorso et al., 2020; Castelli et al., 2021) and its use in studies exploring the role of PPARα in combination with

other substances, either as pre-treatment or co-treatment (Florio et al., 2018; Pierozan et al., 2018).

The optimal concentration of GW6471 was determined through dose-range-finding cytotoxicity tests to determine the maximum non-cytotoxic concentration for BALB/c 3T3 A31-1-1 cells.

To prevent potential molecular competition for receptor binding and to enhance the efficacy of GW6471, it was applied both as a pre-treatment and co-treatment. The inhibitor was initially delivered in half the total volume of the culture medium. After 30 min, the second half of the medium containing twice-concentrated PFOS and the same concentration of GW6471 as in the pretreatment was added. This approach ensured the early and simultaneous exposure of cells to the PPARα receptor inhibitor during PFOS treatment.

CHAPTER 5

Materials and Methods

5.0 – *In vitro* cell culture

In this study, the murine fibroblast cell line BALB/c 3T3, clone A31-1-1 (Fig. 5.1), was used, as outlined in the protocol of the pre-validation study (Sasaki et al., 2012a). Original stock was obtained from the Health Science Research Resource Bank (Osaka, Japan).

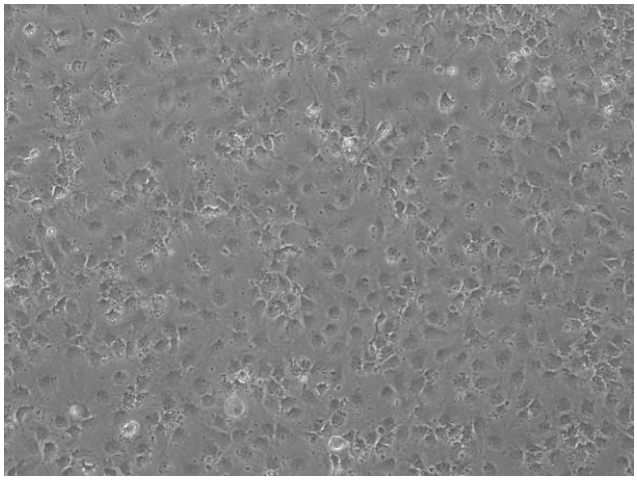

Fig. 5.1 - Live BALB/c A31-1-1 cells at confluence, grown in MEM medium. Magnification 10x (EVOS M5000).

The cells were initially cryopreserved in a freezing solution containing MEM (Minimum Essential Medium) with 10% FBS (Fetal Bovine Serum) and 5% dimethyl sulfoxide (DMSO). They were subsequently cultured in an incubator under modified atmospheric conditions at 37 ± 1°C, 90 ± 5% humidity, and 5.0 ± 1% CO_2, using M10F medium, which consisted of MEM supplemented with 10% FBS and 1% PS (10,000 units/ml penicillin and 10 mg/ml streptomycin). For this experiment, cells at

passage 1 from the original stock were maintained in a subconfluent state after thawing. The cells were detached from sterile culture flasks (BD Falcon, UK) by washing with DPBS (Dulbecco's Phosphate-Buffered Saline, without calcium and magnesium ions, Gibco, UK) and using a solution containing 0.05% trypsin-0.02% Na-EDTA (Gibco, UK). They were then resuspended in the culture medium and counted using a Neubauer chamber.

5.1 – Immunofluorescence Experiment

To evaluate PPARα protein expression in BALB/c 3T3 A31-1-1 cells, an indirect immunofluorescence experiment was conducted. Polyclonal antibodies (Abcam Anti-PPAR alpha antibody_ab61182) and secondary antibodies (Abcam Goat Anti-Rabbit IgG H&L, Alexa Fluor 488_ab150077) were used. U87 MG cells served as the positive control, as recommended by the manufacturer, whereas U87 MG cells treated only with the secondary antibody were used as the negative control.

Hoechst staining was performed to visualize cell nuclei.

BALB/c 3T3 A31-1-1 cells were seeded at a density of 30,000 cells/well in µ-Slide 8 Well supports (Ibidi 80806). Twenty-four hours after seeding, the culture medium was removed and the cells were washed with phosphate-buffered saline (PBS). The cells were fixed with methanol for 10 min. Following additional PBS washes, cells were incubated with a blocking solution containing 2.5% bovine serum albumin (BSA) in PBS for 20 min.

The primary antibody (1:200 in 1% BSA in PBS) was applied and incubated for 1 h at room temperature. After incubation, cells were washed with PBS. The secondary antibody (1:200 in 1% BSA in PBS) was added, followed by a 1-hour incubation at room temperature. After further PBS washes, the cells were incubated for 3 minutes with Hoechst stain at 0.5 µg/ml (Thermo Scientific™ 62249) at room temperature. Finally, cells were observed under a fluorescence microscope (EVOS M5000).

5.2 – Chemicals and Stock solutions

3-Methylcholanthrene (MCA) (CAS 56-49-5, purity 98.9 ± 0.5% w/w) was used as a reference substance in the cell transformation tests at a concentration of 4 µg/ml.

Dimethyl sulfoxide (DMSO, CAS number 67-68-5, Hybri-max Sterile, purity 100%, Sigma/D2650) was used as the vehicle and solvent to dissolve the compounds.

In the first experiment of CTA and microarray transcriptomics, *bis (2-ethylhexyl) phthalate* PESTANAL®, an analytical standard (DEHP, CAS number: 117-81-7, purity ≥ 98.0%, SIAL 36735), was used as the test chemical. DEHP barely dissolves in water, and its solubility in cell culture medium decreases with lower DMSO and higher cell culture medium volumes. A preliminary solubility test was performed to verify the stability of the treatment solutions in the medium. The treatment solutions were incubated under test conditions (37°C, 5% CO_2, and 90% relative humidity) for 72 h to check for precipitates. Two groups of DEHP dilutions in DMSO (1:1,000 with 0.1% DMSO and 1:200 with 0.5% DMSO) were

tested at final DEHP concentrations of 100, 75, and 25 µg/ml. While the initial dissolution in DMSO was complete, the 0.1% DMSO group exhibited turbidity and micelles. Thus, a final concentration of 0.5% DMSO was used in the experiments to ensure the homogeneous dissolution of DEHP. Serial dilutions of the DEHP stock solution in DMSO were prepared and diluted in the complete M10F medium to obtain the final treatment solutions.

In the CTA experiment, the carcinogenic potential of PFOS combined with the PPARα antagonist *GW6471* (CAS number: 880635-03-0, purity: 98.71%, 10 mg, Chemscene) was used as a PPARα receptor antagonist, while the test chemical was a standard solution of PFOS (CAS number: 1763-23-1, purity: 98.4% ± 0.6%, 100 mg, Ultra Scientific Italia srl).

GW6471 was dissolved in DMSO at a concentration of 12 mg/ml. The solution was vigorously vortexed and oscillated for approximately 40 min to promote uniform solubilization.

The solubility of PFOS has already been tested in our laboratory in previous studies, where rapid vortexing (1-2 minutes) was required to completely solubilize the test items (Vaccari et al., 2024). To stabilize the solution further, it was left on a shaker for approximately 1 h. The experimental design of this CTA provided a final DMSO concentration of 0.15%.

5.3 – Colony Formation Efficiency Assay

A Colony Formation Efficiency Assay (CFE) Assay was used to evaluate the cytotoxicity of DEHP, PFOS, and GW6471 in the BALB c/3T3 A31-1-1 cell model.

This assay quantifies the clonogenic potential of cells in the presence of a test chemical, with the number of colonies counted being proportional to cell viability and inversely proportional to cytotoxicity.

Preliminary CFE tests determined the appropriate dose range for CTAs and the maximum non-cytotoxic concentration of GW6471.

A concurrent CFE (CC) assay was performed for each cell transformation test following the reference protocol (Sasaki et al., 2012a).

The CFE test was performed for all the experiments as follows:

cells were seeded at a density of 200 cells per 60 mm Petri dish in 4 ml of M10F medium. After 24 h, treatments were applied. Negative controls consisted of untreated cells and those treated with DMSO alone, with five replicates for each condition.

The cells were incubated under standard conditions. After 72 h, the medium was replaced with a fresh culture medium. Ten days post-seeding, the cells were fixed with methanol (10 min) and stained with 0.04% Giemsa (30 min). Colonies containing at least 50 cells were counted using an inverted phase-contrast microscope following established guidelines (Franken et al., 2006; Sasaki et al., 2012a).

The results are expressed as follows.

- Mean number of colonies per plate ± standard error (SE).

- Absolute Cloning Efficiency (ACE): the fraction of cells surviving post-treatment relative to the number of cells seeded.
- Relative Cloning Efficiency (RCE): The percentage reduction in cloning efficiency in treated groups compared to the solvent-treated negative control.

5.3.1 – Statistical Analysis

Three types of statistical tests were used to analyze the CFE results, as follows:

- A one-tailed or two-tailed Student's t-test for independent samples was used to assess the difference between the mean number of colonies in the treated groups.
- The z-test for the comparison of the two proportions was applied to compare the ACE values of the treated and control groups.
- The chi-square test in 2 × 2 contingency tables was used to evaluate the significance of RCE values.

5.4 – Cell Transformation Assay

To assess the carcinogenicity of the test substances, DEHP, PFOS, and the PFOS-GW6471 mixture, CTAs were used to evaluate the acquisition of malignant characteristics in response to treatments. For detailed information on co-treatment with GW6471, refer to Chapter 4.

Cells were seeded at a density of 10 000 cells/dish in 4 ml of M10F medium and incubated under standard culture conditions. 24 hours after seeding, cells were exposed to the treatments. Positive controls, consisting of cells treated with MCA, and negative controls, consisting of untreated cells and cells treated with DMSO, were prepared. Ten replicates were used for each treatment group.

After 72 hours, the medium was replaced with fresh culture medium. Cells were maintained under standard culture conditions until the 32nd day post-seeding, with medium changes performed twice weekly until the fourth week. From the second week onward, cells were maintained using DF212F culture medium, composed of DMEM/F12 (Dulbecco's Modified Eagle Medium/F12), 2% FBS, 1% PS (10 000 units/ml penicillin and 10 mg/ml streptomycin), and supplemented with 0.1% bovine insulin at 2 mg/ml. Reduced serum concentration in the complete medium promoted the growth of transformed cells. No medium changes were observed in the final week of the assay.

Five weeks after the initial seeding, the plates were fixed with methanol and stained with 0.04% Giemsa. Focus counting and evaluation were conducted according to the guidelines outlined in relevant scientific literature (IARC, 1985; OECD, 2007; Hayashi et al., 2008; Sasaki et al., 2012b). Only type III *foci* were considered in the evaluation of the test outcome (Fig. 5.2).

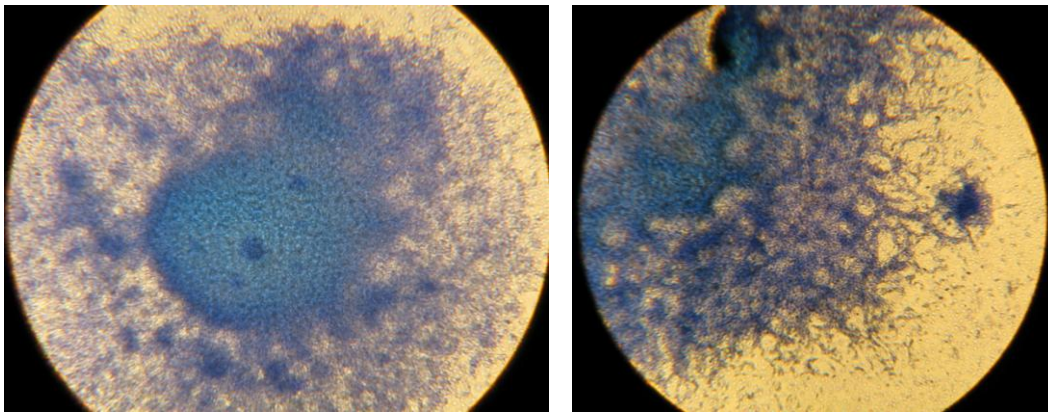

Fig. 5.2 – Example of Type III Foci; CTA with BALB/c 3T3 A31-1-1 cells treated with BaP and 3-MCA, respectively, magnification × 20.

In particular, type III *foci* exhibited the following characteristics.

- Intense basophilia
- Elongated and spindle-shaped cells
- Disorganized and multilayered cell growth
- Invasiveness and infiltration into the monolayer of non-transformed cells

The transforming activity is expressed as:

- Average number of *foci* per plate ± SE
- Percentage of positive plates (showing type III *foci*) relative to the total number of plates examined
- Transformation frequency (TF) was calculated as the ratio of the mean number of *foci* per experimental group to the number of cells at risk, which is the number of cells surviving post-treatment (cells seeded per plate multiplied by the ACE observed in the CC) ± SE."

The test acceptability criteria were defined based on relevant scientific literature (OECD, 2007; Hayashi et al., 2008; Sasaki et al., 2012a; Tanaka et al., 2012):

The transformation test is considered valid if

- The positive control (MCA; 4 *μg/mL*) induced a significant increase in cellular transformation.
- The treatment vehicle did not induce a significant increase in transformation (maximum of 5 total *foci* across 10 plates).
- The total number of positive *foci* observed in the plates treated with the positive control was at least three times higher than that observed in the solvent control plates.

5.4.1 – Statistical Analysis

CTA results were analyzed using the following statistical tests:

- The significance of the number of positive plates (showing type III *foci*) relative to the total number of plates examined was calculated using the one-tailed Fisher-Yates test in 2 × 2 contingency tables.
- Analysis of *foci* distribution was performed using the Mann-Whitney U test for one- or two-tailed independent samples.
- Statistical evaluation of the difference between the transformation frequencies of the treated groups and controls was carried out using the one-tailed Poisson test, after verifying the Poisson distribution pattern of the frequency values.

5.5 – Transcriptomics Experiment

The transcriptomic experiment was conducted following a Transformics Assay-like approach, utilizing the seeding, culture, and treatment protocols of the CTA (Mascolo et al., 2018; Pillo et al., 2022). The selected concentrations of the reference substance DEHP in BALB/c 3T3 A31-1-1 model were 1.97 µg/ml, 6.57 µg/ml, and 19.7 µg/ml. Cell lysis occurred at the end of 24 h and 72 h treatments and 28 d post-72 h treatment (32 d post-seeding).

The experiment comprised of three phases: cell culture and treatment, cell lysis and RNA extraction, RNA labelling and microarray preparation, followed by image analysis. Cells in the logarithmic growth phase were seeded at 10 000 cells per 60 mm dish, with four biological replicates for each treatment and lysis time point, totaling 12 groups. The biological replicates consisted of independent plates that were seeded and treated in parallel. Each replicate was obtained from multiple technical replicates to ensure adequate cell numbers for nucleic acid extraction, without altering the seeding and culture protocol.

M10F medium was used for cell culture and treatment. Treatment solutions, prepared similar to those in the CTA assay, utilized DMSO as a vehicle at a final concentration of 0.5%. The cells were exposed to DEHP (1.97 µg/ml, 6.57 µg/ml, and 19.7 µg/ml) 24 ± 2 h post-seeding, with exposure times of 24 h or 72 h based on the group.

5.5.1 – Cell Lysis, RNA Extraction, and Analysis

The total RNA was extracted using the phenol/chloroform method. For each 60 mm dish, 500 µL of TRIzol Reagent (Invitrogen, San Diego, CA, USA) was used and mechanical scraping was applied. Four type 1 biological replicates were used for each treatment. RNA purification was performed using RNeasy Mini Kit columns (Qiagen, Valencia, CA, USA), and RNA was eluted in 30 µL of RNase-free water. A total of 48 RNA samples were analyzed for concentration, quality, and integrity using a NanoDrop™ OneC spectrophotometer and Agilent 4200 TapeStation system. The analysis provided the RNA concentration (ng/µl), A260/A280 ratio for protein contamination (optimal around 2), and A260/A230 ratio for solvent contamination (optimal around 2). Potential RNA degradation was assessed using the 28S/18S ratio (approximately 2 for high-quality RNA) and RNA Integrity Number (RIN), ranging from 1 (completely degraded) to 10 (intact RNA), with values above 7 indicating acceptable quality.

5.5.2 – RNA Labeling and Microarray Hybridization

RNA labeling was performed using the Low Input Quick Amp Labeling Kit (version 6.9.1, December 2015, Agilent Technologies, Santa Clara, CA, USA), according to the manufacturer's protocol (www.genomics.agilent.com). A total of 100 ng of RNA from each biological replicate was used for labeling.

Labeled RNA was purified using RNeasy Mini columns (Qiagen, Valencia, CA, USA), resulting in 30 µL of labeled RNA solution per sample. RNA concentration and cyanine 3 incorporation levels were

measured using a NanoDrop OneC spectrophotometer at 260 nm and 550 nm, respectively. According to the manufacturer's guidelines, RNA samples were considered acceptable if they contained over 0.825 µg of total RNA and had a specific activity of at least 6 pmol of cyanine 3 per µg of amplified cRNA. The labeled cRNA was then hybridized onto 8x60K oligonucleotide microarray slides (SurePrint G3 Mouse Gene Expression v2 8x60K Microarray Kit, Agilent), which feature 27,122 genes and 4,578 lncRNAs (long non-coding RNAs) (http://www.genomics.agilent.com). The hybridization procedure utilized the Low Input Quick Amp Labeling Kit (version 6.9.1). Each sample, containing 600 ng of labeled and fragmented RNA, was applied to a slide and incubated at 65°C for 17 h.

The microarrays were subsequently washed twice using a Gene Expression Wash Buffer Kit (Agilent Technologies). Fluorescence signal intensities were detected using Scan Control Software on the SureScan Microarray Scanner G2600D.

5.5.3 – Image analysis and biological interpretation

The scanned images were analyzed using Feature Extraction software (version 12.2.0.7, Agilent Technology), and statistical analysis was conducted using the Agilent GeneSpring 14.9.1. Data normalization followed the standard 75th percentile method recommended by Agilent for the one-color protocol.

Data filtering for intensity and quality was conducted using two parallel approaches.

i) The application of “Filtered on Expression” and “Filtered on Flags” functions on the "All Samples" schema.

ii) An additional quality filter, "Filtered probsets by Error," was set to a coefficient of variation (CV) < 50%.

This approach aligns with previously established methods (Grabiec et al., 2016; Elmore et al., 2022). These filtering steps were applied initially in a preliminary analysis of a restricted dataset, including only the DEHP 6.57 µg/ml 72-hour and DMSO 0.5% 72-hour treatment groups, and subsequently in the “All samples analysis”, which comprised the entire dataset.

Statistical analyses were performed using unpaired t-tests (treated vs. control). Post-hoc corrections were applied using the Benjamini-Hochberg and Bonferroni methods. DEGs were then subjected to functional enrichment analysis using MetaCore™ V6.34 software (GeneGo Inc., USA), which utilizes a dynamic database of molecular interactions, signaling pathways, gene-disease associations, and molecular toxicity.

Biological analysis focused on identifying significantly modulated pathway maps with a false discovery rate (FDR) ≤ 0.05. In MetaCore, pathway maps represent “gene sets”, where modulated genes are indirectly represented through the proteins they encode (Fig.5.3). Individual transcripts are identified as network objects (NwOs) and can appear in multiple maps. NwOs are modulated molecular entities including proteins, protein complexes, peptides, and RNA species.

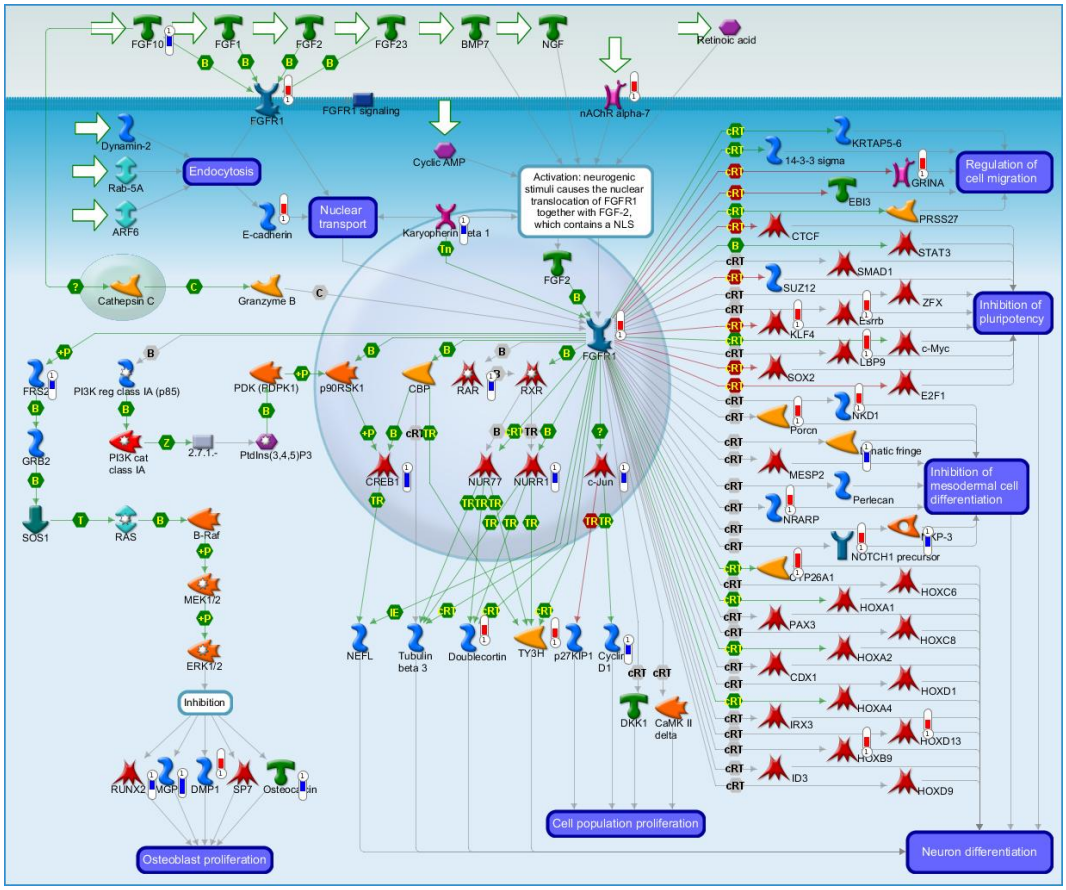

Fig. 5.3 – This example pathway map, which scored third based on enrichment distribution sorted by Statistically Significant Maps (FDR≤0.05), obtained using the 'Analyze Single Experiment – Enrichment Analysis' function by MetaCore (DEHP 19.7 µg/mL). It illustrates how experimental data from all files is linked and visualized. Thermometer-like figures on the map indicate expression levels: upward red thermometers represent upregulated signals, while downward blue thermometers indicate downregulated gene expression.

CHAPTER 6

Results

6.1 – Immunofluorescence Experiment

The immunofluorescence experiment yielded positive results, successfully marking and localizing PPARα protein within the cell nuclei, as shown in the images below, captured using an EVOS M5000 microscope.

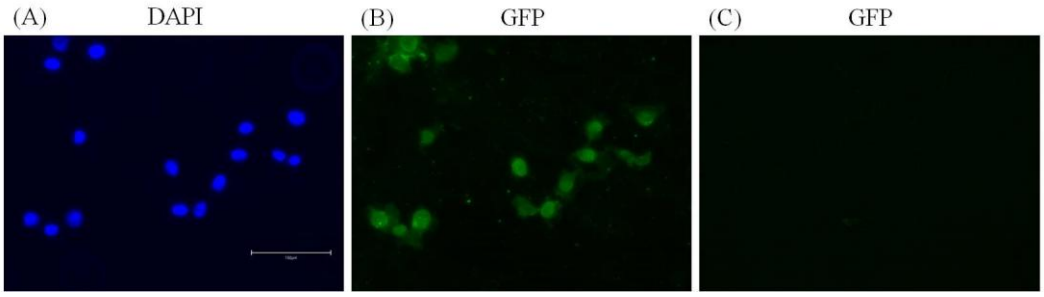

Fig. 6.1 - Images obtained with the EVOS M5000 imaging system of BALB/c 3T3 clone A31-1-1 cells. 20X objective. **A)** DAPI filter for visualizing Hoechst staining. **B)** GFP filter for visualizing Alexa Fluor® 488 (PPARα antibody). **C)** Negative control, cells treated with secondary antibody only.

6.2 – Clonal Efficiency Assays

6.2.1 – Cytotoxicity of DEHP

The initial cytotoxicity study evaluated the effects of DEHP concentrations ranging from 0.05 to 100 µg/mL on the BALB/c 3T3 A31-1-1 cell line (Fig. 6.2 – Test 1). Cytotoxic effects were observed within the range of 25 - 100 µg/mL, with concentrations at or above 50 µg/mL leading to a significant reduction in colony formation, exceeding 90%. The second

study investigated the effects of the compound at concentrations between 2.5 and 50 µg/mL (Fig. 6.2 – Test 2). Results were further confirmed by the CFE conducted as part of the CTA (Fig. 6.2– CTA CC; Tab. 6.2). An interpolation curve was used to identify the reference effect concentrations (IC10, IC50, and IC90) (Tab. 6.1).

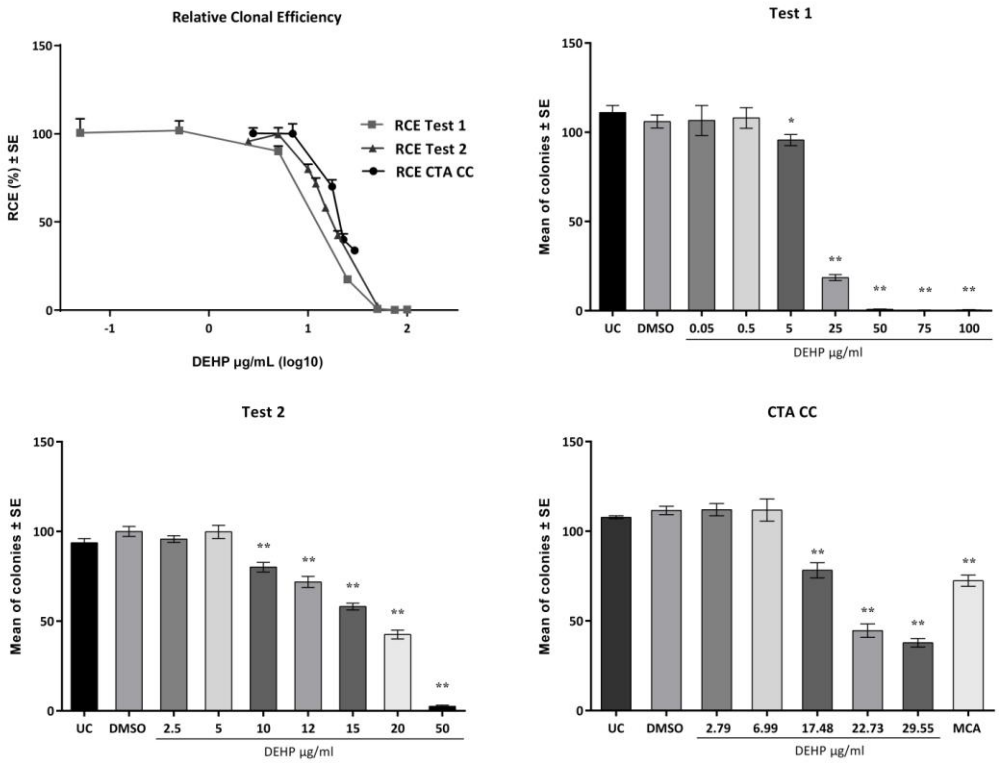

Fig. 6.2 – Clonal efficiency of BALB/c 3T3 A31-1-1 cells exposed to DEHP. Comparison of cytotoxicity assay results expressed as Relative Clonal Efficiency (RCE) linear regression (χ2-test) and Mean of colonies ±SE. *p < 0.05 vs. vehicle control, t-test. **p < 0.01 vs. vehicle control, t-test. Test 1 and Test 2 were performed as preliminary cytotoxicity assay. Cell Transformation Assay (CTA) concurrent cytotoxicity (CC) was performed within the CTA. SE: standard error; UC: Untreated Cells; DMSO: Dimethyl sulfoxide 0.5%; MCA: 3-Methylcholanthrene 4 µg/µL

Tab. 6.1 – IC (Inhibitory Concentration) values obtained from the analysis of Relative Clonal Efficiency (RCE) data using a nonlinear regression model. Test 1-2: Preliminary cytotoxicity tests; CTA CC: Transformation Assay concurrent cytotoxicity.

	IC interpolated (µg/ml)		
	Test 1	**Test 2**	**CTA CC**
IC10	5.02	7.06	9.53
IC50	12.18	17.42	20.82
IC90	34.14	42.08	/

Tab. 6.2 – Clonal efficiency of BALB/c 3T3 A31-1-1 cells exposed to DEHP in the Cell Transformation Assay (CTA) concurrent cytotoxicity (CC). ACE: Absolute Clonal Efficiency; RCE: Relative Clonal Efficiency; UC: untreated cells; DMSO: Dimethyl sulfoxide

Treatment	**Mean of colonies ± SE**	**ACE**	**RCE (%)**
UC	107.80 ± 0.80	0.54	97
DMSO 0.5%	111.60 ± 2.38	0.56	100
Bis(2-ethylhexyl) phthalate (µg/mL)			
2.79	112.00 ± 3.42	0.56	100
6.99	111.80 ± 6.20	0.56	100
17.48	78.20 ± 4.31 [a]	0.39 [b]	70 [c]
22.73	44.60 ± 3.72 [a]	0.22 [b]	40 [c]
29.55	37.80 ± 2.37 [a]	0.19 [b]	34 [c]

[a] *Significantly different (p<0.01) from controls (solvent-treated cells) at the Student t-test.*
[b] *Significantly different (p<0.01) from controls (solvent-treated cells) at the z test.*
[c] *Significantly different (p<0.01) from controls (solvent-treated cells) at the Chi-square test of significance in 2 × 2 contingency tables.*

6.2.2 – Cytotoxicity of GW6471

Two assays were conducted to evaluate the clonogenic efficiency of the BALB/c 3T3 A31-1-1 model treated with the PPARα antagonist, GW6471. The primary aim of these assays was to identify the maximum non-cytotoxic concentration in the BALB/c 3T3 A31-1-1 model as a reference for selecting the appropriate concentration for the next phase of the experiment. The first assay assessed the clonogenic efficiency of the cell model over the concentration range of 0.07 to 6.00 µg/mL. A second cytotoxicity study was performed to confirm the results of the first assay and further explore the relevant concentration range. The results are shown in Figure 6.3.

The concentration of 0.6 µg/mL was identified as the most suitable for use in the subsequent experimental phase. In the first CFE, GW6471 exhibited a significant increase in clonogenic efficiency compared to the control at concentrations of 0.2 and 0.3 µg/mL (Fig. 6.3 – Test 1). Owing to the potential observed proliferative effect, statistical evaluation was performed using an ANOVA variance test with Dunnett's correction (two-tailed). However, this effect was not observed in the second CFE (Fig. 6.3 – Test 2).

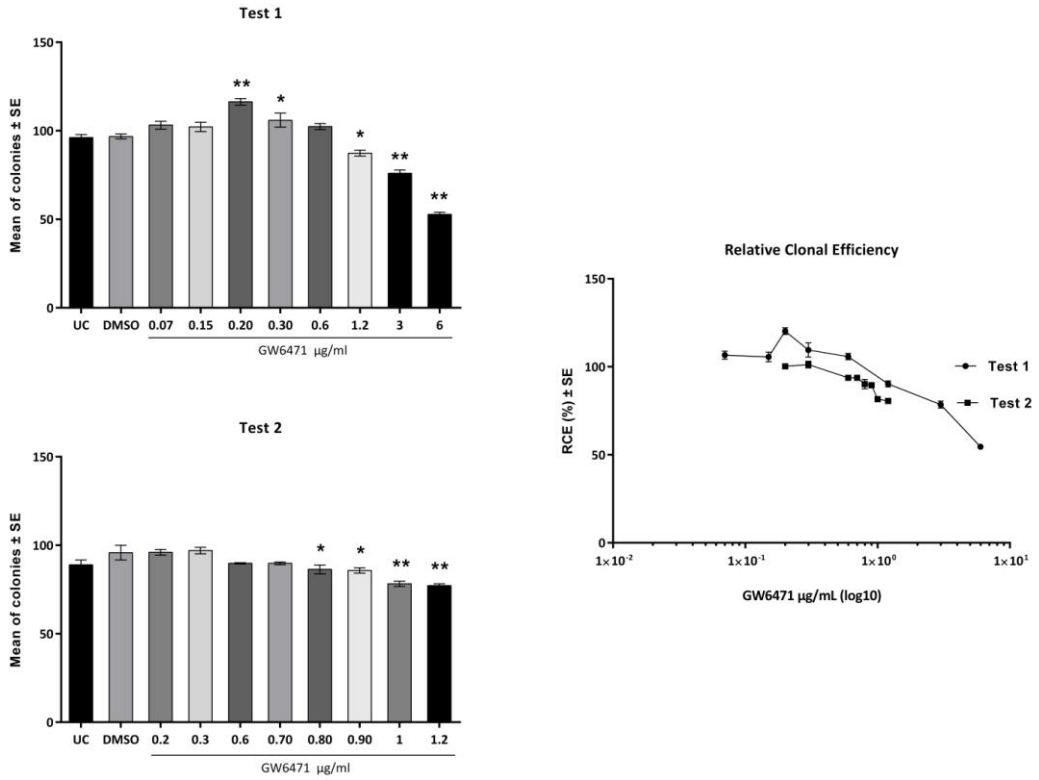

Fig. 6.3 – Clonal efficiency of BALB/c 3T3 A31-1-1 cells exposed to GW6471. Comparison of cytotoxicity assay (Test 1 and Test 2) results expressed as Relative Clonal Efficiency (RCE) linear regression (χ2-test) and mean of colonies ±SE. *p < 0.05 vs. vehicle control; **p < 0.01 vs. vehicle control, Dunnett's test.
SE: standard error; UC: Untreated Cells; DMSO: Dimethyl sulfoxide 0.1%.

6.2.3 – Cytotoxicity of PFOS with reduced PPARα Activation

In the CTA assay set up to evaluate the carcinogenic potential of PFOS in combination with the PPARα-antagonist GW6471, the clonogenic efficiency of the model was assessed under various treatment conditions: exclusive treatment with PFOS at concentrations of 50, 75, and 100 µg/mL, and treatment with PFOS at the same concentrations combined with GW6471 at 0.6 µg/mL. In this assay, DMSO was used as a control for the comparisons, while GW6471 was introduced exclusively to assess the cytotoxicity of the antagonist used as co-treatment.

The addition of the PPARα inhibitor reduced the cytotoxic effect of PFOS on clonogenic efficiency (two-tailed t-test) (Tab. 6.3; Fig. 6.4).

Tab. 6.3 – Clonal efficiency of BALB/c 3T3 A31-1-1 cells exposed to PFOS and GW6471 in the Cell Transformation Assay (CTA) concurrent cytotoxicity (CC). ACE: Absolute Clonal Efficiency; RCE: Relative Clonal Efficiency; UC: untreated cells; DMSO: Dimethyl sulfoxide

Treatment	Mean of colonies ± SE	ACE	RCE (%)
UC	101.60 ± 3.16	0.51	100
DMSO 0.15%	101.60 ± 3.85	0.51	100
GW6471 0.6 *µg/mL*	103.40 ± 2.29	0.52	100
PFOS (µg/mL)			
50	85.00 ± 3.35 [b]	0.42 [c]	84 [d]
75	70.00 ± 2.92 [b]	0.35 [c]	69 [d]
100	67.60 ± 2.16 [b]	0.34 [c]	66 [d]
PFOS (µg/mL) + GW6471 (0.6 µg/mL)			
50	88.60 ± 2.56 [a]	0.44 [c]	87 [d]
75	79.80 ± 2.08 [b]	0.40 [c]	78 [d]
100	79.40 ± 2.79 [b]	0.40 [c]	78 [d]

[a] *Significantly different (p<0.05) from controls (solvent-treated cells) at the Student t-test.*
[b] *Significantly different (p<0.01) from controls (solvent-treated cells) at the Student t-test.*
[c] *Significantly different (p<0.01) from controls (solvent-treated cells) at the z test.*
[d] *Significantly different (p<0.01) from controls (solvent-treated cells) at the Chi-square test of significance in 2 × 2 contingency tables.*

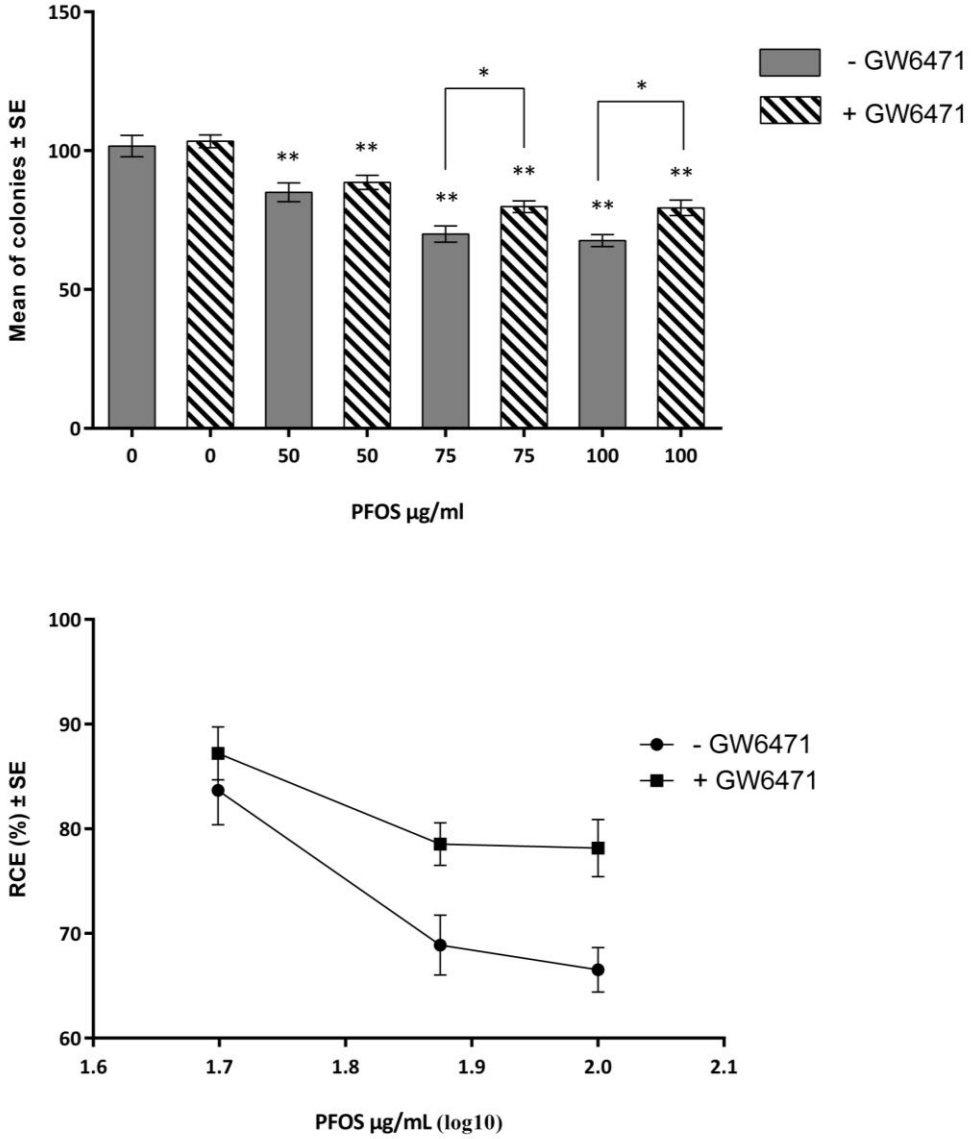

Fig. 6.4 – Clonal efficiency of BALB/c 3T3 A31-1-1 cells exposed to PFOS and GW6471 in the Cell Transformation Assay (CTA) concurrent cytotoxicity (CC), expressed as Mean of colonies ±SE, **p<0.01 vs. vehicle control, t-test; *p<0.05 vs. co-treated, t-test, and Relative Clonal Efficiencies (RCE) linear regression (χ2-test).
SE: standard error; co-treatment: + GW6471 0.6 µg/mL

6.3 – Transformation Assays

6.2.1 – DEHP Transformation Assay

The results of the transformation assay met the acceptability criteria, as the positive control (MCA, 4 µg/mL) induced a significant increase in cellular transformation (10 positive plates out of 10 total plates), whereas the vehicle control (DMSO 0.5%) did not induce any significant increase in transformation (0 positive plates out of 10 total plates). Treatment with DEHP did not significantly increase the average number of *foci* per plate (Fig. 6.5).

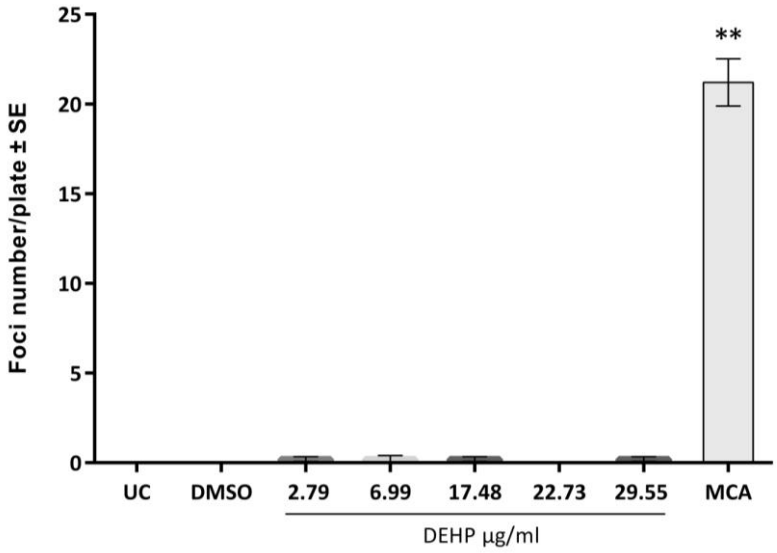

Fig. 6.5 - Effects of the treatment with DEHP on the transformation rate of BALB/c 3T3 A31-1-1 cells expressed as mean number of transformed *foci* per plate ± SE ** p<0.01 vehicle control, Mann–Whitney U test.

6.2.1 – PFOS Transformation Assay

The results of the transformation assay using PFOS and GW6471 met the acceptability criteria. The DMSO 0.15% control did not induce a significant increase in transformation (one positive plate out of 10 total

plates). The treatments resulted in a significant dose-response increase in the average number of *foci* per plate (Tab. 6.4; Fig. 6.6; Fig 6.7). The difference between the average number of *foci* in the groups treated with PFOS alone and those subjected to co-treatment with the PPARα-antagonost GW6471 was assessed, and no significant difference was observed (two-tailed Mann-Whitney U test). In this assay, DMSO was used as a control for the comparisons, while GW6471 was introduced exclusively to assess the effect of the antagonist used as co-treatment.

Tab. 6.4 – Effects of the treatment PFOS without/with GW6471 on the transformation rate of BALB/c 3T3 A31-1-1 cells. UC: untreated cells; DMSO: Dimethyl sulfoxide; TF: Transformation Frequency.

Treatment	Plates with *foci*/plates scored	Mean no. of transformed *foci*/plate ± SE	TF ($\times 10^{-4}$)
UC	0/5	0 ± 0.0	0.00
DMSO 0.15%	1/10	0.10 ± 0.1	0.14
GW6471 0.6 *µg/mL*	1/10	0.10 ± 0.1	0.13
MCA	10/10 [a]	19.30 ± 1.69 [c]	51.06 [d]
PFOS (µg/mL)			
50	7/10 [a]	1.40 ± 0.43 [b]	1.25 [d]
75	8/10 [a]	1.40 ± 0.43 [c]	1.25 [d]
100	10/10 [a]	3.10 ± 0.53 [c]	2.77 [d]
PFOS (µg/mL) + GW6471(0.6 µg/mL)			
50	6/10	0.90 ± 0.28 [b]	2.02 [d]
75	8/10 [a]	2.10± 0.38 [c]	5.56 [d]
100	10/10 [a]	3.30± 0.60 [c]	8.73 [d]

[a] *Significantly different from control (solvent-treated plates) at the Fisher–Yates test of significance in 2 × 2 contingency tables ($p < 0.05$).*
[b] *Significantly different ($p < 0.05$) from controls (solvent-treated cells) at the Mann–Whitney unpaired U test.*
[c] *Significantly different ($p < 0.01$) from controls (solvent-treated cells) at the Mann–Whitney unpaired U test.*
[d] *Significantly different ($p < 0.01$) from controls (solvent-treated cells) at the Poisson test.*

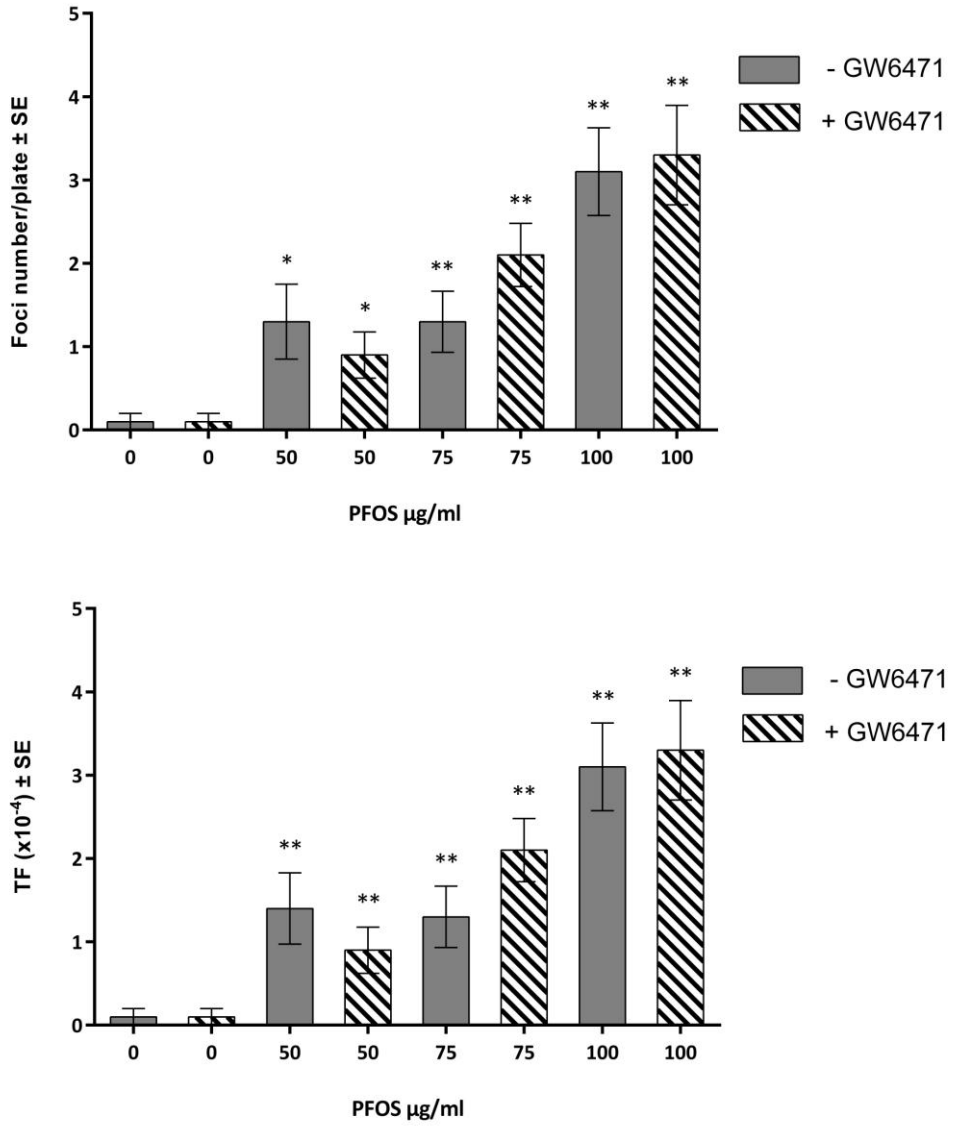

Fig. 6.6 – Effects of the treatment with PFOS without/with GW6471 on the transformation rate of BALB/c 3T3 A31-1-1 cells expressed as mean number of *foci* per plate ± SE and Transformation Frequency (TF). *p < 0.05 vs. vehicle control; ** p≤0.01 vs solvent control respectively at the Mann-Whitney unpaired U test and Poisson Test.

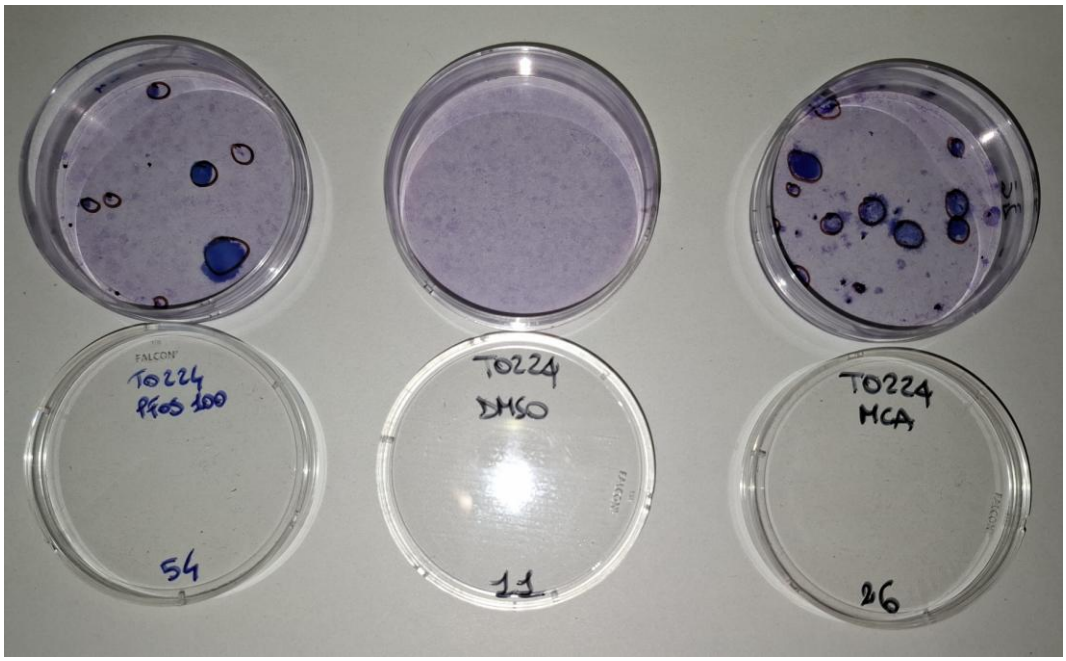

Fig. 6.7 – Three Petri dishes from the CTA experiment corresponding to three different treatment groups, respectively: PFOS, DMSO (vehicle, negative control), and MCA (positive control), from left to right. Visible foci appear blue due to Giemsa staining.

6.4 – Transcriptomic Analysis of DEHP: Transcriptional Profiling and Identification of DEGs

The analysis using Feature Extraction software led to the removal of eight arrays from the dataset because their scanning parameters failed to meet the quality control criteria of the software. As a result, the 24-hour expression profiles for DEHP concentrations of 1.97 µg/mL and 6.57 µg/mL were excluded from further analysis. The remaining array data were subsequently analyzed using the GeneSpring software. Quality assessment was performed, including filtering for signal intensity and quality, followed by normalization using the 75th percentile method.

6.4.1 – Preliminary Statistical Analysis: Limited Dataset of 8 Arrays

First, a preliminary analysis was conducted on a limited dataset comprising the DEHP 6.57 µg/mL samples from the 72-hour group and the respective control. The data were filtered based on the signal quality and intensity, resulting in the identification of 44 406 gene entities. On this list, an unpaired t-test with Benjamini-Hochberg and Bonferroni corrections was applied ($p<0.05$). The resulting list of DEGs consisted of a single modulated gene (unc-13 homolog C) that was identified in both tests.

To increase the number of DEGs and evaluate their characteristics, an additional quality filter was applied based on the CV <50%, which significantly reduced the dataset to 519 entities (Fig. 6.8). An unpaired t-test with Benjamini-Hochberg correction, followed by a t-test with Bonferroni correction, was applied to this dataset, yielding two DEGs lists consisting of 512 and 22 genes, respectively.

Reducing the number of gene entities subjected to the t-test may reduce the stringency of multiple testing corrections (Lu et al., 2011; Marczyk et al., 2013). As shown in the figure below, applying the filter led to an increase in the clustering of replicates and greater a differentiation between treatments (Fig. 6.8).

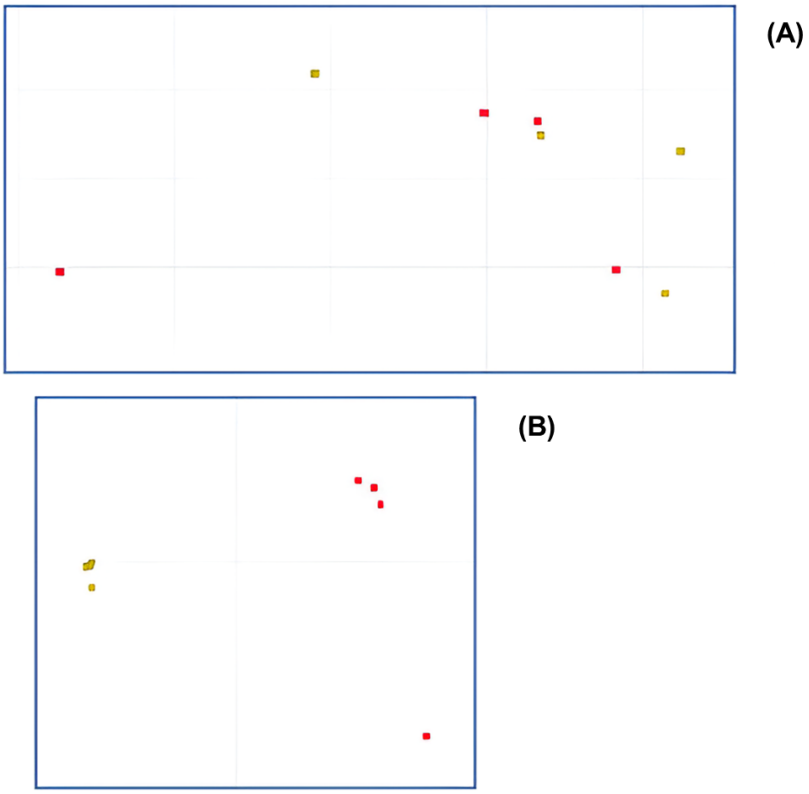

Fig. 6.8 – Comparison of two Principal Component Analyses performed in the preliminary statistical analysis on the limited dataset of 8 Arrays (Benjamini-Hochberg unpaired t-tests, 72-hour 6.57 µg/ml treatment vs. vehicle). **(A)** Cropped view of the first PCA performed on the t-test applied to the dataset analyzed with canonical analysis [X-Axis: Component 1 (34.88%); Y-Axis: Component 2 (18.03%)]; **(B)** Cropped view of the PCA performed on the t-test after filtration (CV<50%) [X-Axis: Component 1 (80.45%); Y-Axis: Component 2 (5.87%)].

6.4.2 – Statistical Analysis of the Complete Dataset

At this stage, a full statistical analysis was performed on the complete dataset, which included all the scanned array data. After filtering the dataset for signal quality (applying expression and flag filters), analysis of variance (ANOVA, $p \leq 0.05$, SNK) was performed to evaluate the differences between the various treatment conditions. The outcome of this analysis is presented as Principal omponent analysis (PCA) in Figure 6.9.

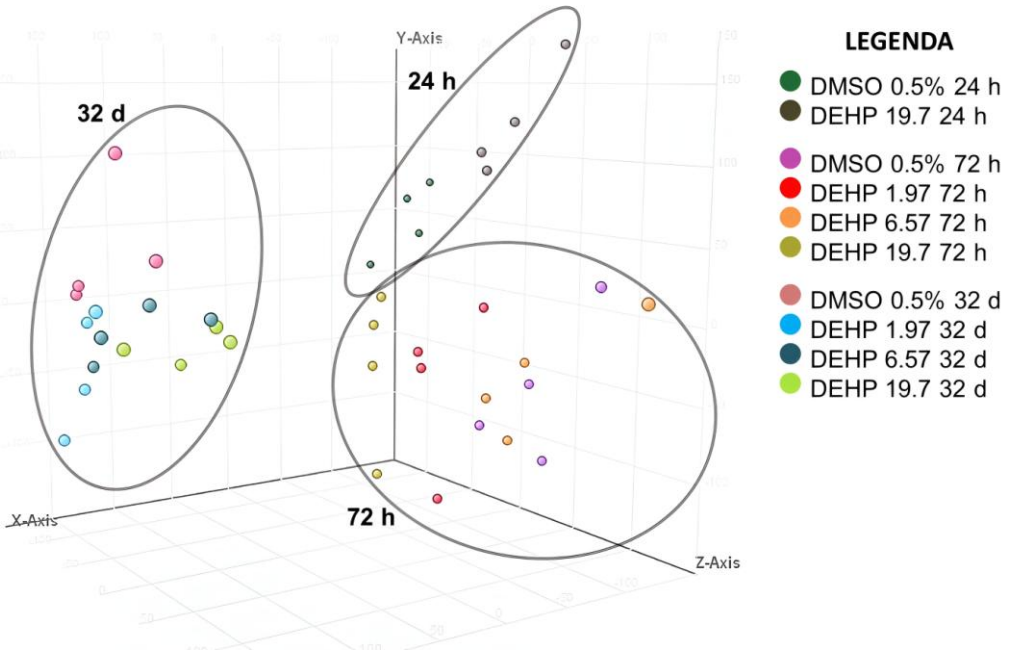

Fig. 6.9 - Principal component analysis performed on gene lists derived from One-way ANOVA, SNK cut-off = 0.05; X-Axis: Component 1 (47.44%); Y-Axis: Component 2 (11.48%); Z-Axis: Component 3 (7.26%).

In PCA, two levels of clustering are clearly identifiable: the grouping of samples based on treatment concentration and grouping based on lysis time. The distribution of samples by treatment concentration relative to the control did not appear to show a strong dose-response relationship (as indicated by the distances between the treatments and the control) (Fig 6.9).

Subsequently, additional ANOVA tests were performed for the 72-hour and 32-day groups. These represent, respectively, the group of samples where lysis occurred after 72 h of DEHP treatment, and the group of samples exposed to treatment for 72 h but subjected to lysis after 28 d of maintenance in culture (32 d post-seeding) to evaluate longer-term effects.

The results of these analyses are presented through two comparative PCAs in the image below (Fig. 6.10).

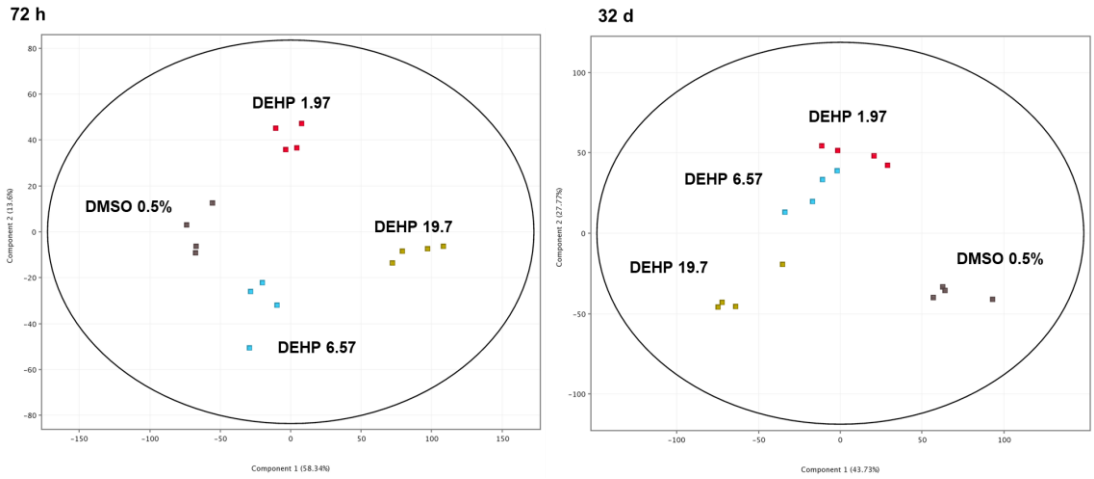

Fig. 6.10 - PCA performed on gene lists derived from a One-way ANOVA (SNK cut-off = 0.05) for two groups of samples treated for 72 hours, with lysis occurring 72 hours post-treatment and 32 d post-seeding, respectively. (72 h): X-Axis: Component 1 (58.34%); Y-Axis: Component 2 (13.6%); (32 d): X-Axis: Component 1 (43.73%); Y-Axis: Component 2 (27.77%).

Unlike the first PCA, which included all the experimental samples, these later analyses showed a clearer distinction between the samples based on the treatment concentration. Notably, the treatment groups exhibited a stronger dose-response relationship, as evident from the relative distances between them and the control. At 72 h, the two lowest concentrations were closer to the control, whereas at 32 d, the treatment groups were clearly separated from the control, with their distribution from bottom to top corresponding to decreasing treatment concentrations (Fig. 6.10).

The analysis then proceeded with multiple comparisons using unpaired t-tests with post hoc correction methods, including the Benjamini-Hochberg and Bonferroni methods. Each t-test was applied to compare

each treatment against the control within the same lysis time, with the aim of identifying statistically significant gene modulations caused by the treatments. The lists of differentially expressed genes (DEGs) obtained are shown in terms of quantity in Tables 6.5 and 6.6.

Tab. 6.5 – Lists of differentially expressed genes (DEGs) ($p \leq 0.05$) identified through t-tests with Benjamini-Hochberg correction, analyzed using GeneSpring software.

Treatment (µg/ml)	DEGs at 24 h	DEGs at 72 h	DEGs at 32 d
DEHP 1.97	/	1	212
DEHP 6.57	/	1	408
DEHP 19.7	13 164	6 523	1 597

Tab. 6.6 – Lists of differentially expressed genes (DEGs) ($p \leq 0.05$) identified through t-tests with Bonferroni correction, analyzed using GeneSpring software.

Treatment (µg/ml)	DEGs at 24 h	DEGs at 72 h	DEGs at 32 d
DEHP 1.97	/	1	3
DEHP 6.57	/	1	7
DEHP 19.7	334	41	6

From an initial examination of the number of DEGs in the lists, we derived some preliminary insights summarized as follows: First, the hypothesized dose-response relationship observed in the two PCA analyses (Fig. 6.10) is confirmed by the fact that the number of entities in each list increases with the treatment concentration. Second, the lower concentrations had a minimal effect at 72 h. Finally, unlike the lower concentrations, the effect of the highest concentration on the

transcriptome diminished as the time after treatment increased (Tab. 6.5; 6.6).

In total, 13 164 genes were modulated by the highest concentration, with 7 870 upregulated and 5 294 downregulated genes. A second unpaired t-test, corrected using the Bonferroni method, confirmed these results, as the resulting gene list was a subset of the initial one, consisting of 240 upregulated and 94 downregulated transcripts.

To further explore the differences between treatments at 72 h and identify relevant gene modulations, we adjusted the statistical approach by employing a method similar to the preliminary analysis. This involved reducing the initial gene lists by applying t-tests to a dataset filtered for CV<50%; this time, filtration was applied to the entire dataset.

However, applying the CV filter did not significantly increase the number of modulated entities for the 72-hour DEHP treatments at 1.97 and 6.57 µg/mL, with only 28 and 2 genes identified, respectively.

The consistency of the gene lists identified by both statistical approaches was further supported by MetaCore™ enrichment analyses, which did not reveal any significantly modulated pathways for low and intermediate concentrations at 72 h.

The application of the filter also resulted in a reduction of the list of DEGs modulated by the highest concentration DEHP 19.7 µg/ml.

Therefore, we proceeded with biological analysis using unfiltered transcriptional profiles (i.e., without the CV<50% filter). Nevertheless, given the high number of DEGs identified in the preliminary analysis

through the CV filter applied to the dataset limited to the 6.57 µg/mL vs. DMSO 0.5% comparison at 72 h, we opted to further analyze this list. First, we compared it with the DEGs from the 19.7 µg/mL concentration, revealing a considerable overlap in gene modulations. This comparison is illustrated in the Venn diagram below, produced using the GeneSpring software (Fig. 6.11). Based on this result, it was deemed valuable to compare the biological analyses of the 6.57 µg/mL 72-hour transcriptional profile generated in the preliminary analysis with the 19.7 µg/mL profile obtained via the canonical method.

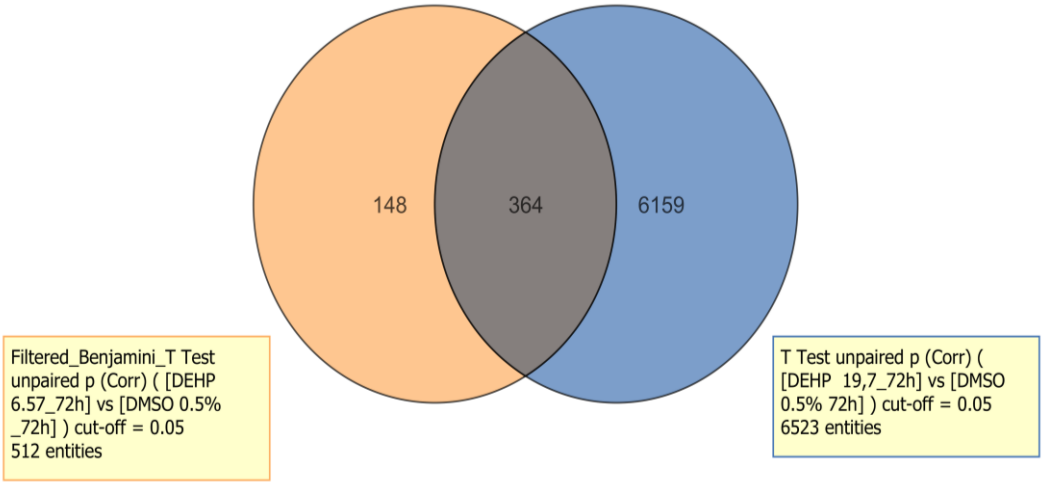

Fig. 6.11 – Venn diagram comparing gene modulations between the transcriptional profile of the 19.7 µg/mL concentration and the profile of the 6.57 µg/mL concentration, the latter obtained in the preliminary analysis with CV<50% filtering on a dataset limited to the comparison pair. Diagram generated using GeneSpring.

Finally, a comparison was made between the gene lists generated for the 19.7 µg/mL concentration across the three different cell lysis times (Fig. 6.12).

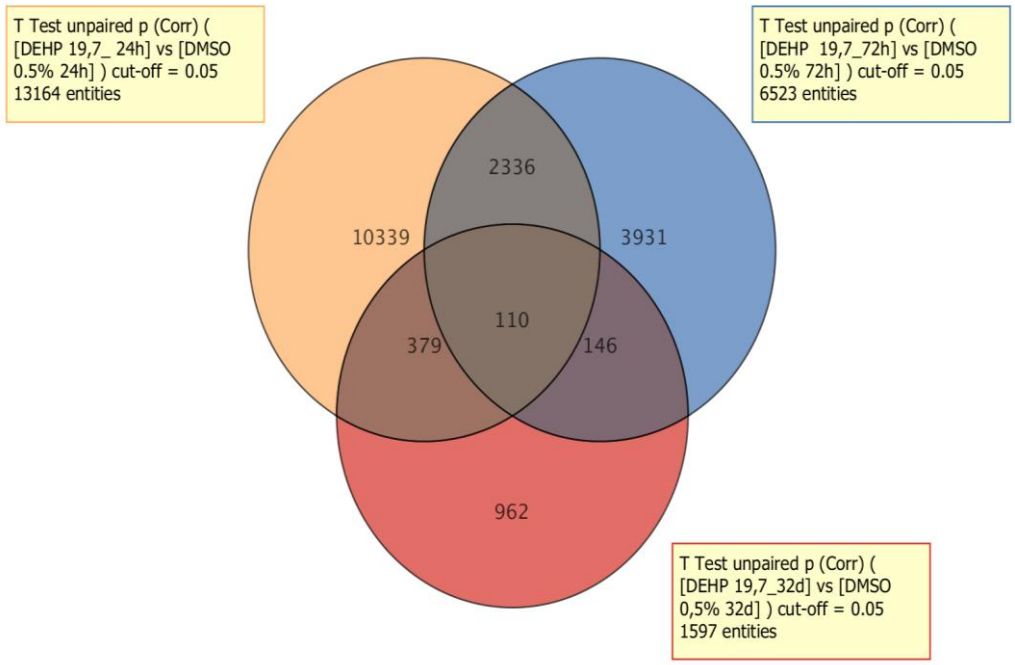

Fig. 6.12 – Venn diagram comparing gene modulations among the transcriptional profiles of the 19.7 µg/mL concentration across the three different cell lysis time points. Diagram generated using GeneSpring

6.5 – Biological interpretation: MetaCore pathway enrichment analysis of DEGs

For biological analysis, enrichment analysis was performed to identify the functional groups of modulated genes linked to disruptions in molecular pathways. This type of analysis was conducted on the DEGs lists generated by GeneSpring, using the MetaCore™ V6.34 software (GeneGo Inc., USA). Network objects (NwOs) are modulated molecular entities or theris attributes (proteins, protein complexes or groups, peptides, RNA species).

6.5.2 – Enriched molecular pathways after 24-hour treatment

Pathway enrichment analyses on DEGs at 24 h, focused exclusively on the DEHP concentration of 19.7 µg/mL. The list of DEGs obtained from the unpaired t-test with Benjamini-Hochberg correction (n=13 164 genes) was imported into the MetaCore™ suite and processed using the “Pathway Map ontology” through the Functional “Ontology Enrichment” tool. A Fold-Change (FC) threshold of ±1.5 was applied.

Enrichment analysis identified and classified 5 573 network objects and more than 200 significantly modulated pathway maps (FDR≤0.05). The top 50 pathway maps ranked by significance are listed in Table 6.7.
A complete list of pathway maps has been published and is available online (Pillo et al., 2024).

Tab. 6.7 – Statistically significant pathway maps after 24 h of treatment with DEHP at 19.7 µg/mL (FDR ≤ 0.05), obtained using the 'Analyze Single Experiment – Enrichment Analysis' function in MetaCore.

#	Pathwaymap	Modulated NwO	FDR
1	Protein folding and maturation_Amyloid precursor protein processing (schema)	25/50	7.137E-08
2	Protein folding and maturation_POMC processing	16/50	2.361E-05
3	Signal transduction_Nuclear FGFR1 signaling	30/88	2.361E-05
4	TGF-beta signaling via SMADs in breast cancer	20/47	4.825E-05
5	Signal transduction_PDGF signaling via MAPK cascades	24/65	5.180E-05
6	CHDI_Correlations from Replication data_Causal network (positive correlations)	27/79	5.180E-05

7	Signal transduction_CXCR4 signaling via MAPKs cascades	21/53	5.823E-05
8	Development_Regulation of epithelial-to-mesenchymal transition (EMT)	23/64	9.200E-05
9	Immune response_Histamine H1 receptor signaling in immune response	19/47	9.200E-05
10	Immune response_IL-17 signaling	22/60	9.200E-05
11	Development_Transcriptional regulation of megakaryopoiesis	16/35	9.200E-05
12	TGF-beta 1-mediated induction of EMT in normal and asthmatic airway epithelium	18/43	9.200E-05
13	Th2 cytokine- and TNF-alpha-induced profibrotic response in asthmatic airway fibroblasts/ myofibroblasts	20/52	9.875E-05
14	Signal transduction_Ephrin reverse signaling	14/28	9.875E-05
15	Immune response_IL-6 signaling via JAK/STAT	24/71	1.146E-04
16	Signal transduction_Thrombospondin 1 signaling	24/71	1.146E-04
17	TGF-beta signaling via kinase cascades in breast cancer	21/58	1.315E-04
18	Cytoskeleton remodeling_Regulation of actin cytoskeleton organization by the kinase effectors of Rho GTPases	21/58	1.315E-04
19	Signal transduction_WNT/Beta-catenin signaling in tissue homeostasis	17/42	1.985E-04
20	Inhibition of Ephrin receptors in colorectal cancer	14/30	1.985E-04
21	TNF-alpha and IL-1 beta-mediated regulation of contraction and secretion of inflammatory factors in normal and asthmatic airway smooth muscle	22/65	2.311E-04
22	Neurogenesis_NGF/ TrkA MAPK-mediated signaling	30/105	2.311E-04
23	Signal transduction_MIF signaling	21/61	2.625E-04
24	Macrophage-induced immunosuppression in the tumor microenvironment	28/97	3.479E-04

25	Inflammatory mechanisms of pancreatic cancerogenesis	22/67	3.479E-04
26	Beta-catenin-dependent transcription regulation in colorectal cancer	15/36	3.836E-04
27	Immune response_IL-1 signaling	25/83	4.368E-04
28	Angiogenesis in hepatocellular carcinoma (HCC)	18/50	5.050E-04
29	Role of red blood cell adhesion to endothelium in vaso-occlusion in Sickle cell anemia	15/37	5.050E-04
30	Chemotaxis_SDF-1/ CXCR4-induced chemotaxis of immune cells	24/79	5.050E-04
31	TGF-beta-induced fibroblast/ myofibroblast migration and extracellular matrix production in asthmatic airways	20/60	5.732E-04
32	Signal transduction_Relaxin family peptides signaling via RXFP1 and RXFP2 receptors	22/70	6.026E-04
33	Regulation of metabolism_GLP-1 signaling in beta cells	26/91	6.802E-04
34	Epigenetic regulation of neuronal hyperexcitability in neuropathic pain	28/102	7.191E-04
35	Development_WNT/Beta-catenin signaling in embryogenesis	16/43	7.715E-04
36	Signal transduction_S1P1 receptor signaling	31/119	7.715E-04
37	Ethanol/Acetaldehyde-dependent stimulation of MMP-9 expression in hepatocellular carcinoma (HCC)	10/19	7.932E-04
38	ErbB2-induced breast cancer cell invasion	21/67	8.320E-04
39	Immune response_IFN-alpha/beta signaling via MAPKs	22/73	1.035E-03
40	Development_Negative regulation of WNT/Beta-catenin signaling in the nucleus	25/89	1.103E-03
41	IFN-gamma and Th2 cytokines-induced inflammatory signaling in normal and asthmatic airway epithelium	15/40	1.103E-03
42	G-protein signaling_Rac1 activation	22/74	1.127E-03
43	Transcription_HIF-1 targets	26/95	1.127E-03

44	E-cadherin signaling and its regulation in gastric cancer	14/36	1.127E-03
45	WNT signaling in gastric cancer	14/36	1.127E-03
46	Development_Positive regulation of WNT/Beta-catenin signaling at the receptor level	20/64	1.127E-03
47	Development_NOTCH/ TGF-beta crosstalk in EMT	16/45	1.135E-03
48	Signal transduction_Nitric oxide synthesis	25/90	1.144E-03
49	Development_Role of Ceramide 1-phosphate, Sphingosine 1-phosphate and Complement cascade in hematopoietic stem cell homing	13/32	1.144E-03
50	Hedgehog signaling in breast cancer	11/24	1.144E-03

Given the large number of modulated pathway maps, we decided to proceed with a critical analysis of the modulations using two approaches: one based solely on modulations and statistical significance, and the other based on the specific functions of the pathway maps, applying category filters available in MetaCore. These filters allowed the selection of pathway groups based on four biological functions: metabolic maps, regulatory maps, toxicity processes, and maps related to pathological processes. It should be noted that the subsequent discussion also considered pathway maps not listed in Table 6.7, as they were identified and integrated into the analysis using the category filter. Specifically, Figure 6.13 lists the pathway maps belonging to the "Toxicity Processes" category.

Figure 6.14 shows the distribution of modulated pathway maps across the four MetaCore categories: regulatory pathways were the most perturbed by the treatment, followed by pathways related to pathological

processes and those associated with toxicological outcomes. It is important to note that this result is closely tied to the types of pathway maps available in MetaCore and should be regarded primarily as a general guideline (Fig. 6.14).

The modulation of the "*Aryl hydrocarbon receptor signaling pathway*" (Pathway map #103) (FDR 4.720e-3) is particularly noteworthy, as it represents the third most significant pathway within the "Toxicity Processes" category (Fig. 6.13).

Although the filter did not highlight modulated pathway maps in the metabolic map category, the enrichment analysis identified modulated pathways and genes related to DEHP metabolism, tissue-specific pathways involved in systemic metabolism and neurophysiological balance, as well as basic cellular signaling pathways with potential pleiotropic effects.

Among the latter, NOTCH, WNT, and TGF-β signaling pathways are particularly notable. Additionally, modulation of numerous pathway maps associated with inflammatory processes and immune responses was observed, as well as signaling pathways involved in cell cycle regulation (proliferation/apoptosis).

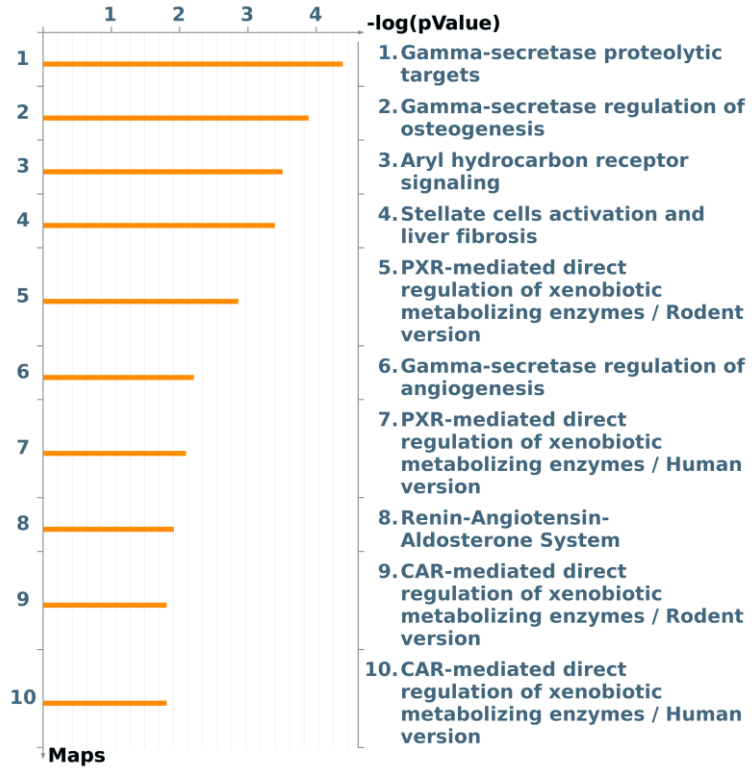

Fig. 6.13 – Pathways Maps derived from the “Toxic Process” filtertering function

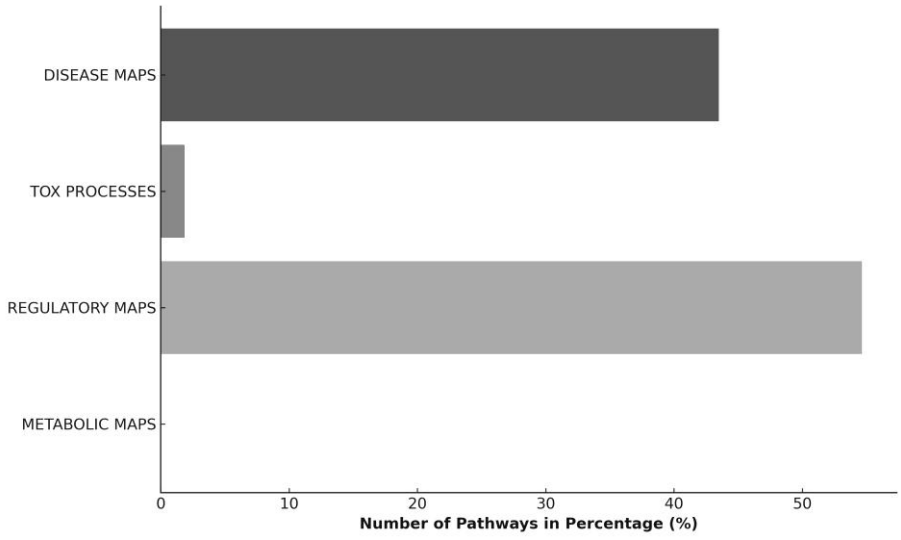

Fig. 6.14 – This figure shows the percentage distribution of MetaCore pathway maps across different categories, using the "Filter Pathway Maps by Category" function in MetaCore. Each pathway map may belong to more than one category. Only pathway maps with FDR≤0.05 were included.

6.5.1.1 Three most significantly enriched pathway maps and key genes related to neuro-endocrine disruption

The most significantly modulated pathway after 24 h of treatment is the "*Protein folding and maturation_Amyloid precursor protein processing (schema)*" (Pathway map #1) (FDR 7.303e-8; 25 modulated network objects out of 50) (Tab. 6.7). Specifically, this pathway map was characterized by the modulation of three transcripts: amyloid precursor protein (APP, FC 1.81), beta secretase 2 (BACE2, FC 1.58), and matrix metalloproteinase 9 (MMP9, FC -3.14).

APP is a type 1 membrane glycoprotein that plays critical roles in neural transmission, neuronal homeostasis, and development.

The second most significant pathway map involved the proteolytic modification and maturation of a specific peptide: "*Protein folding and maturation_POMC*" (Pathway map #2) (FDR 2.518e-5). Pro-opiomelanocortin (POMC) is a prohormone involved in the regulation of the leptin-melanocortin signaling pathway in response to leptin and insulin.

This finding is further supported by the significant modulation of the "*POMC, alpha-MSH, and AGRP in the regulation of food intake and energy expenditure in obesity in the hypothalamus*" pathway (Pathway map #149, FDR 1.118e-2; 13 modulated network objects out of 43) (Tab. 6.7). In this pathway, overexpression of melanocortin receptor 4 (MCR-4, FC 1.69) and agouti-related neuropeptide (AGRP, FC 1.67), which act as antagonists of melanocortin receptor signaling, was observed, along with the downregulation of brain-derived neurotrophic factor (BDNF, FC -1.62).

It is important to note that despite the high statistical significance, the modulation of these two pathways is supported by only a few modulated transcripts owing to the small number of genes involved.

The third most significant pathway is "*Signal transduction_Nuclear FGFR1 signaling*" (Pathway map #3; FDR 2.418e-5) (Tab. 6.7). The fibroblast growth factor (FGF) signaling pathway through tyrosine kinase receptors (FGFR) regulates many cellular processes and plays essential roles in early embryonic development. Unlike the first two pathway maps, this map consisted of 88 genes, 30 of which were modulated by treatment with 19.7 µg/mL DEHP.

Although a slight upregulation was observed upstream of FGFR1 (FC 1.5), the overall modulation of this pathway appeared to be inhibitory due to the downregulation of several downstream target genes, while various FGF inhibition targets were upregulated. Modulation of this pathway may indicate alterations in the cell cycle in DEHP-treated cells. A study conducted on the BALB/c 3T3 cell line identified two groups of growth factors capable of stimulating DNA synthesis and making cells "competent" to enter the S phase: i) the group associated with platelet-derived growth factor (PDGF) and ii) the group associated with fibroblast growth factor (FGF). Competent cells respond to other growth factors, including epidermal growth factor (EGF) and insulin-like growth factor-1 (IGF-1), which drive cell cycle progression (Jones and Kazlauskas, 2001).

In our dataset, several FGF-related transcripts were upregulated, including EGF [FC 1.59 for Egf (A_55_P2733187) and FC 1.64 for Egf

(A_55_P2822952)]. In contrast, several PDGF-related transcripts were downregulated, including PDGFB [FC -2.43 for Pdgfb (A_55_P2047310) and FC -2.32 for Pdgfb (A_55_P2733467)] and the receptor subunit PDGFR (PDGF-Rα) [FC -2.00 for Pdgfra (A_51_P345649), FC -1.71 for Pdgfra (A_55_P2734892), and FC -2.03 for Pdgfra (A_55_P2735715)]. Similarly, transcripts related to insulin, insulin receptor substrate-1 (ISR-1), and insulin-like growth factor 1 receptor (IGF-1 Receptor) were downregulated [FC -2.21 for Isr-1 and FC -1.69 for Igf1r (A_52_P668647) and FC -1.72 for Igf1r (A_55_P2804885)].

In the context of modulations with potential endocrine regulatory effects, the modulation of the "*Aryl hydrocarbon receptor signaling pathway*" (Pathway map # 103) (FDR 4.720e-3) is notable, with 19 modulated transcripts out of 53, including estrogen receptor 1 (ESR1) (also present in pathways # 70,103, 113, 167, FDR ≤0.05) (Tab. 6.7).

Other modulations of interest included the transcript for gonadotropin-releasing hormone (GnRH) (Pathway map # 65, FDR 1.879e-3) and the slight upregulation of the transcript NR4A3 (nuclear receptor subfamily 4 group A member 3; FC 1.59), which was strongly downregulated in the 32-day transcriptional profiles. NR4A3 is associated with many tissue-specific functions, including the regulation of cell proliferation, metabolism, differentiation, apoptosis, carbohydrate and lipid metabolism and energy homeostasis in muscle cells (Zhang et al., 2020).

Finally, noteworthy modulations include the transcripts for the SH3 domain and tetratricopeptide repeats 2 (SH3TC2, FC 6.17), calcium-

dependent potassium channel KCNMA1 (FC 17.61), and SCO-spondin (FC 21.34), which encode proteins specific to neural tissue.

6.5.1.2 Enriched Pathway maps and key genes related to inflammation and oxidative stress

Continuing the analysis of the significantly modulated pathway maps, several signaling pathways related to cytokine production, inflammation, and immune responses were identified. These pathways included "*Immune response_Histamine H1 receptor signaling in immune response*" (pathway #9) (FDR 9.344e-5), "*Immune response_IL-17 signaling*" (pathway #10) (FDR 9.344e-5), and "*Immune response_IL-6 signaling via JAK/STAT*" (pathway #15) (FDR 1.168e-4) (Tab. 6.7). Additionally, pathways such as "*Th2 cytokine- and TNF-alpha-induced profibrotic response in asthmatic airway fibroblasts/myofibroblasts*" (pathway #13) (FDR 1.000e-4) and "*TNF-alpha and IL-1 beta-mediated regulation of contraction and secretion of inflammatory factors in normal and asthmatic airway smooth muscle*" (pathway # 21) (FDR 2.361e-4) were altered (Tab. 6.7).

Within these pathways, various cytokine signaling factors, including IL-21, IL-17, IL-17R, IL6R, IFN-α, and IL8RA, were found to be upregulated. Notably, the pro-inflammatory transcription factor NFAT [Nfatc4 (A_55_P2745072) FC 1.91] was also overexpressed. These modulations could be linked to the activation of the IP3 receptor signaling pathway in the mitochondria, supported by the upregulation of its corresponding transcript. Additionally, in the 24-hour expression profile,

the transcription factor Nuclear factor erythroid 2-related factor 2 (NRF2) and heme oxygenase were upregulated, indicating an antioxidant response.

Other transcripts related to inflammatory processes, such as IL13Ra (FC 1.66) and TLR4 (FC 3.12) were also modulated. However, at the same time, some important factors in pro-inflammatory signaling pathways showed downregulation or discordant signaling. These included NF-kB (FC -1.65), COX-2 (FC -2.68), CCL20 (FC -3.43), VCAM [FC -2.41 for Vcam1 (A_51_P210956) and -1.91 for Vcam1 (A_52_P520495)], IGF-1 receptor, MMP-2 (FC -1.55), and the previously mentioned MMP-9.

Despite the upregulation of the IL6R (interleukin-6 receptor), several downstream factors in this signaling pathway were downregulated. IL-6 activation can induce STAT3 and activator protein 1 [AP-1, a complex of different subunits: FOS (FC -1.51), FOSL2 (FC -2.31), JUN (FC -1.79) e JUNB (FC -1.56)], RUNX2, IL1RAP, c-JUN, and c-FOS, all of which are associated with inflammation and immune responses. On the other hand, IL-6 can also promote the activation of Mucin 4 and the angiogenic factor VEGF-A, both of which were upregulated (FC 2.43 and 1.61, respectively).

Finally, several gene markers associated with cellular stress and DNA damage were modulated, including activating transcription factor 3 (ATF3, FC 6.12), growth arrest and DNA-damage-inducible 45 alpha (GADD45α, FC 6.00), NALP1B (FC 6.72), Serpinb1b (FC 8.57), and nicotinamide N-methyltransferase (NNMT, FC 6.56). The latter may play a role in epigenetic modifications and hypomethylation effects and has also

been implicated in the regulation of hepatic gluconeogenesis, cholesterol biosynthesis, and xenobiotic detoxification (Liang et al., 2023).

6.5.1.3 Enriched Pathway maps and key genes related to apoptosis and proliferation

Using the pathway filter option and focusing on regulatory pathways related to apoptosis and survival, the modulation of the pathway map "*Signal transduction_WNT/β-catenin signaling in tissue homeostasis*" (pathway #42) (FDR 2.010e-4; 17 modulated network objects out of 42) was identified (Tab. 6.7). Several other significantly modulated pathways further support the modulation of the WNT pathway. In the 24-hour dataset, various WNT ligands and receptors were found to be regulated: FC 1.60 for Wnt3a (A_51_P210970), FC −2.46 for Wnt5b (A_55_P1984976), FC −1.54 for Wnt7b (A_52_P231691), and FC 2.39 for Wnt9a (A_55_P2032147). WNT ligands bind to Frizzled receptors [FC 2.25 for Fzd4 (A_51_P361220) and FC 2.38 for Fzd4 (A_66_P132734)], which activate signaling via β-catenin and SNAIL1 (FC −1.75). After translocation into the nucleus, β-catenin regulates the expression of several genes, including LEF-1 (FC 2.54), TCF7 (FC 1.58), and TCF7L2 (FC −1.60).

Additionally, modulation of pathway maps related to TGF-β signaling (pathways # 4, 8, 12, 17, 31 and 47) was observed, suggesting a possible inhibition of TGF-β signalling (Tab. 6.7). Several transcripts associated with proteins involved in extracellular matrix reorganization

were downregulated, such as MMP-2 (FC −1.55), MMP-9 (FC −3.14), Stromelysin-1 (FC −9.44), and MMP-13 (FC −5.34).

The "*Signal transduction_PDGF signaling via MAPK cascades*" pathway map (pathway #5) (FDR 5.293e-5) (Tab. 6.7) is hypothesized to be inhibited due to the downregulation of upstream factors PDGFβ (FC −2.43) and PDGFRα (FC −2.03), along with modulation of HAS2 synthase (FC −3.44) and HAS1 (FC 1.58).

Moreover, downregulation was noted in the Ephrin signaling pathway, with the EphrinB4 receptor (FC −1.80) and Ephrin-B ligands downregulated [Efnb1 (FC −1.76); Efnb2 (FC −2.78); and Efnb3 (FC −1.74)] (pathways # 6, 14, 20, 28, 54 and 104). The modulation of the pathway "*Cytoskeleton remodeling and regulation of actin cytoskeleton organization by the kinase effectors of Rho GTPases*" (pathway #18) (FDR 1.337e-4) is linked to these downregulations (Tab. 6.7).

Finally, the modulation of several transcripts related to tumor suppression and activation of apoptotic processes was noted, including N-myc downstream regulated gene 4 (FC 1.58), N-myc downstream regulated gene 1 (FC 8.05), HIV-1 Tat interactive protein 2 (FC 14.47), mitochondrial tumor suppressor 1 (MTUS1, FC 2.93), serine (or cysteine) peptidase inhibitor, clade B, member 9h (SERPINB9, FC 21.44), GADD45 (FC 6), and tumor protein p73 (TP73, FC 3.66).

These data indicate an influence on cell cycle regulation, survival processes, and proliferation; however the overall modulations are difficult

to interpret, making it challenging to clearly define the direction of these stimuli.

6.5.1.4 Enriched Pathway maps and key genes related to xenobiotic metabolization and cell metabolism

Among the significantly modulated pathway maps identified through the application of the *regulatory pathway maps/metabolic pathways* filter, the following were highlighted: 1) "*Signal transduction_WNT/β-catenin signaling in tissue homeostasis*" (pathway # 19) (FDR 2.010e-4; 17 modulated network objects out of 42); 2) "*Regulation of metabolism of GLP-1 signaling in beta cells*" (pathway # 34) (FDR 6.727e-4; 26 modulated network objects out of 91); and 3) "*Regulation of metabolism: glucocorticoid receptor signaling in glucose and lipid metabolism*" (FDR 5.027e-2; 17 modulated network objects out of 80).

Figure 6.13 was generated using the *filter by Map Categories: Tox processes* function to display the top ten pathway maps, ranked by significance, related to toxicity processes that may be induced by DEHP treatment in the BALB/c 3T3 A31-1-1 cell model. The first three pathways on the list are all related to the gamma-secretase complex, where modulation of NOTCH1 (FC 1.59), APP (FC 1.88), and presenilin (FC 1.99) was observed.

Next on the list are signaling pathways related to xenobiotic metabolism: the "*Aryl hydrocarbon receptor signalling"* (pathway # 103) (FDR 4.720e-3) and "*PXR signaling (Rodent/human version)"* (pathway

#172) (FDR 1.291e-2) (Figure 6.13). In the latter, the transcription factor HNF4α (FC 1.61) was upregulated.

The PXR and CAR signaling pathways regulate several genes encoding phase I and II enzymes and transporters involved in xenobiotic detoxification and elimination. Notably, the CAR pathway map was not significantly modulated with an FDR of 6.229e-2 (Figure 6.13).

Additionally, in the 24-hour enrichment analysis of the 19.7 µg/mL DEHP concentration, several enzymes involved in fatty acid metabolism and β-oxidation were found to be modulated, likely activated by PPARα. These included EHHADH (FC 1.59), ACLS1 (FC 1.58), ACAA1 [Acaa1a (A_52_P155990) FC 1.94 and Acaa1a (A_55_P2076580) FC 1.74], ACOX1 (FC 1.51), ACOX2 (FC 7.38), ACOX3 (FC 1.81), and CPT-1A (FC 2) (Tab. 6.10).

6.5.2 – Enriched molecular pathways after 72-hour treatments: amplification of the initial inflammatory response

As previously indicated in the results of the statistical analysis using GeneSpring, the 72-hour treatments with DEHP at 1.97 µg/mL and 6.57 µg/mL did not result in significant gene regulation compared to the control, with the exception of a single entity in both treatment groups (Tab. 6.5, 6.6, and 6.8).

Tab. 6.8 – Gene modulations after 72 h of treatment with DEHP 1.97 µg/mL and 6.57 µg/mL; unpaired t-test with Benjamini-Hochberg correction, p<0.05.

72 h-treatment (µg/ml)	Gene	p Value	FC	Biologic Function
1.97	UPF3 regulator of nonsense transcripts homolog B (yeast)	0.01	3.32	unfolded protein response
6.57	unc-13 homolog C	0.03	1.71	glutamatergic neuron-specific gene

It should be noted that the only gene modulated at 72 h at the 6.57 µg/mL concentration, unc-13 homolog C, was also confirmed to be modulated in the preliminary analysis, even without the application of the CV-related quality filter.

In contrast, the unpaired t-test with Benjamini-Hochberg correction for the 72-hour treatment with DEHP 19.7 µg/mL resulted in a substantial list of DEGs, with 6 523 entities, of which 3 520 were downregulated and 3 003 upregulated compared to the control. From this list, only transcripts with FC≥ 1.5 were considered for the Enrichment Analysis in MetaCore. The software identified and recognized 3 052 Network objects, whose modulation was associated with over 50 significantly modulated pathway maps (Tab. 6.9).

As can be observed, many of the modulated pathway maps are attributed to biological processes such as apoptosis, oxidative stress, and immune response. Additionally, after 72 h, many genes associated with the AhR pathway (pathway # 29), including CYP1A1, CYP1B1, and some UDP-glucuronosyltransferase (UGTs) such as UGT1A1, remained upregulated (Tab. 6.10).

Tab. 6.9 – Statistically significant Pathway Maps after 72 h of treatment with DEHP 19.7 µg/mL (FDR≤0.05), obtained using the 'Analyze Single Experiment – Enrichment Analysis' function in MetaCore.

#	Pathwaymap	Modulated NwO	FDR
1	Apoptosis and survival_Granzyme A signaling	18/41	3.953E-07
2	Oxidative stress_ROS signaling	30/108	3.953E-07
3	Immune response_IL-6 signaling via JAK/STAT	21/71	3.119E-05
4	Signal transduction_RANKL-dependent osteoclast differentiation	21/81	2.730E-04
5	DNA damage_ATM/ATR regulation of G2/M checkpoint: cytoplasmic signaling	16/51	2.877E-04
6	Signal transduction_Calcium-mediated signaling	19/72	4.564E-04
7	Signal transduction_mTORC1 downstream signaling	17/60	4.664E-04
8	Immune response_IL-6 signaling via MEK/ERK and PI3K/AKT cascades	19/74	4.760E-04
9	G-protein signaling_Rac1 activation	19/74	4.760E-04
10	Eosinophil adhesion and transendothelial migration in asthma	18/68	4.855E-04
11	DNA damage_ATM/ATR regulation of G1/S checkpoint	14/44	5.168E-04
12	Signal transduction_Angiotensin II/AGTR1 signaling via Notch, Beta-catenin and NF-kB pathways	19/78	8.275E-04
13	Ovarian cancer (main signaling cascades)	17/65	8.323E-04
14	Immune response_HMGB1/RAGE signaling	15/53	9.329E-04
15	DNA damage_p53 activation by DNA damage	17/68	1.307E-03
16	IL-6 signaling in colorectal cancer	12/37	1.307E-03

17	Development_Positive regulation of WNT/Beta-catenin signaling in the nucleus	17/69	1.307E-03
18	Development_Positive regulation of WNT/Beta-catenin signaling in the cytoplasm	18/76	1.307E-03
19	Development_YAP/TAZ-mediated co-regulation of transcription	15/56	1.307E-03
20	Interleukins-induced inflammatory signaling in normal and asthmatic airway epithelium	11/32	1.307E-03
21	Proteases and EGFR-activated mucin production in airway epithelium in COPD	14/50	1.307E-03
22	Vascular endothelial cell damage in SLE	16/63	1.307E-03
23	Apoptosis and survival_p53 and p73-dependent apoptosis	19/84	1.307E-03
24	Mechanisms of drug resistance in small cell lung cancer (SCLC)	17/70	1.307E-03
25	DNA damage_ATM activation by DNA damage	17/71	1.531E-03
26	Development_NOTCH1 signaling in the epidermis	16/65	1.753E-03
27	Role of alpha-V/ beta-6 integrin in colorectal cancer	9/23	1.803E-03
28	IL-6 signaling in tumor-associated monocytes/macrophages in breast cancer	7/14	2.016E-03
29	Aryl hydrocarbon receptor signaling	14/53	2.031E-03
30	EGFR signaling pathway in lung cancer	14/53	2.031E-03
31	Inflammatory mechanisms of pancreatic cancerogenesis	16/67	2.154E-03
32	Interleukins-induced inflammatory response in asthmatic airway fibroblasts	11/35	2.154E-03
33	Development_Muscle progenitor cell migration in hypaxial myogenesis	12/41	2.154E-03
34	Development_Negative regulation of WNT/Beta-catenin signaling in the nucleus	19/89	2.154E-03
35	Signal transduction_Mu-type opioid receptor signaling in non-neuronal cells	15/61	2.322E-03

36	GTP-XTP metabolism	19/90	2.392E-03
37	Signal transduction_Relaxin family peptides signaling via RXFP3 and RXFP4 receptors	12/42	2.440E-03
38	Development_Beta adrenergic receptors in brown adipocyte differentiation	11/36	2.440E-03
39	PGE2 pathways in cancer	14/55	2.440E-03
40	Immune response _CCR3 signaling in eosinophils	17/77	2.893E-03
41	Immune response_Plasmin signaling	16/70	2.917E-03
42	NETosis in SLE	10/31	2.917E-03
43	Immune response_Oncostatin M signaling via MAPK	11/37	2.928E-03
44	Development_Thromboxane A2 signaling	13/50	3.033E-03
45	TGF-beta 1-induced transactivation of membrane receptors signaling in hepatocellular carcinoma (HCC)	13/50	3.033E-03
46	Development_Regulation of epithelial-to-mesenchymal transition (EMT)	15/64	3.197E-03
47	Development_Role of Ceramide 1-phosphate, Sphingosine 1-phosphate and Complement cascade in hematopoietic stem cell homing	10/32	3.351E-03
48	Role of IL-6 in obesity and type 2 diabetes in adipocytes	10/32	3.351E-03
49	TNF-alpha and IL-1 beta-mediated regulation of contraction and secretion of inflammatory factors in normal and asthmatic airway smooth muscle	15/65	3.351E-03
50	Signal transduction_PDGF signaling via MAPK cascades	15/65	3.351E-03

Signals indicative of PPARγ activation are also observed. In general, signals related to PPARα activation and other metabolic pathways showed a decrease, particularly in enzymatic activities (Tab. 6.10 and 6.12).

Analysis of specific modulations of interest revealed that the transcriptional response at 72 h showed an amplification of inflammatory signaling, with the upregulation of transcripts such as COX-1 and COX-2, cFOS, and other transcripts linked to the AP-1 complex [Fos (A_55_P2910184) FC 3.01; Fosl1 (A_51_P308796) FC 2.28; Junb (A_51_P159194) FC 2.47, and Junb (A_55_P2011106) FC 2.63], unlike what was observed at 24 h.

These modulations may also be associated with an increase in apoptotic signaling, as supported by other previously noted modulations and the numerous related pathway maps (pathways # 1, 5, 11, 15, 23 and 25). Additionally, activation of the innate immune response mediated by IL-17 and IL-6 (pathways #3, 8, 17, 21, 29 and 50) was observed (Tab. 6.9).

In the transcriptional profile of the 72-hour treatment with DEHP 19.7 µg/mL, downregulation of transcripts linked to lipid biosynthesis processes, including Acetyl-CoA carboxylase 1 (ACACA; FC -1.81), Stearoyl-CoA desaturase [Scd1 (A_52_P682382) FC -1.85 and Scd1 (A_55_P2099594) FC -1.55] and Fatty acid synthase (FASN; FC -1.61), is noted (Tab. 6.12).

Interestingly, some of these regulations were also detected in the enrichment analysis performed as part of the preliminary analysis for the 6.57 µg/mL treatment profile (reviced dataset) (Tab. 6.13 and 6.14). This is further supported by Figure 6.10, which shows that over 75% of the DEGs from the preliminary analysis of the effects of DEHP 6.57 µg/mL were

shared with the canonical analysis of the higher treatment concentration of 19.7 µg/mL.

In this context, it is also noted that the higher concentration treatment induced a more intense inflammatory response in terms of both gene number and FC values, highlighting a dose-response relationship. Among these, the upregulation of transcripts IL-6 (FC 5.37), IL-6R (FC 1.66 and 1.94 for the two concentrations, respectively), IL6st (FC 2.54), COX-2 (FC 2.16) (pathways #3 and 8), components of the NF-kB complex [Rel (A_55_P2723629) FC 1.62], and the membrane receptor TLR4 (FC 3.3; pathway # 1) (Tab. 6.9) is particularly noteworthy.

Additionally, the strong upregulation of the transcript of TXNIP [Txnip (A_55_P2006255) FC 5.09; Txnip (A_66_P131361) FC 4.77], associated with the amplification of inflammatory signals through inflammasome activation, is highlighted.

Compared to the 24-hour data, the upregulation of the transcription factor NRF2 was confirmed at both concentrations at 72 h, with FC values of 3.37 for the higher concentration and 2.09 for the intermediate concentration, confirming the activation of oxidative stress response signals.

The modulation of several transcripts linked to fatty acid β-oxidation persisted at 72 h (Tab. 6.12 and 6.14). Additionally, the modulation of ANGPTL4 (FC 1.73 and 2), PPARγ (FC 1.72 and 2.99), and CPT1A (FC 1.34 and 1.83) is noted for both the 6.57 µg/mL and 19.7 µg/mL concentrations.

The downregulation of other transcripts related to fatty acid synthesis, such as acetyl-CoA carboxylase 1, is also highlighted.

In addition to these shared modulations, the exclusive modulation of the 19.7 µg/mL concentration profile included the upregulation of FABP4 (FC 1.89), which is also linked to fatty acid beta-oxidation, and LPL (FC 1.55), which encodes a key lipase in the metabolism of triglyceride-rich lipoproteins, as well as the downregulation of Fatty acid synthase (FASN FC -1.61) and Acyl-CoA desaturase (SCD FC -1.85) (Tab. 6.15).

Moreover the upregulation of the transcript related to Apolipoprotein E Protein [Apoe (A_55_P2736230) FC 1.71] further confirmed its effect on lipoprotein metabolism.

The upregulation of EGF, described at 24 h, was also confirmed at 72 h for both 19.7 µg/mL and 6.57 µg/mL concentrations.

The AhR receptor pathway was also modulated at 72 h, with greater modulation at higher concentrations. Within this pathway, the common modulation of CYP1A1 (FC 1.89 and 6.91) and UGT1A6 (FC 1.54 and 2.27) was noted, along with the following exclusive modulations at higher concentrations: CYP1B1 (FC 2.34), c-FOS (FC 3.01), related to immune and inflammatory responses, and the upregulation of the tumor suppressor gene BRCA1 (FC 2.11).

In the intermediate concentration profile, downregulation of the transcript linked to angiotensin AGT (FC -1.94), was also observed, which may be related to the regulation of the inflammatory response.

Based on these results, the intermediate concentration had a lesser effect on inflammatory response.

As for the lowest concentration profile of 1.97 µg/mL, even after applying the filter, only five genes with FC≥1.5 were identified in MetaCore, and no modulated pathways were linked to the observed gene regulations.

Tab. 6.10 – Modulated xenobiotic metabolism and cellular metabolic genes (enzymes) after 24 and 72 h of treatment (DEHP 19.7 µg/ml).

GENE NAME	GENE SYMBOL	24 h	72 h
Glutathione S-transferase, alpha 2 (Yc2)	Gsta2	up	
Glutathione S-transferase, alpha 3	Gsta3	up	
Glutathione S-transferase, alpha 4	Gsta4	up	
Glutathione S-transferase, mu 3	Gstm3		down
Glutathione S-transferase, mu 7	Gstm7	up	
Glutathione S-transferase kappa 1	Gstk1	down	down
Glutathione S-transferase omega 2	Gsto2	up	up
Glutathione S-transferase pi 3	Gstp3	up	
Glutathione S-transferase, theta 1	Gstt1	down	
Glutathione S-transferase, theta 2	Gstt2	down	
Glutathione S-transferase, theta 4	Gstt4	down	
Glutathione transferase zeta 1	Gstz1	up	down
Glutathione peroxidase 8 (putative)	Gpx8	down	
Microsomal glutathione S-transferase 1	Mgst1	up	
Microsomal glutathione S-transferase 2	Mgst2		down
UDP glucuronosyltransferase 1 Family, polypeptide A1	Ugt1a1	up	
UDP glucuronosyltransferase 1 Family, polypeptide A6A	Ugt1a6a	up	
UDP glucuronosyltransferase 1 Family, polypeptide A6B	Ugt1a6b	up	up
UDP glucuronosyltransferase 1 Family, polypeptide A8	Ugt1a8	up	
UDP glucuronosyltransferase 2 Family, polypeptide A1	Ugt2a1	down	
UDP glucuronosyltransferase 2 Family, polypeptide B1	Ugt2b1	up	
Aldehyde dehydrogenase Family 3, Subfamily A2	Aldh3a2	up	

Aldehyde dehydrogenase 16 Family, Member A1	Aldh16a1	up	
Aldehyde dehydrogenase Family 1, Subfamily A7	Aldh1a7	up	
Aldehyde dehydrogenase Family 6, Subfamily A1	Aldh6a1	up	
Aldehyde dehydrogenase 1 Family, Member L2	Aldh1l2	up	
Aldehyde dehydrogenase 1 Family, Member B1	Aldh1b1	up	
Aldehyde dehydrogenase 2, Mitochondrial	Aldh2		up
Aldehyde dehydrogenase 18 Family, Member A1	Aldh18a1		down
Aldehyde dehydrogenase 1 Family, Member L1	Aldh1l1		down
Alcohol dehydrogenase 1 (class I)	Adh1	up	up
Alcohol dehydrogenase, iron containing, 1	Adhfe1	up	up
Alcohol dehydrogenase 7 (class IV), mu or sigma polypeptide	Adh7	up	
Alcohol dehydrogenase 5 (class III), chi polypeptide	Adh5	up	down
Lipase, Family Member N	Lipn	up	
Diacylglycerol lipase, beta	Daglb	down	
Lipase, Member I	Lipi	up	
Lipase, Family Member M	Lipm	up	
pancreatic lipase	Pnlip	up	
Lipase, hormone sensitive	Lipe	up	
Lipase, Member O1	Lipo1	up	
Lipoprotein lipase	Lpl		up
Carnitine palmitoyltransferase 1a, liver	Cpt1a	up	up
Cytochrome P450 Family 1 Subfamily B Member 1	Cyp1b1		up
Cytochrome P450 Family 1 Subfamily A Member 1	Cyp1a1	up	up
Cytochrome P450 Family 11 Subfamily A Member 1	Cyp11a1	up	
Cytochrome P450 Family 27 Subfamily A Member 1	Cyp27a1	up	
Cytochrome P450 Family 2 Subfamily C Member 19	Cyp2c19	up	
Cytochrome P450 Family 2 Subfamily C Member 8	Cyp2c8	up	
Cytochrome P450 Family 2 Subfamily C Member 9	Cyp2c9	up	
Cytochrome P450 Family 3 Subfamily A Member 5	Cyp3a5	up	
Cytochrome P450 Family 3 Subfamily A Member 7	Cyp3a7	up	
Elongation of very long chain fatty acids protein 6	Elovl6	down	
Multidrug resistance protein 1 Protein	Mdr1	up	
Solute carrier organic anion transporter Family Member 1A5 Protein	Slc21a7	down	

Tab- 6.11 – Modulated gap junctions transcripts after 24 h and 72 h of treatment (DEHP 19.7 µg/ml)

GENE NAME	GENE SYMBOL	24 h	72 h
Gap junction protein, alpha 1	Gja1	down	up
Gap junction protein, beta 3	Gjb3	down	up
Gap junction protein, beta 5	Gjb5	down	up
Gap junction protein, beta 4	Gjb4	down	up
Gap junction protein, gamma 1	Gjc1	down	
Gap junction protein, epsilon 1	Gje1	up	

6.5.3 – Enriched Pathway maps and key genes related to PPARα

Although the MetaCore pathway map "*Regulation of lipid metabolism_Regulation of lipid metabolism by PPAR*" did not show significant modulation in the 24-hour enrichment analysis (FDR 4.901e-1), several genes associated with the PPARα signaling pathway, fatty acid metabolism, and β-oxidation were modulated in this experiment (Tab. 6.12). These modulations indicate the activation of fatty acid transport factors that may support ligand-mediated transactivation of PPARα, potentially by direct binding to PPAR agonists (Hughes et al., 2015).

Tab. 6.12 – Modulated transcripts with FC≥ ±1.5 associated with the PPARα signaling pathway, fatty acid metabolism, and beta-oxidation

GENE NAME	GENE SYMBOL	24 h	72 h
Fatty acid binding protein 1	Fabpl	up	
Fatty acid binding protein 7	Fabp7	up	
Fatty acid binding protein 4	Fabp4		up
Solute carrier family 27 (fatty acid transporter), member 1	Fatp1	up	up
Lipoprotein lipase Protein	Lpl		up
Enoyl-Coenzyme A, hydratase/3-hydroxyacyl Coenzyme A dehydrogenase	Ehhadh	up	
3-ketoacyl-CoA thiolase, peroxisomal Protein	Acaa1	up	
Peroxisomal acyl-coenzyme A oxidase 1	Acox1	up	

Peroxisomal acyl-coenzyme A oxidase 2	Acox2	up	up
Peroxisomal acyl-coenzyme A oxidase 3	Acox3	up	up
Carnitine O-palmitoyltransferase 1	Cpt1-A	up	up
Long-chain-fatty-acid--CoA ligase 1	Acsl1	up	
Peroxisome proliferator-activated receptor gamma	Pparγ		up
Solute carrier family 2, facilitated glucose transporter member 4 Protein (Glut4)	Slc2a4	up	
Fatty acid synthase	Fasn		down
Acyl-CoA desaturase Protein	Scd		down
Fatty acid-binding protein, adipocyte Protein	Afab-p		up
Niemann-Pick C1-like protein 1 Protein	Npc1l1	up	down
Low-density lipoprotein receptor Protein	Ldlr	down	
Apolipoprotein E	Apoe		up
Apolipoprotein B-100 receptor	Apobr	up	
Phospholipase A2	Pla2g2e	up	up
ATP-binding cassette sub-family A member 1	Abca1	down	down
Low-density lipoprotein receptor	Ldlr	down	
Very low-density lipoprotein receptor	Vldlr	up	
Prolow-density lipoprotein receptor-related protein 1	Lrp1	down	up
Adiponectin receptor protein 1	AdpoR1	down	
Adiponectin receptor protein 2	AdpoR2		down
Lysosome membrane protein 2	Cd36l2	up	
Niemann-Pick C1 protein	Npc1	up	up
Niemann-Pick C1-like protein 1	Npc1l1	down	up
StAR-related lipid transfer protein 5	Stard5	up	
StAR-related lipid transfer protein 4	Stard4		down
Versican proteoglycan	Vcan		up

6.5.4 – Enriched molecular pathways after 72 h 6.57µg/ml - treatment: exploring DEGs derived from the preliminary analysis

To further investigate the lists of DEGs obtained in the preliminary analysis of the 6.57 µg/mL concentration, an enrichment analysis was performed on these data.

As previously explained, statistical analysis of these data was carried out on a reduced dataset, consisting only of the transcriptional profiles from the DEHP 6.57 µg/mL 72-hour treatment groups and the

respective control, and a quality filter based on the CV was applied to this dataset.

The t-tests, corrected using both Benjamini-Hochberg and Bonferroni methods, resulted in DEG lists ($p \leq 0.05$) of 512 and 22 genes, respectively, with the latter constituting a subset of the former.

These gene lists were analyzed using MetaCore and the "Enrichment analysis/analyze single experiment" function to identify significantly modulated pathways. Pathway maps with a FDR ≤ 0.05 were evaluated (Tab. 6.13 and 6.14). The gene list obtained through the unpaired t-test with Benjamini-Hochberg correction was further filtered in MetaCore, considering only genes with FC ≥ ±1.5.

The biological analyses of the two datasets performed using MetaCore showed consistent and concordant results in terms of biological interpretation, with both converging on the involvement of adverse cytotoxicity pathways mediated by oxidative stress, inflammatory response, and modulation of detoxification pathways. Of particular interest is the pathway "*Aberrant lipid trafficking and metabolism in age-related macular degeneration pathogenesis*" (Pathway # 11; FDR 3.861E-02) (Tab. 6.13). Additionally, in both analyses, the "*Aryl hydrocarbon receptor signaling*" pathway is significantly modulated, with an FDR of 0.03 (Tab. 6.13) and 0.0008 (Tab. 6.14), respectively.

Tab. 6.13 – Significantly modulated pathways (unpaired T-test with Benjamini-Hochberg correction, FDR ≤ 0.05) by DEHP 6.57 µg/mL 72 h-treatments. Preliminary analysis was performed on a dataset consisting only of the pair of treatment groups being compared: DEHP 6.57 µg/mL and DMSO 0.5%, with a quality filter of CV < 50% (set to < 50.0 percent for at least 1 out of 2 conditions). The list was further analysed with an Analyze Single Experiment – Enrichment Analysis (MetaCore).

#	Pathwaymap	Modulated NwO	FDR
1	Immune response_IFN-alpha/beta signaling via JAK/STAT	9/62	1.625E-07
2	Protein folding and maturation_Angiotensin system maturation	8/48	2.679E-07
3	Immune response_IFN-alpha/beta signaling via MAPKs	7/73	1.095E-04
4	Immune response_Antiviral actions of Interferons	5/52	3.605E-03
5	Immune response_IFN-gamma actions on extracellular matrix and cell differentiation	5/54	3.605E-03
6	Inflammatory mechanisms of pancreatic cancerogenesis	5/67	8.571E-03
7	Regulation of Tissue factor signaling in cancer	4/43	1.674E-02
8	Aryl hydrocarbon receptor signaling	4/53	3.303E-02
9	HBV-dependent transcription regulation leading to hepatocellular carcinoma (HCC)	3/25	3.861E-02
10	COVID-19: SARS-CoV-2 effects on the vascular endothelium	4/59	3.861E-02
11	Aberrant lipid trafficking and metabolism in age-related macular degeneration pathogenesis	4/60	3.861E-02
12	Immune response_IL-4-induced regulators of cell growth, survival, differentiation and metabolism	4/62	4.009E-02

Tab.6.14 Significantly modulated pathway maps (unpaired T-test with Bonferroni correction, FDR ≤ 0.05) by DEHP 6.57 µg/mL 72 h-treatments. Preliminary analysis was performed on a dataset consisting only of the pair of treatment groups being compared: DEHP 6.57 µg/mL and DMSO 0.5%, with a quality filter of CV < 50% (set to < 50.0 percent for at least 1 out of 2 conditions). The list was further analysed with an Analyze Single Experiment – Enrichment Analysis (MetaCore).

#	Pathwaymap	Modulated NwO	FDR
1	The role of KEAP1/NRF2 pathway in skin sensitization	2.179E-04	3.615E-02
2	Aryl hydrocarbon receptor signaling	6.007E-04	3.615E-02
3	Aberrant lipid trafficking and metabolism in age-related macular degeneration pathogenesis	7.696E-04	3.615E-02
4	Immune response_IFN-alpha/beta signaling via JAK/STAT	8.216E-04	3.615E-02
5	Glutathione metabolism	1.076E-03	3.788E-02
6	SHH signaling in oligodendrocyte precursor cells differentiation in multiple sclerosis	9.154E-03	5.415E-02
7	Role of inflammasome in macrophages, adipocytes and pancreatic beta cells in type 2 diabetes	1.266E-02	5.415E-02
8	Role of IL-8 in colorectal cancer	1.335E-02	5.415E-02
9	Schema: Initiation of T cell recruitment in allergic contact dermatitis	1.335E-02	5.415E-02
10	Endothelin-1- and TNF-alpha-induced inflammatory response in asthmatic airway fibroblasts	1.405E-02	5.415E-02

6.5.5 – Enriched molecular pathways following 72-hour treatments and 28 d of culture

RNA extracted 32 d after the start of the experiment was obtained from cell cultures treated with DEHP at three different concentrations for 72 h and then maintained in culture for an additional 28 d.

The DEG lists for the 32-day samples showed an increase in size with treatment concentration. These lists were individually uploaded to the MetaCore software suite to perform the functional enrichment analysis.

The DEG list resulting from the t-test with Benjamini-Hochberg correction, comparing the 1.97 µg/mL treatment to its respective control, led to the identification of 124 network objects in MetaCore, with the modulation of only one pathway map with an FDR≤0.05: "*Signal transduction_Activin A signalling"* (Tab. 6.15).

It is interesting to note that the set of modulated network objects with FC≥ ±1.5 shows a predominance of downregulation (95 out of a total of 124).

For the DEHP 6.57 µg/mL treatment, from the initial DEG list of 512 entities, MetaCore software identified 340 network objects, of which 208 had FC≥ ±1.5, and a list of 22 modulated pathway maps with FDR≤ 0.05 (Tab. 6.16). In this case, a more balanced distribution of upregulated and downregulated signals was observed, with 132 network objects downregulated out of the total 208. The list of significantly modulated pathway maps includes several pathways related to neurophysiological mechanisms (Pathway maps # 1, 5, 13, 21) (Tab. 6.16).

Tab. 6.15 – Modulated genes of the only pathway map with FDR≤0.05 perturbeded by DEHP 1.97 µg/mL 72 h-treatments after 28 d of culture: "*Signal transduction_Activin A signalling"*, with 4/65 modulated entities; FDR 0.027. Analyze Single Experiment – Enrichment Analysis (MetaCore).

Modulated NwO	**FC**
c-Fos	-5.722
Otx1	-2.582
p21	2.382
Vegf-a	1.502

Tab. 6.16 – Significantly modulated pathway maps (FDR≤0.05) from DEHP 6.57 µg/mL 72 h-treatments after 28 d of culture. Enrichment analysis. Analyze Single Experiment – Enrichment Analysis (MetaCore).

#	Pathwaymap	Modulated NwO	FDR
1	Regulation of intrinsic membrane properties and excitability of striatopallidal medium spiny neurons in Huntington's disease	5/57	4.494E-02
2	Influence of multiple myeloma cells on bone marrow stromal cells	4/33	4.851E-02
3	Signal transduction_PDGF signaling via MAPK cascades	5/65	4.851E-02
4	Signal transduction_Erk Interactions: Inhibition of Erk	4/34	4.851E-02
5	Neurophysiological process_Regulation of intrinsic membrane properties and excitability of cortical pyramidal neurons	5/74	4.953E-02
6	Immune response_CD28 signaling	5/87	4.953E-02
7	Stimulation of TGF-beta signaling in lung cancer	4/48	4.953E-02
8	Immune response_IL-3 signaling via JAK/STAT, p38, JNK and NF-kB	5/93	4.494E-02
9	Macrophage and dendritic cell phenotype shift in cancer	5/100	4.851E-02
10	Signal transduction_FGFR2 signaling	5/104	4.851E-02
11	Development_WNT/Beta-catenin signaling in the nucleus	4/62	4.851E-02
12	Immune response_IL-10 signaling	4/62	4.953E-02
13	Regulation of intrinsic membrane properties and excitability of striatonigral medium spiny neurons in Huntington's disease	4/62	4.953E-02
14	Signal transduction_Genomic ESR1 and ESR2 signaling	4/67	4.953E-02
15	Immune response_Plasmin signaling	4/70	4.494E-02
16	Immune response_IL-4-responsive genes in type 2 immunity	4/70	4.851E-02

17	Reproduction_Gonadotropin-releasing hormone (GnRH) signaling	4/73	4.851E-02
18	Immune response_IL-11 signaling via JAK/STAT	3/34	4.851E-02
19	Oxidative stress_ROS-mediated activation of MAPK via inhibition of phosphatases	3/34	4.953E-02
20	Interleukins-induced inflammatory response in asthmatic airway fibroblasts	3/35	4.953E-02
21	Alzheimer disease: synaptic dysfunction	4/78	4.953E-02
22	E-cadherin signaling and its regulation in gastric cancer	3/36	4.494E-02

Finally, functional enrichment analysis of the DEG list from the highest DEHP concentration (19.7 µg/mL) identified 1399 network objects, of which 732 had FC≥ ±1.5, with 353 entities being downregulated. This functional enrichment analysis revealed more than 50 modulated pathway maps with FDR≤0.05 (Tab. 6.17).

The DEHP 19.7 µg/mL 32-day transcriptional profile, expressed by the statistically modulated pathway maps, shows a significant involvement of pathways associated with inflammatory/immune mechanisms (pathway maps # 3, 4, 7, 11, 12, 17, 19, 26, 28, 31, 33, 34, 35, 38, 42, 49, 50) and the presence of pathways associated with neurophysiological processes (pathway maps # 2, 15, 18, 24, 47) (Tab. 6.17).

Tab.6.17 – Significantly modulated pathway maps (FDR≤0.05) from DEHP 19.7µg/ml 72 h-treatments after 28 d of culture. Analyze Single Experiment – Enrichment Analysis (MetaCore).

#	Pathwaymap	Modulated NwO	FDR
1	Signal transduction_Calcium-mediated signaling	10/72	1.877E-03
2	Neurophysiological process_Glutamic acid regulation of Dopamine D1A receptor signaling	8/45	1.877E-03
3	Immune response_Oncostatin M signaling via MAPK	7/37	3.350E-03
4	Immune response_Fc epsilon RI pathway: Lyn-mediated cytokine production	10/87	3.350E-03
5	Reproduction_Gonadotropin-releasing hormone (GnRH) signaling	9/73	4.148E-03
6	CHDI_DEGs from Replication data_Causal network	9/81	6.149E-03
7	Immune response_Histamine H1 receptor signaling in immune response	7/47	6.149E-03
8	Development_TGF-beta-dependent induction of EMT via MAPK	7/47	6.149E-03
9	Stimulation of TGF-beta signaling in lung cancer	7/48	6.149E-03
10	Signal transduction_PDGF signaling via MAPK cascades	8/65	6.149E-03
11	Immune response_CD28 signaling	9/87	7.741E-03
12	AIDS: HIV-1 signaling via CCR5 in macrophages and T lymphocytes	6/39	1.268E-02
13	Cytoskeleton remodeling_Regulation of actin cytoskeleton organization by the kinase effectors of Rho GTPases	7/58	1.561E-02
14	Signal transduction_Angiotensin II/ AGTR1 signaling via RhoA and JNK	8/78	1.561E-02
15	Nicotine signaling in dopaminergic neurons, Pt. 2 - axon terminal	6/43	1.561E-02
16	TGF-beta 1-mediated induction of EMT in normal and asthmatic airway epithelium	6/43	1.561E-02

17	Immune response_Substance P-stimulated expression of proinflammatory cytokines via MAPKs	6/43	1.561E-02
18	Signal transduction_Mu-type opioid receptor signaling in non-neuronal cells	7/61	1.564E-02
19	Chemotaxis_Lysophosphatidic acid signaling via GPCRs	10/129	2.026E-02
20	Signal transduction_Non-apoptotic FasR(CD95) signaling	8/86	2.121E-02
21	Putative glucocorticoid- and LABA-mediated inhibition of pro-fibrotic signaling in asthmatic airway fibroblasts/myofibroblasts	5/31	2.121E-02
22	ErbB2-induced breast cancer cell invasion	7/67	2.257E-02
23	Apoptosis and survival_IL-17-induced CIKS-dependent MAPK signaling	5/32	2.257E-02
24	Neurophysiological process_HTR2A signaling in the nervous system	6/49	2.286E-02
25	Angiogenesis in hepatocellular carcinoma (HCC)	6/50	2.451E-02
26	Oxidative stress_ROS-mediated activation of MAPK via inhibition of phosphatases	5/34	2.667E-02
27	Signal transduction_Activation of PKC via G-Protein coupled receptor	6/52	2.809E-02
28	Signal transduction_CXCR4 signaling via MAPKs cascades	6/53	2.994E-02
29	Transcription_HIF-1 targets	8/95	2.994E-02
30	Immune response_TCR alpha/beta signaling	8/97	3.308E-02
31	Immune response_Platelet activating factor/ PTAFR pathway signaling	6/55	3.308E-02
32	Role of TGF-beta 1 in fibrosis development after myocardial infarction	5/38	3.654E-02
33	COVID-19: Regulation of antiviral response by SARS-CoV-2	9/124	3.676E-02
34	Immune response_TLR5, TLR7, TLR8 and TLR9 signaling	6/58	3.885E-02
35	Immune response_CCR5 signaling in macrophages and T lymphocytes	6/58	3.885E-02

36	Signal transduction_RANKL-dependent osteoclast differentiation	7/81	4.102E-02
37	Role of stellate cells in progression of pancreatic cancer	6/60	4.102E-02
38	Immune response_TREM1 signaling	6/60	4.102E-02
39	Pro-tumoral TNF-alpha signaling in melanoma	5/41	4.102E-02
40	Signal transduction_Non-canonical WNT5A signaling	7/82	4.102E-02
41	HBV-dependent transcription regulation leading to hepatocellular carcinoma (HCC)	4/25	4.102E-02
42	Immune response_IL-1 signaling	7/83	4.102E-02
43	Effect of H. pylori infection on gastric epithelial cells motility	5/42	4.102E-02
44	Signal transduction_Relaxin family peptides signaling via RXFP3 and RXFP4 receptors	5/42	4.102E-02
45	Signal transduction_S1P2 receptor activation signaling	8/107	4.102E-02
46	Development_WNT/Beta-catenin signaling in the nucleus	6/62	4.102E-02
47	Regulation of intrinsic membrane properties and excitability of striatonigral medium spiny neurons in Huntington's disease	6/62	4.102E-02
48	Regulation of Tissue factor signaling in cancer	5/43	4.158E-02
49	Immune response_CD40 signaling in B cells	7/85	4.158E-02
50	Immune response_IL-18 signaling	6/63	4.158E-02

It is noteworthy that many of the pathway maps related to inflammatory and immune processes indicate a general inhibition, which was also observed at the lower concentrations. The comparative analysis at 32 d for the two highest concentrations (6.57 µg/ml and 19.7 µg/ml)

revealed concordance between the datasets, with several common gene modulations and FC values consistent with a dose-response relationship.

Gene modulations in the pathway maps at 32 d were predominantly downregulated. Furthermore, particularly at the highest concentration, many of the modulated transcripts consisted of kinases and phosphatases involved in cytoplasmic signal transduction. These notable modulations are believed to be related to the metabolic imbalances induced by treatment in a dose-dependent manner.

Some modulations suggesting different effects of the concentrations include: the COX-2 transcript (FC -3.24), which is strongly downregulated only at the 6.57 µg/mL concentration; the downregulation of Snail1 (FC -1.7 and -2.1) and Vinculin (FC -2.9 and -2.3), both related to epithelial-mesenchymal transition, in the profiles of 6.57 µg/mL and 19.7 µg/mL concentrations; the DNA (cytosine-5)-methyltransferase 3B Protein transcript, downregulated at 1.97 µg/mL and 6.57 µg/mL concentrations (DNMT3B, FC -1.6 and -1.55) but not at the highest concentration; while the upregulation of the p21 transcript (CDKN1A, FC 2.38) is an exclusive modulation at the lowest concentration.

Also of interest is the presumed downregulation of the calcium signaling pathway at both the 6.57 µg/mL and 19.7 µg/mL concentrations, as evidenced by the downregulation of several calcium-regulated transcripts. Notably, the top pathway for the 6.57 µg/mL concentration, "*Regulation of intrinsic membrane properties and excitability of striatopallidal medium spiny neurons in Huntington's disease*," shows gene

modulations related to the regulation of intracellular calcium and ion flow across the plasma membrane (Tab. 6.16 and 6.18).

Tab. 6.18 – Modulated NwO (FC≥ ±1.5) within the "*Regulation of intrinsic membrane properties and excitability of striatopallidal medium spiny neurons in Huntington's disease*" signaling pathway (pathway map #1 Tab. 6.16), signifincantly perturbed by DEHP 6.57 µg/mL 72 h-treatment after and 28 d of culture.

Gene Symble	Gene Name	Modulation by 6.57 µg/ml	Modulation by 19.7 µg/ml	Biological Function
Acm1	Muscarinic acetylcholine receptor M1	down	down	Cholinergic receptor (acetylcholine) sensitive to the action of muscarine
Itpr2	Receptor for the second messenger inositol 1,4,5-trisphosphate (IP3)		down	Inositol receptor, intracellular calcium release channel
Plcb1	1-phosphatidylinositol-4,5-bisphosphate phosphodiesterase beta-1		down	Phospholipase involved in the inositol signaling pathway
Ppp3cb	Calcineurin A (catalytic)	down	down	Serine/threonine phosphatase regulated by intracellular calcium
Kcnma1	Calcium-activated potassium channel subunit alpha-1	down	down	Large-conductance calcium-activated potassium channel
Na(v) I α	Sodium channel protein type 1 subunit alpha	down	down	Voltage-dependent sodium channel
Shank	SH3 and multiple ankyrin repeat domains 2	down		Structural protein involved in synaptic neurotransmission

CHAPTER 7

Discussion

7.1 – Cytotoxicity and carcinogenic potential of DEHP

The primary objective of this study was to evaluate the carcinogenic potential of the chemical compound DEHP using the standardized *in vitro* CTA method with the BALB/c 3T3 A31-1-1 cell model, followed by a microarray transcriptomic experiment to identify and explore the molecular and cellular events, as well as potential mechanisms of action, which could be associated with its toxicological profile and *in vitro* activity.

In this study, an in-depth literature review was conducted, focusing on results and methods from other studies that have tested DEHP in various types of CTAs. The data from this literature review have been published and are available online (Pillo et al., 2024).

Our experiment demonstrated a relatively high cytotoxicity of DEHP in the BALB/c 3T3 A31-1-1 model compared to other studies, along with a clear dose-response relationship, which is often absent in other studies (Pillo et al., 2024).

However, the CTA yielded negative results, which is consistent with other studies conducted with different BALB/c 3T3 clones (Pillo et al., 2024).

As described in the Materials and Methods section, particular attention was paid to the dissolution of DEHP in cell medium in this study. The final concentration of DMSO used was 0.5% (v/v), which was chosen

over the more conventional 0.1% (v/v) to enhance the stability of the compound in the cell medium and ensure a more homogeneous distribution, as recommended in the standard protocol (Sasaki et al., 2012a).

A significant concentration-dependent reduction in colony formation was observed starting at 10 µg/mL, corresponding to 10.20 µL/mL.

The higher concentration of DMSO used in this study may have improved the bioavailability of DEHP, resulting in a stronger cytotoxic effect. This hypothesis was supported by the dose-response curves observed in the results.

Interestingly, the only CTA study with BALB/c 3T3 showing positive results for cell transformation with DEHP was conducted using the A31 clone, in the absence of S9 metabolic activation, at a very high concentration range (9.8-980 µg/ml) under good laboratory practice (GLP) conditions. A significant increase in *foci*, with a dose-response correlation, was also observed in this study (European Chemicals Bureau - Joint Research Centre, 2008; Pillo et al., 2024). It is important to note that these results were evaluated in the JRC report EUR 23384 EN_2008. However, information regarding the vehicle used and further details on the outcomes could not be obtained. Additionally, the test yielded negative results in the presence of metabolic supplements with S9 subcellular enzyme fractions.

The varying sensitivities of different BALB/c 3T3 clones to different classes of chemical substances have been previously reported. In particular, A31 and A31-1-1 clones have shown different responses to

substances like 1,2-Dibromoethane, which requires bioactivation through glutathione conjugation (Colacci et al., 2011). Glutathione conjugation is a primary detoxification pathway for DEHP, both in humans and mice, although the resulting conjugates are biologically inactive unless the molecule undergoes specific cleavage, catalyzed by β-glucuronidases (SCENIHR, 2016). Other studies have shown that DEHP treatment causes a reduction in glutathione levels both *in vivo* and *in vitro* (She et al., 2017; Zhao et al., 2018; Amara et al., 2020).

As reported in Pillo et al., DEHP has an extensive dataset of results from CTAs using various protocols and cell models, showing predominantly positive results in the SHE model and negative results in BALB/c 3T3 clones (Pillo et al., 2024).

It is widely recognized that the results obtained from SHE and BALB/c 3T3 CTAs can vary significantly, with several KEs and biomarkers identified for each model. The SHE model, in particular, has been identified as more sensitive to a broader range of carcinogens and capable of detecting less specific mechanisms involved in the early stages of cell transformation (Benigni et al., 2015; Colacci et al., 2023).

Although evidence suggests that DEHP-mediated cell transformation in the SHE model proceeds independently of PPARα activation, the specific mechanisms involved have not been fully elucidated (Tsutsui et al., 1993; Landkocz et al., 2011; Colacci et al., 2023). Notably, one study demonstrated that DEHP, MEHP, clofibrate, and WY-14,643 did not induce peroxisome proliferation in the SHE model

in the absence of exogenous metabolic activation; however DEHP was still able to induce cell transformation under such conditions (Tsutsui et al., 1993).

Nevertheless, it is important to note that also certain significant differences between the two CTA protocols may theoretically have contributed to the differing results.

The duration of exposure is considered a critical variable, particularly when evaluating substances such as DEHP, which show reversible effects that may have toxicological or carcinogenic significance under repeated exposure conditions, including the inhibition of gap junction intercellular communication (GJIC), peroxisomal β-oxidation, and increased cell replication. These effects, observed *in vivo* throughout the treatment, regressed once treatment was stopped (Isenberg et al., 2000, 2001). In addition, GJIC inhibition has been described as a transient effect *in vitro* in the SHE model (Cruciani et al., 1997).

It is interesting to note that positive results were obtained in the SHE model at different exposure times, ranging from 7 days to 24 hours (Pillo et al., 2024).

In the study by Tsutsui et al., the exposure time was set to 48 hours, resulting in a weak induction of morphological transformation in SHE cells. However, unlike what was observed in the GLP study on BALB/c 3T3 A31 cells, the frequency of cell transformation induced by DEHP was enhanced by exogenous metabolic activation (S9) and further increased with extended treatment duration. In contrast, other studies

using lower concentrations found that DEHP induced transformation in SHE cells after a 7-day exposure but not after a 24-hour exposure (LeBoeuf et al., 1996).

It is also noteworthy that some *in vitro* studies using different cell models have shown that the limited or slow metabolization of DEHP can result in insufficient concentrations of its active metabolites, thereby reducing its biological effects (Schaedlich et al., 2018). MEHP, the primary bioactive metabolite of DEHP, directly binds to and activates various PPAR isoforms, including PPARα and PPARγ, usually exhibiting greater potency than DEHP when used directly *in vitro*. While Matthews et al. (1993) observed limited or equivocal activity of MEHP in BALB/c 3T3 A31-1-13 cells, a recent study by Wang et al. (2024) demonstrated that MEHP induces anchorage-independent growth, a hallmark of cellular transformation, suggesting its potential intestinal carcinogenicity (Matthews et al., 1993; Wang et al., 2024)

In our study, a greater bioactivity of DEHP was observed in the cytotoxicity assay, with cytotoxicity levels higher than those reported in other studies, showing that improved solubilization can increase the bioactivity of DEHP.

Further studies will be needed to clarify whether the absence of transformation is related to limited metabolization of the compound and lower bioavailability of reactive metabolites, or to the ability of the cells to neutralize these metabolites through detoxification mechanisms. Additionally, it should be noted that many studies have reported the use of

lower vehicle concentrations (e.g., DMSO) compared to those used in our study, and that DEHP exhibits lower solubility (<0.1 mg/mL) compared to MEHP, which has a solubility of approximately 1 mg/mL.

Therefore, the negative results observed in the BALB/c 3T3 CTA should be further explored by analyzing the metabolite composition profile and conducting CTAs with DEHP metabolites, such as MEHP. Moreover, extending the treatment duration could provide additional insights. Given that the mechanisms involved may be transient, treatment duration is also considered a key factor in assessing the carcinogenicity of DEHP and should be carefully evaluated in *in vitro* studies of non-genotoxic carcinogens.

7.2 – Transcriptional profiling of DEHP

The transcriptomic experiment with DEHP followed a cell culture and treatment protocol typical of the BALB/c 3T3 A31-1-1 CTA. The aim was to analyze transcriptional profiles at different time points corresponding to critical phases of the CTA test: 24 h of treatment to assess early cellular responses; 72 h, marking the end of the CTA treatment period, to evaluate cellular stress responses and resilience; and 32 d, marking the conclusion of the CTA, where potential cell transformation and/or long-term effects were observed and assessed.

7.2.1 – Possible involvement of PPARα and Dysregulation of Lipid Metabolism

Immunofluorescence experiments confirmed the nuclear localization of PPARα in our cell line. This suggests that the negative

outcome observed in the transformation experiment is not likely due to the absence of PPARα, which is commonly considered the primary receptor for DEHP, although tissue-specific transcriptional response should still be considered. While the MetaCore pathway map "*Lipid Metabolism Regulation by PPAR*" did not show significant modulation in the enrichment analysis (FDR 4.901e-1), several PPARα target genes were modulated by DEHP in the BALB/c 3T3 A31-1-1 model following DEHP treatments of 24 h and 72 h at a concentration of 19.6 µg/ml (Tab. 6.12). These genes are involved in lipid transport and uptake, including carnitine palmitoyltransferase 1 (CPT1), mitochondrial and peroxisomal β-oxidation, microsomal ω-oxidation of fatty acids (such as ACOX3, ACAA1, EHHADH, and P450 ω-hydroxylase), and lipoprotein metabolism (e.g., lipases such as LPL and APOE).

Additionally, the data suggest inhibition of insulin signaling, alongside transcriptional upregulation of the insulin-regulated glucose transporter GLUT4 (Slc2a4, FC 2.04), compared to the control at the 24-hour time point. Interestingly, this upregulation of GLUT4 and downregulation of the insulin receptor have also been observed in murine myoblasts treated with Bisphenol A (Kang et al., 2023).

One notable transcript modulated is CPT1, which has been identified as a marker of PPARα activation in DEHP-exposed mice (Lv et al., 2016). The known toxicity and hepatocarcinogenic pathway of DEHP in rodents, linked to PPARα activation, involve a cascade of events: (1) receptor activation, (2) peroxisome proliferation, (3) enhanced fatty acid

metabolism, (4) increased cell proliferation and apoptosis inhibition, (5) ROS production, (6) oxidative DNA damage, and (7) inhibition of GJIC (Isenberg et al., 2000; Ito et al., 2007; Corton et al., 2014; Rajesh and Balasubramanian, 2014). Dysregulation of PPARα and its hyperactivation can lead to alterations in cholesterol transport at cellular and systemic levels (Corton et al., 2014; Takada and Makishima, 2020).

In this context, our dataset showed downregulation of the LDL receptor (LDLR) (FC -1.79), alongside the modulation of key transcripts involved in intracellular cholesterol trafficking (Tab. 6.12). Specifically, NPC1 and NPC1L1, both critical for cholesterol movement within cells, were modulated, with NPC1 upregulated at both 24 h and 72 h, and NPC1L1 downregulated at 24 h but upregulated at 72 h.

It is important to highlight that NPC1L1 is differently expressed across species. In mice, its expression is primarily intestinal, whereas in humans and rats, it is expressed in both the intestine and liver, where it plays a crucial role in cholesterol absorption. In the liver, NPC1L1 is localized to the canalicular membrane and is involved in the reabsorbtion of cholesterol from bile into hepatocytes. This protein is a key factor in the regulation of hepatic lipid levels and has been linked to hepatic steatosis (Sugizaki et al., 2014; Toyoda et al., 2019).

The upregulation of NPC1 and NPC1L1 could indicate increased intracellular cholesterol, potentially linked to the observed downregulation of ABCA1 at 72 h (FC -4.95 at 6.57 µg/ml; FC -8.25 at 19.7 µg/ml). ABCA1 is responsible for cholesterol efflux from cells and plays a critical role in

preventing intracellular cholesterol accumulation by facilitating the export of excess cholesterol and phospholipids to lipid-poor apolipoproteins such as ApoA-I for HDL formation (Wang et al., 2022). The observed downregulation of ABCA1 in our study could indicate impaired cholesterol efflux, which contributes to intracellular cholesterol accumulation.

Consistent with this, prolonged exposure to low concentrations of DEHP disrupted cholesterol metabolism in rat liver cells, resulting in hepatic steatosis and fibrosis exacerbation (Lee et al., 2020). In that study, ABCA1, STARD4, and NPC1 were also downregulated, with a dose-dependent increase in intracellular cholesterol levels. Additionally, in our 24-hour transcriptional profile for the highest DEHP concentration, SOAT1 (sterol O-acyltransferase 1), an enzyme responsible for storing cholesterol by esterifying it with long-chain fatty acids (Tu et al., 2023), was upregulated (FC 1.61).

In the 19.7 µg/ml profile, STARD4, which is involved in intracellular cholesterol transport, was downregulated (FC -1.59), along with mild downregulation of the cholesterol-metabolizing enzymes AMACR (FC -1.33) and CYP1A7 (FC -1.17).

Finally, PPARγ was upregulated in the 72-hour transcriptional profile. Some studies suggest that DEHP may activate PPARγ, leading to the downregulation of insulin receptor and GLUT4 protein expression and disruption of insulin signaling (Mariana and Cairrao, 2023), indicating possible PPARγ activation in our model.It is noteworthy that PPARα and PPARγ can be activated by direct binding with DEHP metabolites, such as

MEHP, rather than by DEHP itself (Kratochvil et al., 2019; Useini et al., 2023). Otherwise, PPARγ is upregulated during adipogenesis, and its transcription can be mediated by several transcription factors (Lee and Ge, 2014)***.***

7.2.2 – Molecular Initiating Event and early downstream Key Events

The Enrichment analysis conducted using MetaCore for the 24-hour transcriptional profile indicated significant modulation of the AhR and PXR pathways, which are involved in xenobiotic metabolism and the activation of phase I and phase II enzymes. Due to their primary role in metabolism and detoxification processes, these receptors are known as "xeno-sensors." However, it has been demonstrated that their activity can influence several cellular processes such as lipid and glucose homeostasis and immune responses, thereby playing a potential role in the development of cardiometabolic diseases (Rakateli et al., 2023).

Modulation of the AhR signaling pathway is supported by the upregulation of CYPs and UGTs, as well as other network objects in the "*Aryl hydrocarbon receptor signaling pathway*" (pathway map #103) (FDR 4.720e-3), which ranks as the third most significant pathway in the "Toxicity Processes" category (Fig. 6.13). These findings are consistent with those of other studies in which DEHP exposure affected various human and rodent cell types (Ernst et al., 2014; Zou et al., 2020; Ge et al., 2022; Hsieh et al., 2022).

Notably, the observed downregulation of FASN, SCD-1 and ACACA has been linked to AhR activation in response to TCDD exposure, leading to decreased fatty acid synthesis in both *in vivo* and primary human hepatocytes (Rakateli et al., 2023). Alongside these downregulations, the notable induction of CYP2C8 (FC 23.92) points to an interesting crosstalk between PPAR and AhR in our model. It has been suggested that DEHP may induce CYP2C8 expression through ligand-independent AhR activation (Hsieh et al., 2022). Induction of CYP2C8 has also been associated with epithelial-mesenchymal transition (EMT), driven by AhR/ERK signaling (Hsieh et al., 2022).

In addition to PPARα and AhR crosstalk, there appears to be transcriptional coordination with the PXR signaling pathway.

PXR is a member of the nuclear receptor subfamily 1 and can be activated by a wide range of molecules, including xenobiotics and endogenous metabolites such as steroids and bile acids (Mackowiak and Wang, 2016). Other studies have noted that both RXR ligands and partner receptors activate a "cooperative" transcriptional response, highlighting the overlapping and crosstalk between PPARs, PXR, and CAR (Evans and Mangelsdorf, 2014; Shizu et al., 2021).

In our study, the activation of PXR was evidenced by the modulation of its associated pathway (Fig. 6.13), along with the previously discussed modulation of genes involved in xenobiotic metabolism and detoxification, such as CYP2C9 (FC 4.21), CYP2C19 (FC 1.58), and the ABC transporter MDR1, which has been extensively studied in multidrug

resistance (Burk et al., 2005; Jadhao et al., 2021). The upregulation of this xenobiotic transporter suggests the activation by cells of a detoxification and chemical stress elimination response, even though DEHP and MEHP are unknown substrates for this transporter. MDR1 upregulation has also been linked to DEHP treatment (Takeshita et al., 2006; Jones et al., 2015; Jadhao et al., 2021).

Several studies have identified PXR as a key factor in maintaining lipid homeostasis and atherogenesis and as a potential mediator of the effects of phthalates and other plastic-associated chemicals such as Bisphenol A and Bisphenol B (Sui et al., 2021). The exact mechanism of PXR activation by DEHP remains unclear and can occur through either direct ligand-binding and ligand-independent (indirect) mechanisms (Mackowiak and Wang, 2016).

Additionally, we observed the upregulation of the transcription factor HNF4α (FC 1.61), which plays a crucial role in hepatic fat metabolism and bile acid production (Lv et al., 2021) .

Given the significant transcriptional overlap and the complex interplay between these so-called "xeno-sensors," including AhR, PXR, CAR, and PPARα, our data do not allow for a definitive activation-transcription link, nor can we distinguish the specific roles these receptors play in the observed transcriptional responses.

The interaction between these factors remains poorly understood, with varied and sometimes contradictory findings in the literature, suggesting tissue- and species-specific crosstalk (Evans and Mangelsdorf,

2014; Mackowiak and Wang, 2016; Shizu et al., 2021). For instance, a recent study proposed that PXR activation might inhibit PPARα target gene expression in HepaRG cells, whereas, PPARα activation can induce PXR target genes (Shizu et al., 2021).

Although PPARα binding was not directly assessed in this study, the molecular data presented so far suggest that DEHP-induced lipid metabolism disorders are supported by perturbation of the PPARα/PPARγ pathways. Based on these results, we hypothesized that a key molecular initiating event in our experiment was the activation of the PPARα. Indeed, PPARα activation triggers a cascade of molecular events related to compound metabolism, alterations in energy homeostasis and lipid metabolism, and immune responses, events in which AhR and PXR may also play a role.

The induction of CYP2C8, which was strongly upregulated at 24 h (Cyp2c65 (A_51_P471126) FC 9.39 and Cyp2c65 (A_52_P652059) FC 23.93), could be associated with the joint action of multiple signaling pathways, PPARα/AhR/PXR (Makia and Goldstein, 2016; Hsieh et al., 2022). Furthermore, the 24-hour profile showed the activation of detoxification enzymes, UGTs (phase II metabolic enzymes), such as UGT1A1, whose expression is regulated by both AhR and PXR, UGT1A6, which is specifically regulated by AhR, and UGT1A8, which is regulated by HNF4α and associated with MEHP metabolism (Aueviriyavit et al., 2007; Hanioka et al., 2017). The upregulation of these enzymes may support DEHP metabolism and detoxification via glucuronidation, which is the

primary route for DEHP metabolite elimination in humans (Hanioka et al., 2017). However, further experiments and metabolomics investigations are needed to substantiate this hypothesis.

Previous studies have identified UGTs activation as a key detoxification event for carcinogens in BALB/c 3T3 A31-1-1 CTA (Mascolo et al., 2018; Pillo et al., 2022; Colacci et al., 2023). These data further support the hypothesis that the negative results observed in the BALB/c 3T3 CTA compared with the SHE model may be attributed to the active detoxification of DEHP metabolites in this model. Supporting this hypothesis, no UGTs were identified in the SHE model following DEHP exposure (Landkocz et al., 2011).

These key molecular events associated with DEHP metabolism and detoxification are particularly evident in the 24-hour exposure profile and tend to diminish in the 72-hour transcriptional profiles (Tab. 6.10), where downstream cellular responses, such as oxidative stress response, DNA damage, and apoptotic processes, predominate.

7.2.2 – Oxidative Stress, Inflammatory Response, and Cellular Remodeling Pathways after DEHP Exposure

Pathway analysis of the 24-hour transcriptional profile supports the activation of signaling pathways related to oxidative stress defense and pro-inflammatory responses following treatment with cytotoxic concentrations of DEHP (19.7 µg/ml). At the same time, downregulation of the NF-kB/AP-1 signaling pathway was observed. This inhibition could be linked to negative interference and crosstalk with PPARα signaling. Indeed

PPARα activation can inhibit the nuclear translocation of the NF-kB/p65 subunit, which in turn prevents the phosphorylation of nuclear c-Jun/AP-1, thereby suppressing the production of pro-inflammatory cytokines such as TNFα, IL-1β, COX-2, and iNOS (Delerive et al., 1999; Xu et al., 2001; Korbecki et al., 2019).

On the other hand, the "*Immune response_IL-17 signaling*" pathway (pathway #10) (FDR 9.344e-5) shows upregulation of IL-21, IL-17, and IL-17R, cytokines involved in the differentiation, maintenance, and expansion of Th17 cells, playing a crucial role in oxidative stress regulation and inflammation.

Additionally, modulation of numerous transcripts related to extracellular matrix remodeling was observed, including LAMA3 (Epiligrin, FC −2.27), Thrombospondin 1 [Thbs1 (A_55_P2746459) FC −3.67 and Thbs1 (A_65_P13588) FC −3.88 for], and downregulation of ephrin signaling, as seen in the "*CHDI_Correlations from Discovery data_Causal network (positive)*" pathway (pathway #6) (FDR 5.293e-5). Further downregulation of several matrix metalloproteinases, including MMP10 (FC -20.11), MMP1 (FC -8.64), and MMP3 (FC -9.44), along with upregulation of hyaluronidase HYAL1 (FC 6.18), suggests that DEHP may influence cell-cell and cell-matrix adhesion. Overall, DEHP treatment appeared to promote cell adhesion and matrix interactions, although many of the modulated factors showed contrasting effects.

Interestingly, in the gene expression analysis of SHE cells exposed to DEHP in Landkocz et al., reduced cell adhesion and anti-apoptotic

signaling activation were observed (Landkocz et al., 2011). In contrast to the SHE model at 24 h, we observed opposite modulation in this study, with downregulation of CORO1C, KIF23, COL1A1, and DCLK, and upregulation of NRP2 and CTTNBP2, which are associated with cytoskeletal remodeling, along with the downregulation of the anti-apoptotic factors BCL10, NFKB1, and SH3KBP1.

However, some gene modulations observed here that relate to cytoskeletal changes, such as downregulation of THBS1, FLRT2, HAS2, and CTNNBIP1, are in agreement with DEHP-induced changes in the SHE model.

Furthermore, we identified significant modulation of tumor suppressor genes and apoptotic activators, such as HTATIP2 (FC 14.47) GADD45α (FC 4.2) and TP73 (FC 3.66), as well as subsequent THBS1 upregulation at 72 h (FC 2.9).

Another notable finding in this study was the downregulation of transcripts encoding gap junction proteins in the 24-hour profile (Tab. 6.11). These modulations confirm the hypothesis that GJIC inhibition is a temporary effect of DEHP exposure, as observed both *in vivo* and *in vitro* (Cruciani et al., 1997; Isenberg et al., 2000, 2001).

As shown in the results, inflammatory signaling intensified after 72 h of treatment, becoming dominant in the transcriptional profile alongside the oxidative stress response, DNA damage, and apoptosis induction at a 19.7 µg/ml concentration. The increased activation of the inflammatory and immune response pathways may be attributed to reduced PPARα

activation after DEHP metabolism at 72 h, as well as to the continued cytotoxic and stress-related effects on the cells.

This robust cellular stress response and the activation of defense mechanisms may be another critical factor contributing to the negative outcome of the transformation assay.

7.2.3 – Metabolic Stress and Neuroendocrine Disruption

Transcriptional profiles from DEHP-treated BALB/c 3T3 A31-1-1 cells revealed modulation of transcripts associated with neurophysiological and hormonal functions. These findings align with the literature that highlights the relationship between neurophysiological balance and metabolism, which is often observed in metabolic and neurological disorders (Farris et al., 2021; Hamzé et al., 2022).

The presence of neurophysiological transcript modulation is evident both as an early molecular interaction at 24 h and as a delayed effect observed 28 d after treatment cessation. Among these, modulation of transcripts for anion channels, neurotransmitter receptors, and neuropeptides stands out. Interestingly, these tissue-specific transcripts were found to be modulated in a murine embryonic fibroblast model.

Notably, the APP transcript, a precursor of neurotoxic amyloid β peptides in Alzheimer's disease, was upregulated at 24 h, along with its substrate enzyme BACE2. Although initially deemed of limited relevance in this model, this finding gained significance in light of recent epidemiological evidence linking diabetes and Alzheimer’s disease, potentially through APP processing (Farris et al., 2021; Hamzé et al.,

2022). Moreover, early life exposure to DEHP in Caenorhabditis elegans has been linked to increased amyloid-β toxicity (Yen et al., 2021).

These data support the hypothesis that DEHP influences APP expression and processing, potentially affecting cholesterol metabolism and LDL receptor expression (Wang et al., 2014).

In this study, downregulation of the LDL receptor (LDLR, FC −1.79) and LDL-related receptor 1 (LRP1, FC −2.01) was observed at 24 hours, followed by upregulation at 32 d for both the 6.57 µg/ml and 19.7 µg/ml concentrations (FC 1.67 and 2.26, respectively).

Modulation of pathway maps #2 and #149 was also associated with upregulation of the POMC transcript, which can be post-translationally processed in the pituitary gland into ACTH, endorphins (α-, β-, γ-EP), and melanotropins (α-, β-, γ-MSH). These biopeptides are active in the central melanocortin system and regulate energy metabolism and body weight homeostasis (Li et al., 2023). These findings are consistent with the DEHP-induced endocrine disruption and neurotoxicity observed *in vivo* in rodents, particularly in the hypothalamus and limbic system (Lv et al., 2016). Lv et al. identified a link between DEHP-induced hypothyroidism and obesity, supported by the downregulation of the thyroid hormone receptor (TR) -β and RXR genes in C3H/He mice treated with DEHP.

Many studies have shown that DEHP disrupts the integrity of the hypothalamic-pituitary-thyroid axis, affecting thyroid hormone synthesis, secretion, and metabolism. Oral exposure studies in rats revealed thyroid hyperactivity, increased lysosome size and number, Golgi apparatus

hypertrophy, and endoplasmic reticulum stress (Rowdhwal and Chen, 2018).

Our data revealed the upregulation of two TRs at 24 h: TR-β [Thrb (A_51_P388835) FC 2.95 and Thrb (A_52_P532559) FC 1.58] and TR-α (FC 1.66), along with a slight upregulation of the parathyroid hormone transcript (PTH), which regulates calcium ion homeostasis. The upregulation persisted at 72 h (at the higher concentration) [Thrb (A_51_P388835) FC 2.69], along with the upregulation of the thyroid-stimulating hormone-releasing hormone transcript (Trh, FC 2.03). Notably, TR-α was downregulated at 32 d for the higher concentration [Thra (A_52_P666930) FC -1.66 and Thra (A_66_P102879) FC -1.73].

The nuclear hormone receptor NR4A3 transcript was strongly downregulated at 32 d across all three concentrations (FC -7.83, -28.41, and -18.08, respectively). This gene encodes a member of the steroid-thyroid-retinoid hormone receptor superfamily. *In vivo* knockout mouse studies have shown that silencing the NR4A3 gene induces obesity, glucose intolerance, and elevated blood glucose levels (Yang et al., 2020).

Fibroblast growth factor 1 (FGF1), another key regulator of metabolism, especially in bile acid, lipid, and carbohydrate metabolism, was slightly upregulated in this study, although the downstream signaling pathway was generally inhibited. FGFR1 and FGF1 play a role in adipogenesis regulation and may contribute to obesity by modulating adipocyte numbers (Wang et al., 2020; Hamzé et al., 2022; Sancar et al., 2022).

Notably, the 24-hour DEGs list revealed a strong upregulation of the FGF21 transcript (FC 22.03). FGF21 is a peptide hormone with pleiotropic effects on the regulation of insulin sensitivity, glucose and lipid homeostasis. In fact, *in vitro* evidence suggests that FGF21 secretion enhances basal glucose uptake in MEHP-treated adipocytes (Hsu et al., 2019). Hsu et al. found glucose uptake and GLUT1 upregulation to be independent of insulin signaling, which may also provide a possible explanation for the GLUT4 upregulation observed in our study, along with the downregulation of insulin signaling. Interestingly, both FGF1 and FGF21 expression in adipose tissue are regulated by PPARγ (Hsu et al., 2019; Sancar et al., 2022).

PPARγ upregulation at 72 h was confirmed for both the 19.7 µg/ml and 6.57 µg/ml concentrations (with the latter identified from a reduced dataset analysis filtered by CV).

Additionally, our dataset showed upregulation of EGF transcripts at both 24 h and 72 h, along with downregulation of transcripts related to PDGF, insulin and modulation of pathways associated with metabolism and cell cycle regulation.

Overall, these findings support the toxic effects of DEHP on cellular metabolism, suggesting that the disruption of insulin signaling could lead to impaired glucose utilization and lipid synthesis. These results are consistent with literature linking DEHP to obesity, hypothyroidism, lipid metabolism disorders, liver toxicity, adrenal dysfunction, elevated blood glucose, energy imbalance, and insulin resistance in both humans and

rodents (Tickner et al., 2001; Lv et al., 2016; Dales et al., 2018; Zhang et al., 2023).

Notably the EGF signaling pathway plays a role in mediating the early effects of phthalates on placental function (Grindler et al., 2018).

Thyroid dysfunction associated with DEHP exposure has also been linked to its estrogenic activity, as it can act as an antagonist of 17-beta estradiol, altering estrogen synthesis by inducing CYP19A1 aromatase expression (Chen et al., 2016; Xu et al., 2022; Zheng et al., 2023).

Simultaneously, as previously discussed, DEHP can modulate AhR and PPAR signaling pathways, potentially interfering with estrogen synthesis by upregulating CYP1B1 (upregulated in this study with FC 1.4 at 24 h and FC 2.34 at 72 h) and inhibiting CYP19 expression (Villard et al., 2007; Ernst et al., 2014).

Both PPARα and PPARγ have also been shown to interfere with estradiol synthesis via molecular competition, affecting estrogen signaling (Mu et al., 2000; Yanase et al., 2001; Fan et al., 2005).

As seen in the results, the 24-hour transcriptional profile shows modulation of several enzymes involved in estrogen biosynthesis (CYP2C19 FC 1.58; HSD17B7 FC -2.67; HSD17B8 FC 1.64; HSD17B1 FC 1.5; CYP2C29 FC 4.21), estradiol metabolism (CYP2C65 FC 9.39; CYP2C65 FC 23.92; CYP3A16 FC 1.6; CYP1A1 FC 1.69; UGT1A10 FC 2.58; UGT2A1 FC -1.78), with some modulations persisting at 72 hours, alongside upregulation of the estrogen receptor ESR1 (FC 1.61). Modulation of the GnRH receptor observed in the 24-hour transcriptional

profile could also be linked to AhR signaling disruption, as demonstrated in a study with TCDD (Horling et al., 2011).

In vivo studies confirmed that DEHP exposure increased GnRH secretion and protein expression in the hypothalamus of adolescent female rats. This hormonal dysregulation can interfere with the IGF-1/PI3K/Akt/mTOR signaling pathway in the hypothalamus, affecting the function of the hypothalamic-pituitary-gonadal axis (Shao et al., 2019). These results are supported by the modulation of GnRH signaling pathways in the 32-day transcriptional profiles for both 19.7 µg/ml and 6.57 µg/ml concentrations.

7.2.4 – Comprehensive Analysis of molecular effects of DEHP and Final Remarks

Based on the comparison of the various transcriptional profiles obtained, a comprehensive analysis of the temporal evolution of the molecular effects of DEHP in the BALB/c 3T3 A31-1-1 model was proposed (Fig. 7.1).

First, a recurring modulation of the ERK/c-Fos signaling pathway was observed. It began with downregulation in the 24-hour dataset, followed by upregulation at 72 h, indicated by increased expression of genes such as p-300, c-Fos, and AP-1 complex members. Finally, a strong downregulation was observed in the 32-day transcriptional profile (FC -5.72 for 1.97 µg/ml; FC -24.65 for 6.57 µg/ml, and FC -39.46 for 19.7 µg/ml). While the ERK/c-Fos signaling pathway is typically involved in early and transient cellular responses to environmental stimuli, in this

case, the most pronounced modulation occurred 28 d after treatment. The highest concentration (19.7 µg/ml) resulted in a ~50% reduction in cell viability in the cytotoxicity assay, compared to ~10% for the intermediate concentration (6.57 µg/ml), and no cytotoxic effect at the lowest one (1.97 µg/ml). This suggests that the ERK/c-Fos pathway modulation is not directly linked to the cytotoxicity of the substance.

The calcium signaling pathway also displayed dynamic modulation, with activation at 24 h and 72 h, supported by upregulation of the IP3 receptor and modulation of the "*Signal transduction_Calcium-mediated signaling*" pathway, followed by downregulation at 32 d for both 6.57 µg/ml and 19.7 µg/ml concentrations. In the transcriptional profiles following 72 h of treatment, only the 19.7 µg/ml concentration led to significant gene modulation involving apoptosis, oxidative stress response, and inflammation. Although the 6.57 µg/ml concentration did not show significant gene regulation at 72 h through canonical analysis, preliminary data from the filtered, reduced dataset indicated significant modulations consistent with those observed in the 19.7 µg/ml profile, showing a dose-response relationship. This suggests that beyond applying a CV filter, the dataset size also affects DEGs identification. Consistent with the CTA assay results, the intermediate concentration showed a moderate response compared with the highest concentration, both in terms of cellular metabolism modulation and inflammatory response. These findings further support the modulations observed in the highly cytotoxic 19.7 µg/ml concentration profile.

At day 32, gene modulation exhibited a concentration-dependent pattern, with downregulation being the predominant effect. These changes suggest the potential mechanisms of action mediated by DEHP, involving similar entities observed at 24 h and 72 h, though often differing in their specific modulations. Furthermore, the absence of signaling pathways typical of a tumor microenvironment was noted. This finding was consistent with the lack of cellular transformation observed at the end of the CTA. Figure 7.1 shows the evolution of the DEHP toxicogenomic profile in our model, in relation to the phenotypic endpoints observed in the CTA assay.

Interestingly, despite the use of mouse embryonic fibroblasts in this model, neuroendocrine transcript alterations emerged both at 24 h as early molecular interactions and at 32 d, indicating a lasting imbalance in the cells.

In this study, mode of action of DEHP, linked to energy homeostasis disruption as described in *in vivo* models, was similarly observed in the molecular toxicity data from 3T3 cells. Additionally, the data support receptor activation as a critical mechanism mediating effects of DEHP, particularly through the activation of PPARα, AhR, and PXR.

It is also noteworthy that HNF4α, whose downregulation has been associated with the development of various cancers and in hepatocarcinogenesis, was upregulated in this study.

Additionally, the activation of AhR signaling and the induction of detoxifying enzymes, such as UGTs, are proposed to facilitate the efficient elimination of DEHP and mitigate cellular transformation.

At the same time, other studies have suggested a potential role for UGT1A1 in mediating hypothyroxinemia (Zhang et al., 2018).

These hypotheses could be further investigated through CTAs using DEHP metabolites, particularly MEHP, which exhibits higher bioactivity, as well as by examining the metabolic capacity of the BALB/c model.

In this study, modulation of various gap junctions was also observed, with downregulation after 24 h of treatment and upregulation at the end of 72 h. This downregulation may represent the cell's attempts to cope with chemical stress. Additionally, GJIC inhibition is considered to be a late key event in the chain of events leading to hepatotoxicity and hepatocarcinogenesis in rodents (Ito et al., 2007; Corton et al., 2014; Rajesh and Balasubramanian, 2014).

In the BALB/c 3T3 A31-1-1 model, GJIC inhibition appears to be a reversible mechanism, consistent with findings in other models (Cruciani et al., 1997; Isenberg et al., 2000). This raises the question of whether the repeated induction of this mechanism could contribute to carcinogenic outcomes.

Sustained cell proliferation can be considered a hallmark necessary, although not sufficient, for the progression toward malignancy in CTA models and *in vivo* tumor processes (Colacci et al., 2023). The

absence of clear signals related to sustained proliferation, particularly those supporting EMT and cytoskeleton remodeling at 72 h, suggests that the process leading to oncotransformation was not initiated or was interrupted, potentially through apoptosis induction, to prevent damaged cell replication.

This hypothesis is further supported by comparing the gene modulations observed in this study with those observed in the SHE model by Landkocz et al., particularly regarding the downregulation of anti-apoptotic factors and upregulation of tumor suppressor transcripts at 24 h and 72 h. In summary, the SHE model revealed cancer biomarkers associated with sustaining cell proliferation. In contrast, the present study using the BALB/c 3T3 A31-1-1 model identified molecular biomarkers more closely related to cell death.

In conclusion, the observed gene modulations aligned with the phenotypic endpoint of no cellular transformation.

. Additionally, the study combining CTA with transcriptomics demonstrated a high concordance with existing literature on the endocrine-disrupting activity of DEHP. The comparison with data obtained from the SHE model provided a deeper understanding of the mechanisms underlying the results observed in the different CTA models. Understanding this aspect is important to improve both the use of CTA in the IATA for non-genotoxic compounds and the choice of model when testing a potentially non-carcinogenic chemicall.

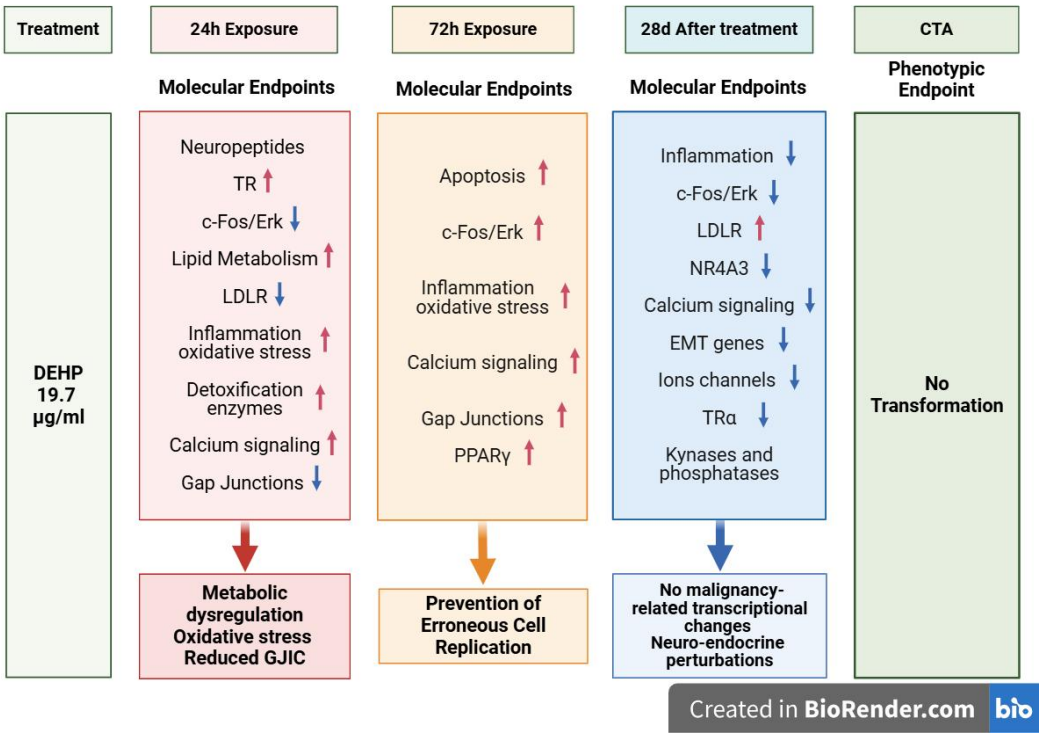

Fig 7.1 – Temporal dynamics of key molecular endpoints during DEHP treatment. This scheme summarizes the molecular and phenotypic changes observed at different time points (24 h, 72 h, and 28 d after 72-hour treatment) following exposure to 19.7 µg/ml DEHP. No transcriptional alterations associated with malignancy were detected, consistent with the non-transforming results from the Cell Transformation Assay (CTA). TR: Thyroid Receptors; LDLR: Low-Density Lipoprotein Receptor; GJIC: Gap Junction Intercellular Communication; PPARγ: Peroxisome Proliferator-Activated Receptor Gamma; NR4A3: Nuclear Receptor Subfamily 4 Group A Member 3; EMT: Epithelial-Mesenchymal Transition.

7.3 – Cytotoxicity and Carcinogenic Potential of PFOS with PPARα Antagonist GW6471 Co-Treatment: Evidence of PPARα-Independent Mechanisms

In this study, we used a CTA to explore whether altering the activity of the PPARα receptor, a key carcinogenic mechanism for PFAS, could affect the transforming potential of PFOS in the BALB/c 3T3 A31-1-1 model.

The synthetic compound GW6471 was used for this purpose (both as a pre-treatment and co-treatment), as it is a specific PPARα antagonist. GW6471 acts by directly binding to the receptor, inducing a conformational change that inhibits co-activator binding, while promoting the recruitment of co-repressors (SMRT and NCoR) (Xu et al., 2002). The PPARα antagonist activity of GW6471 shows an IC50 of 0.15 µg/ml (0.24 µM) for inhibiting receptor activity (Xu et al., 2002).

It is also worth noting that GW6471 has shown antiproliferative activity in several tumor cell lines (Abu Aboud et al., 2015; Ammazzalorso et al., 2020; Castelli et al., 2021).

To maximize the inhibitory effect, GW6471 was administered both before and during the PFOS treatment. This co-treatment approach likely allowed GW6471 to bind to PPARα preemptively, in the absence of molecular competition, and during PFOS exposure. The chosen inhibitor concentration, 0.6 µg/ml, was close to the maximum non-cytotoxic concentration observed in the clonogenic assay (CFE).

As shown in the results, the first CFE revealed a statistically significant increase in cloning efficiency compared to the DMSO control for

concentrations of 0.20 µg/ml and 0.30 µg/ml, based on Dunnet's two-way test. However, this proliferative effect was not confirmed in the second CFE, indicating a need for further investigation. Conversely, both assays consistently showed reduced clonogenic efficiency and confirmed the non-cytotoxic nature of the 0.6 µg/ml concentration, as also observed in the CFE conducted parallel to the CTA.

Regarding the co-treatment effects tested in the CTA, the assay showed a higher clonogenic efficiency in the PFOS + GW6471 treatment group than in the PFOS-only group (Fig.6.4; $p<0.05$). A similar effect was observed in an MCF-10A model using an MTT assay with PFOA (Pierozan et al., 2018).

This higher clonogenic efficiency may be attributed to its inhibitory effect on PPARα, which reduces downstream signaling cascades following receptor activation.

In the transformation test, PFOS concentrations demonstrated a significant effect on cellular transformation, consistent with findings from CTA performed by Vaccari et al., according to GLP principles (Vaccari et al., 2024). Co-treatment with GW6471 did not produce a statistically significant change in the transforming potential of PFOS based on the Mann-Whitney test. Similarly, Poisson regression analysis revealed no significant differences in transformation frequency (TF) between the various PFOS doses and their combinations with GW6471. Although TF appears to increase in the GW6471 co-treated samples (Tab. 6.4), this increase is not statistically significant. The observed rise in TF is likely due

to the reduction in cytotoxicity induced by the co-treatment, allowing a greater number of cells to survive and potentially undergo transformation.

These findings support the hypothesis that PPARα activation is not sufficient to explain PFOS carcinogenicity, and that PFOS may induce cellular transformation in the BALB/c 3T3 A31-1-1 model through PPARα-independent mechanisms.

Two considerations from other studies support this hypothesis: i) PFOA, which showed reduced cytotoxicity in the MCF-10A model in the presence of GW6471, had higher PPARα agonist activity than PFOS; ii) PFOA yielded negative results in the BALB/c 3T3 A31-1-1 CTA (Vaccari et al., 2024).

However, it is important to emphasize that this study did not quantify the activation or inhibition of PPARα during co-treatment with GW6471. The inhibitor tends to reduce receptor activation rather than fully suppress it; therefore, it is plausible that some level of PPARα activation occurred following PFOS treatment. Nonetheless, given that the transformation effect was dose-dependent, with increased cellular transformation correlated with concentration, it is reasonable to expect that a reduction in the primary mechanism of action would similarly reduce this effect, as observed in the cytotoxicity assay.

In conclusion, the use of CTA in this study provides valuable mechanistic insights into the role of PPARα in PFOS-induced cellular transformation. The absence of a significant effect of GW6471 co-treatment on PFOS transforming potential suggested that PPARα

activation may play a secondary role in the transformation process in the BALB/c 3T3 A31-1-1 model. This highlights the complexity of the mechanisms involved and underscores the utility of CTA in unraveling the carcinogenic pathways of PFAS.

Moreover, although simple in design, this approach exemplifies the versatility of *in vitro* assays such as CTA, which, through different types of implementation, can facilitate the study of carcinogenic mechanisms *in vitro*.

CHAPTER 8

Conclusions

This thesis provides new insights into non-genotoxic carcinogenesis and methodologies for assessing non-genotoxic carcinogens, focusing on DEHP and PFOS through the use of NAMs based on the BALB/c 3T3 A31-1-1 CTA.

Non-genotoxic compounds, such as DEHP and PFOS, present challenges in chemical risk assessment due to their multifaceted mechanisms of action, which include, receptor-mediated events, endocrine disruption, and metabolic alterations. This study examined these mechanisms, supporting the application of *in vitro* models for evaluating non-genotoxic carcinogens and the inclusion of the Transformics approach in an IATA for non-genotoxic carcinogens.

Key findings indicated that DEHP, did not induce cellular transformation in the BALB/c 3T3 A31-1-1 cell line, whereas PFOS exhibited transforming effects. Transcriptomic analysis of DEHP-treated cells revealed concentration-dependent modulation of gene expression related to cellular signaling and metabolic pathways, consistent with its endocrine-disrupting effects. These dose-related changes in expression at different time points allowed for a distinction between adaptive and adverse responses. The study underscores the critical role of assessing the solubility of tested compounds, as this property significantly affects

their bioavailability and bioactivity, ultimately influencing the reliability of experimental outcomes

Moreover the potential presence of diverse DEHP metabolites with different reactivities underscores the importance of metabolic competence in assessing effects, and adds an interpretive layer to the varying CTA results in previous studies. In this context, it is important to acknowledge some potential limitations. Specifically the metabolic competence of the BALB/c 3T3 A31-1-1 model, iparticularly its capacity to metabolize DEHP and generate active metabolites, cannot be conclusively determined within the scope of this study.

Further studies are needed to clarify whether the absence of cellular transformation is due to insufficient metabolization of DEHP and the lack of reactive metabolites, or to the ability of the cells to neutralize reactive metabolites through detoxification mechanisms. This highlights the critical importance of considering the metabolic capacity and specific metabolite profiles of the experimental model when interpreting *in vitro* results. To address this issue, additional CTAs using DEHP metabolites, particularly MEHP,could offer more definitive insights.

These findings also emphasize the necessity of a comprehensive panel of tests that evaluating multiple biological endpoints to accurately assess the carcinogenic potential of chemicals.

Nevertheless the integration of transcriptomics with CTA is particularly valuable, as it enhances sensitivity, specificity, and predictivity within a battery of tests aligned with an IATA framework. This approach

not only facilitates the screening of new chemicals by covering a broad spectrum of molecular activities but also enables deeper mechanistic investigations into molecular interactions among multiple KEs. Additionally, the role of PPARα activation in PFOS-induced transformation was explored using co-treatment with a receptor antagonist. The results revealed that PPARα alone may not fully account for the transforming effects of PFOS, suggesting the involvement of alternative pathways in our model.

Evaluation of biological plausibility plays a critical role in data interpretation for risk assessment applications. This process involves extrapolating findings from model systems to human health contexts and developing a mechanistic understanding that links the relevant KEs to compound biological activity. Transcriptomics combined with CTA provides extensive molecular data that support the identification and interconnection of KEs, including MIEs, which are essential for a comprehensive understanding of non-genotoxic carcinogenesis.

The consistency of the DEHP-associated signaling pathways with those documented in rodent and human studies further supports the robustness of our approach. Moreover, although extrapolating these findings to human biology remains challenging, our study suggests certain metabolic pathways may be associated with human DEHP exposure. In conclusion, the integrated approaches employed in this study, combining CTA with transcriptomics and receptor-specific antagonists, demonstrated the versatility and applicability of these *in vitro* assays to elucidate the

complex mechanisms of non-genotoxic carcinogenesis. The insights gained contribute to enhancing chemical assessment methodologies and underscore the need for continued advancement of *in vitro* methods that bridge mechanistic understanding with predictive power for human health outcomes.

References

Aaronson, S.A., Todaro, G.J., 1968. *Development of 3T3-like lines from Balb/c mouse embryo cultures: Transformation susceptibility to SV40*. Journal of Cellular Physiology 72, 141–148. https://doi.org/10.1002/jcp.1040720208

Abu Aboud, O., Donohoe, D., Bultman, S., Fitch, M., Riiff, T., Hellerstein, M., Weiss, R.H., 2015. *PPARα inhibition modulates multiple reprogrammed metabolic pathways in kidney cancer and attenuates tumor growth*. American Journal of Physiology-Cell Physiology 308, C890–C898. https://doi.org/10.1152/ajpcell.00322.2014

Albro, P.W., Corbett, J.T., 1978. *Distribution of Di- and Mono-(2-Ethylhexyl) Phthalate in Human Plasma*. Transfusion 18, 750–755. https://doi.org/https://doi.org/10.1046/j.1537-2995.1978.18679077962.x

Alexander, B.H., Ryan, A., Church, T.R., Kim, H., Olsen, G.W., Logan, P.W., 2024. *Mortality and cancer incidence in perfluorooctanesulfonyl fluoride production workers*. American Journal of Industrial Medicine 67, 321–333. https://doi.org/https://doi.org/10.1002/ajim.23568

Amara, I., Timoumi, R., Annabi, E., Salem, I. Ben, Abid-Essefi, S., 2020. *Di(2-ethylhexyl) phthalate inhibits glutathione regeneration and dehydrogenases of the pentose phosphate pathway on human colon carcinoma cells*. Cell Stress and Chaperones 25, 151–162. https://doi.org/10.1007/s12192-019-01060-5

Ames, B.N., 1979. *Identifying Environmental Chemicals Causing Mutations and Cancer*. Science 204, 587–593. https://doi.org/10.1126/science.373122

Ammazzalorso, A., Bruno, I., Florio, R., de Lellis, L., Laghezza, A., Cerchia, C., de Filippis, B., Fantacuzzi, M., Giampietro, L., Maccallini, C., Tortorella, P., Veschi, S., Loiodice, F., Lavecchia, A., Cama, A., Amoroso, R., 2020. *Sulfonimide and Amide Derivatives as Novel PPARα Antagonists: Synthesis, Antiproliferative Activity, and Docking Studies*. ACS Medicinal Chemistry Letters 11, 624–632. https://doi.org/10.1021/acsmedchemlett.9b00666

Andersen, C., Krais, A.M., Eriksson, A.C., Jakobsson, J., Löndahl, J., Nielsen, J., Lindh, C.H., Pagels, J., Gudmundsson, A., Wierzbicka, A., 2018. *Inhalation and Dermal Uptake of Particle and Gas-Phase Phthalates? A Human Exposure Study*. Environmental Science & Technology 52, 12792–12800. https://doi.org/10.1021/acs.est.8b03761

Arbuckle, T.E., Fisher, M., MacPherson, S., Lang, C., Provencher, G., LeBlanc, A., Hauser, R., Feeley, M., Ayotte, P., Neisa, A., Ramsay, T., Tawagi, G., 2016. *Maternal and early life exposure to phthalates: The Plastics and Personal-care Products use in Pregnancy (P4) study*. Science of The Total Environment 551–552, 344–356. https://doi.org/https://doi.org/10.1016/j.scitotenv.2016.02.022

Armstrong, L.E., Guo, G.L., 2019. *Understanding Environmental Contaminants' Direct Effects on Non-alcoholic Fatty Liver Disease Progression*. Current Environmental Health Reports 6, 95–104. https://doi.org/10.1007/s40572-019-00231-x

Asgharzadeh, F., Memarzia, A., Alikhani, V., Beigoli, S., Boskabady, M.H., 2024. *Peroxisome proliferator-activated receptors: Key regulators of tumor progression and growth*. Translational Oncology 47, 102039. https://doi.org/https://doi.org/10.1016/j.tranon.2024.102039

Ashby, J., Tennant, R.W., 1988. Chemical structure, Salmonella mutagenicity and extent of carcinogenicity as indicators of genotoxic carcinogenesis among 222 chemicals tested in rodents by the U.S. NCI/NTP, Mutation Research.

ATSDR, 2022. Toxicological Profile for Di(2-Ethylhexyl)Phthalate (DEHP). Atlanta.

Audebert, M., Assmann, A.S., Azqueta, A., Babica, P., Benfenati, E., Bortoli, S., Bouwman, P., Braeuning, A., Burgdorf, T., Coumoul, X., Debizet, K., Dusinska, M.,

Ertych, N., Fahrer, J., Fetz, V., Le Hégarat, L., López de Cerain, A., Heusinkveld, H.J., Hogeveen, K., Jacobs, M.N., Luijten, M., Raitano, G., Recoules, C., Rundén-Pran, E., Saleh, M., Sovadinová, I., Stampar, M., Thibol, L., Tomkiewicz, C., Vettorazzi, A., Van de Water, B., El Yamani, N., Zegura, B., Oelgeschläger, M., 2023. *New approach methodologies to facilitate and improve the hazard assessment of non-genotoxic carcinogens-a PARC project*. Frontiers in toxicology 5. https://doi.org/10.3389/FTOX.2023.1220998

Aueviriyavit, S., Furihata, T., Morimoto, K., Kobayashi, K., Chiba, K., 2007. *Hepatocyte nuclear factor 1 alpha and 4 alpha are factors involved in interindividual variability in the expression of UGT1A6 and UGT1A9 but not UGT1A1, UGT1A3 and UGT1A4 mRNA in human livers.* Drug metabolism and pharmacokinetics 22, 391–398. https://doi.org/10.2133/dmpk.22.391

Bajagain, R., Panthi, G., Park, J.H., Moon, J.K., Kwon, J., Kim, D.Y., Kwon, J.H., Hong, Y., 2023. *Enhanced migration of plasticizers from polyvinyl chloride consumer products through artificial sebum*. Science of the Total Environment 874. https://doi.org/10.1016/j.scitotenv.2023.162412

Ballesteros, V., Costa, O., Iñiguez, C., Fletcher, T., Ballester, F., Lopez-Espinosa, M.-J., 2017. *Exposure to perfluoroalkyl substances and thyroid function in pregnant women and children: A systematic review of epidemiologic studies*. Environment International 99, 15–28. https://doi.org/https://doi.org/10.1016/j.envint.2016.10.015

Balmain, A., 2020. *The critical roles of somatic mutations and environmental tumor-promoting agents in cancer risk*. Nature Genetics. https://doi.org/10.1038/s41588-020-00727-5

Barrett, E.S., Corsetti, M., Day, D., Thurston, S.W., Loftus, C.T., Karr, C.J., Kannan, K., LeWinn, K.Z., Smith, A.K., Smith, R., Tylavsky, F.A., Bush, N.R., Sathyanarayana, S., 2022. *Prenatal phthalate exposure in relation to placental corticotropin releasing hormone (pCRH) in the CANDLE cohort*. Environment International 160, 107078. https://doi.org/https://doi.org/10.1016/j.envint.2022.107078

Baumert, B.O., Fischer, F.C., Nielsen, F., Grandjean, P., Bartell, S., Stratakis, N., Walker, D.I., Valvi, D., Kohli, R., Inge, T., Ryder, J., Jenkins, T., Sisley, S., Xanthakos, S., Rock, S., La Merrill, M.A., Conti, D., McConnell, R., Chatzi, L., 2023. *Paired Liver:Plasma PFAS Concentration Ratios from Adolescents in the Teen-LABS Study and Derivation of Empirical and Mass Balance Models to Predict and Explain Liver PFAS Accumulation*. Environmental Science and Technology 57, 14817–14826. https://doi.org/10.1021/acs.est.3c02765

Beesoon, S., Martin, J.W., 2015. *Isomer-Specific Binding Affinity of Perfluorooctanesulfonate (PFOS) and Perfluorooctanoate (PFOA) to Serum Proteins*. Environmental Science & Technology 49, 5722–5731. https://doi.org/10.1021/es505399w

Benigni, R., Bossa, C., Tcheremenskaia, O., Battistelli, C.L., Giuliani, A., 2015. *The Syrian hamster embryo cells transformation assay identifies efficiently nongenotoxic carcinogens, and can contribute to alternative, integrated testing strategies*. Mutation Research/Genetic Toxicology and Environmental Mutagenesis 779, 35–38. https://doi.org/https://doi.org/10.1016/j.mrgentox.2015.02.001

Benjamin, S., Masai, E., Kamimura, N., Takahashi, K., Anderson, R.C., Faisal, P.A., 2017. Phthalates impact human health: Epidemiological evidences and plausible mechanism of action, Journal of Hazardous Materials.

Berenblum, I., Shubik, P., 1947. *A New, Quantitative, Approach to the Study of the Stages of Chemical Carcinogenesis in the Mouse's Skin*. British Journal of Cancer 1, 383. https://doi.org/10.1038/BJC.1947.36

Berwald, Y., Sachs, L., 1963. *In Vitro Cell Transformation with Chemical Carcinogens*. Nature 200, 1182–1184. https://doi.org/10.1038/2001182a0

Biggeri, A., Stoppa, G., Facciolo, L., Fin, G., Mancini, S., Manno, V., Minelli, G., Zamagni, F., Zamboni, M., Catelan, D., Bucchi, L., 2024. *All-cause, cardiovascular disease and cancer mortality in the population of a large Italian area contaminated by perfluoroalkyl and polyfluoroalkyl substances (1980–2018)*. Environmental Health 23, 42.

https://doi.org/10.1186/s12940-024-01074-2

Bline, A.P., DeWitt, J.C., Kwiatkowski, C.F., Pelch, K.E., Reade, A., Varshavsky, J.R., 2024. *Public Health Risks of PFAS-Related Immunotoxicity Are Real*. Current Environmental Health Reports 11, 118–127. https://doi.org/10.1007/s40572-024-00441-y

Bray, F., Laversanne, M., Sung, H., Ferlay, J., Siegel, R.L., Soerjomataram, I., Jemal, A., 2024. *Global cancer statistics 2022: GLOBOCAN estimates of incidence and mortality worldwide for 36 cancers in 185 countries*. CA: A Cancer Journal for Clinicians 74, 229–263. https://doi.org/10.3322/caac.21834

Burk, O., Arnold, K.A., Geick, A., Tegude, H., Eichelbaum, M., 2005. *A role for constitutive androstane receptor in the regulation of human intestinal MDR1 expression*. Biological Chemistry 386, 503–513. https://doi.org/doi:10.1515/BC.2005.060

Butenhoff, J.L., Chang, S.-C., Olsen, G.W., Thomford, P.J., 2012. *Chronic dietary toxicity and carcinogenicity study with potassium perfluorooctanesulfonate in Sprague Dawley rats*. Toxicology 293, 1–15. https://doi.org/https://doi.org/10.1016/j.tox.2012.01.003

Cao, L., Guo, Y., Chen, Y., Hong, J., Wu, J., Hangbiao, J., 2022. *Per-/polyfluoroalkyl substance concentrations in human serum and their associations with liver cancer*. Chemosphere 296, 134083. https://doi.org/https://doi.org/10.1016/j.chemosphere.2022.134083

Castelli, V., Catanesi, M., Alfonsetti, M., Laezza, C., Lombardi, F., Cinque, B., Cifone, M.G., Ippoliti, R., Benedetti, E., Cimini, A., D'angelo, M., 2021. *Pparα-selective antagonist gw6471 inhibits cell growth in breast cancer stem cells inducing energy imbalance and metabolic stress*. Biomedicines 9, 1–17. https://doi.org/10.3390/biomedicines9020127

Chen, F.-P., Chien, M.-H., Chern, I.Y.-Y., 2016. *Impact of low concentrations of phthalates on the effects of 17β-estradiol in MCF-7 breast cancer cells*. Taiwanese Journal of Obstetrics and Gynecology 55, 826–834. https://doi.org/https://doi.org/10.1016/j.tjog.2015.11.003

Chen, Y.-M., Guo, L.-H., 2009. *Fluorescence study on site-specific binding of perfluoroalkyl acids to human serum albumin*. Archives of Toxicology 83, 255–261. https://doi.org/10.1007/s00204-008-0359-x

Chen, Y., Lv, D., Li, X., Zhu, T., 2018. *PM2.5-bound phthalates in indoor and outdoor air in Beijing: Seasonal distributions and human exposure via inhalation*. Environmental Pollution 241, 369–377. https://doi.org/10.1016/j.envpol.2018.05.081

Cheng, W., Ng, C.A., 2017. *A Permeability-Limited Physiologically Based Pharmacokinetic (PBPK) Model for Perfluorooctanoic acid (PFOA) in Male Rats*. Environmental Science and Technology 51, 9930–9939. https://doi.org/10.1021/acs.est.7b02602

Choi, K., Joo, H., Campbell, J.L., Clewell, R.A., Andersen, M.E., Clewell, H.J., 2012. *In vitro metabolism of di(2-ethylhexyl) phthalate (DEHP) by various tissues and cytochrome P450s of human and rat*. Toxicology in Vitro 26, 315–322. https://doi.org/https://doi.org/10.1016/j.tiv.2011.12.002

Clewell, R.A., Sochaski, M., Edwards, K., Creasy, D.M., Willson, G., Andersen, M.E., 2013. *Disposition of diisononyl phthalate and its effects on sexual development of the male fetus following repeated dosing in pregnant rats*. Reproductive Toxicology 35, 56–69. https://doi.org/https://doi.org/10.1016/j.reprotox.2012.07.001

Colacci, A., Corvi, R., Ohmori, K., Paparella, M., Serra, S., Da Rocha Carrico, I., Vasseur, P., Jacobs, M.N., 2023. *The Cell Transformation Assay: A Historical Assessment of Current Knowledge of Applications in an Integrated Approach to Testing and Assessment for Non-Genotoxic Carcinogens*. International Journal of Molecular Sciences. https://doi.org/10.3390/ijms24065659

Colacci, A., Mascolo, M.G., Perdichizzi, S., Quercioli, D., Gazzilli, A., Rotondo, F., Morandi, E., Guerrini, A., Silingardi, P., Grilli, S., Vaccari, M., 2011. *Different sensitivity of BALB/c 3T3 cell clones in the response to carcinogens*. Toxicology in Vitro 25, 1183–1190. https://doi.org/10.1016/j.tiv.2011.05.032

Coperchini, F., Croce, L., Ricci, G., Magri, F., Rotondi, M., Imbriani, M., Chiovato, L., 2021. *Thyroid Disrupting Effects of Old and New Generation PFAS*. Frontiers in Endocrinology. https://doi.org/10.3389/fendo.2020.612320

Corton, J.C., Cunningham, M.L., Hummer, B.T., Lau, C., Meek, B., Peters, J.M., Popp, J.A., Rhomberg, L., Seed, J., Klaunig, J.E., 2014. *Mode of action framework analysis for receptor-mediated toxicity: The peroxisome proliferator-activated receptor alpha (PPARα) as a case study*. Critical Reviews in Toxicology. https://doi.org/10.3109/10408444.2013.835784

Corton, J.C., Peters, J.M., Klaunig, J.E., 2018. *The PPARα-dependent rodent liver tumor response is not relevant to humans: addressing misconceptions*. Archives of Toxicology 92, 83–119. https://doi.org/10.1007/s00204-017-2094-7

Corvi, R., Madia, F., 2017. *In vitro genotoxicity testing–Can the performance be enhanced?* Food and Chemical Toxicology 106, 600–608. https://doi.org/10.1016/j.fct.2016.08.024

Corvi, R., Madia, F., Guyton, K.Z., Kasper, P., Rudel, R., Colacci, A., Kleinjans, J., Jennings, P., 2017. *Moving forward in carcinogenicity assessment: Report of an EURL ECVAM/ ESTIV workshop*. Toxicology in Vitro 45, 278–286. https://doi.org/10.1016/j.tiv.2017.09.010

Creton, S., Aardema, M.J., Carmichael, P.L., Harvey, J.S., Martin, F.L., Newbold, R.F., O'Donovan, M.R., Pant, K., Poth, A., Sakai, A., Sasaki, K., Scott, A.D., Schechtman, L.M., Shen, R.R., Tanaka, N., Yasaei, H., 2012. *Cell transformation assays for prediction of carcinogenic potential: state of the science and future research needs.* Mutagenesis 27, 93–101. https://doi.org/10.1093/mutage/ger053

Cruciani, V., Mikalsen, S.O., Vasseur, P., Sanner, T., 1997. *Effects of peroxisome proliferators and 12-O-tetradecanoyl phorbol-13- acetate on intercellular communication and connexin43 in two hamster fibroblast systems*. International Journal of Cancer 73, 240–248. https://doi.org/10.1002/(SICI)1097-0215(19971009)73:2<240::AID-IJC14>3.0.CO;2-J

Dales, R.E., Kauri, L.M., Cakmak, S., 2018. *The associations between phthalate exposure and insulin resistance, β-cell function and blood glucose control in a population-based sample*. Science of The Total Environment 612, 1287–1292. https://doi.org/https://doi.org/10.1016/j.scitotenv.2017.09.009

Delerive, P., De Bosscher, K., Besnard, S., Vanden Berghe, W., Peters, J.M., Gonzalez, F.J., Fruchart, J.-C., Tedgui, A., Haegeman, G., Staels, B., 1999. *Peroxisome Proliferator-activated Receptor α Negatively Regulates the Vascular Inflammatory Gene Response by Negative Cross-talk with Transcription Factors NF-κB and AP-1 *.* Journal of Biological Chemistry 274, 32048–32054. https://doi.org/10.1074/jbc.274.45.32048

Den Braver-Sewradj, S.P., Piersma, A., Hessel, E.V.S., 2020. *An update on the hazard of and exposure to diethyl hexyl phthalate (DEHP) alternatives used in medical devices*. Critical Reviews in Toxicology. https://doi.org/10.1080/10408444.2020.1816896

EC, 2020. Chemicals Strategy for SustainabilityTowards a Toxic-Free Environment. Brussels.

ECHA, 2023. Bis(2-ethylhexyl) phthalate [WWW Document]. URL https://echa.europa.eu

ECHA, 2024. Key Areas of Regulatory Challenge. Helsinki. https://doi.org/10.2823/858284

ECVAM, 2010. Balb/c 3T3 Cell Transformation Assay Prevalidation study Report. Ispra, Italy.

EFSA Panel on Contaminants in Food Chain, Schrenk, D., Bignami, M., Bodin, L., Chipman, J.K., del Mazo, J., Grasl-Kraupp, B., Hogstrand, C., Hoogenboom, L., Leblanc, J.C., Nebbia, C.S., Nielsen, E., Ntzani, E., Petersen, A., Sand, S., Vleminckx, C., Wallace, H., Barregård, L., Ceccatelli, S., Cravedi, J.P., Halldorsson, T.I., Haug, L.S., Johansson, N., Knutsen, H.K., Rose, M., Roudot, A.C., Van Loveren, H., Vollmer, G., Mackay, K., Riolo, F., Schwerdtle, T., 2020. *Risk to human health related to the presence of perfluoroalkyl substances in food*. EFSA Journal 18, 1–391. https://doi.org/10.2903/j.efsa.2020.6223

EFSA Panel on Food Contact Materials Enzymes and Processing Aids, Silano, V., Barat

Baviera, J., Bolognesi, C., Chesson, A., Cocconcelli, P., Crebelli, R., Gott, D., Grob, K., Lampi, E., Mortensen, A., Rivière, G., Steffensen, I.-L., Tlustos, C., Van Loveren, H., Vernis, L., Zorn, H., Cravedi, J.-P., Fortes, C., Poças Tavares, MF Waalkens-Berendsen, I., Wölfle, D., Arcella, D., Cascio, C., Castoldi, A., Volk, K., Castle, L., 2019. Technical report of the public consultation on the 'Draft update of the risk assessment of di-butylphthalate (DBP), butyl-benzyl-phthalate (BBP), bis(2-ethylhexyl)phthalate (DEHP), di-isononylphthalate (DINP) and di-isodecylphthalate (DIDP) for use in foo, EFSA Supporting Publications. John Wiley & Sons, Ltd. https://doi.org/https://doi.org/10.2903/sp.efsa.2019.EN-1747

Elmore, J., Carter, C., Redko, A., Koylass, N., Bennett, A., Mead, M., Ocasio-Rivera, M., Huang, W., Singh, A., August, A., 2022. *ITK independent development of Th17 responses during hypersensitivity pneumonitis driven lung inflammation*. Communications Biology 5. https://doi.org/10.1038/s42003-022-03109-1

Ernst, J., Jann, J.-C., Biemann, R., Koch, H.M., Fischer, B., 2014. *Effects of the environmental contaminants DEHP and TCDD on estradiol synthesis and aryl hydrocarbon receptor and peroxisome proliferator-activated receptor signalling in the human granulosa cell line KGN*. Molecular Human Reproduction 20, 919–928. https://doi.org/10.1093/molehr/gau045

European Chemicals Bureau - Joint Research Centre, 2008. EU RISK ASSESSMENT – BIS(2-ETHYLHEXYL) PHTHALATE. SUNDBYBERG.

Evans, R.M., Mangelsdorf, D.J., 2014. *Nuclear Receptors, RXR, and the Big Bang*. Cell 157, 255–266. https://doi.org/10.1016/j.cell.2014.03.012

Fan, W., Yanase, T., Morinaga, H., Mu, Y.-M., Nomura, M., Okabe, T., Goto, K., Harada, N., Nawata, H., 2005. *Activation of Peroxisome Proliferator-Activated Receptor-γ and Retinoid X Receptor Inhibits Aromatase Transcription via Nuclear Factor-κB*. Endocrinology 146, 85–92. https://doi.org/10.1210/en.2004-1046

Farris, F., Matafora, V., Bachi, A., 2021. *The emerging role of β-secretases in cancer*. Journal of Experimental & Clinical Cancer Research 40, 147. https://doi.org/10.1186/s13046-021-01953-3

Feige, J.N., Gelman, L., Tudor, C., Engelborghs, Y., Wahli, W., Desvergne, B., 2005. *Fluorescence imaging reveals the nuclear behavior of peroxisome proliferator-activated receptor/retinoid X receptor heterodimers in the absence and presence of ligand*. Journal of Biological Chemistry 280, 17880–17890. https://doi.org/10.1074/jbc.M500786200

Felter, S.P., Boobis, A.R., Botham, P.A., Brousse, A., Greim, H., Hollnagel, H.M., Sauer, U.G., 2020. *Hazard identification, classification, and risk assessment of carcinogens: too much or too little?–Report of an ECETOC workshop*. Critical Reviews in Toxicology 50, 72–95. https://doi.org/10.1080/10408444.2020.1727843

Fenton, S.E., Ducatman, A., Boobis, A., DeWitt, J.C., Lau, C., Ng, C., Smith, J.S., Roberts, S.M., 2021. *Per- and Polyfluoroalkyl Substance Toxicity and Human Health Review: Current State of Knowledge and Strategies for Informing Future Research*. Environmental Toxicology and Chemistry. https://doi.org/10.1002/etc.4890

Florio, R., De Lellis, L., Veschi, S., Verginelli, F., di Giacomo, V., Gallorini, M., Perconti, S., Sanna, M., Mariani-Costantini, R., Natale, A., Arduini, A., Amoroso, R., Cataldi, A., Cama, A., 2018. *Effects of dichloroacetate as single agent or in combination with GW6471 and metformin in paraganglioma cells*. Scientific Reports 8. https://doi.org/10.1038/s41598-018-31797-5

Foreman, J.E., Koga, T., Kosyk, O., Kang, B.H., Zhu, X., Cohen, S.M., Billy, L.J., Sharma, A.K., Amin, S., Gonzalez, F.J., Rusyn, I., Peters, J.M., 2021. *Species Differences between Mouse and Human PPARα in Modulating the Hepatocarcinogenic Effects of Perinatal Exposure to a High-Affinity Human PPARα Agonist in Mice*. Toxicological Sciences 183, 81–92. https://doi.org/10.1093/toxsci/kfab068

Fragki, S., Dirven, H., Fletcher, T., Grasl-Kraupp, B., Bjerve Gützkow, K., Hoogenboom, R., Kersten, S., Lindeman, B., Louisse, J., Peijnenburg, A., Piersma, A.H., Princen, H.M.G., Uhl, M., Westerhout, J., Zeilmaker, M.J., Luijten, M., 2021. *Systemic PFOS*

and PFOA exposure and disturbed lipid homeostasis in humans: what do we know and what not? Critical Reviews in Toxicology. https://doi.org/10.1080/10408444.2021.1888073

Franken, N.A.P., Rodermond, H.M., Stap, J., Haveman, J., van Bree, C., 2006. *Clonogenic assay of cells in vitro*. Nature Protocols 1, 2315–2319. https://doi.org/10.1038/nprot.2006.339

Frisbee, S.J., Shankar, A., Knox, S.S., Steenland, K., Savitz, D.A., Fletcher, T., Ducatman, A.M., 2010. *Perfluorooctanoic Acid, Perfluorooctanesulfonate, and Serum Lipids in Children and Adolescents: Results From the C8 Health Project*. Archives of Pediatrics & Adolescent Medicine 164, 860–869. https://doi.org/10.1001/archpediatrics.2010.163

Garvey, G.J., Anderson, J.K., Goodrum, P.E., Tyndall, K.H., Cox, L.A., Khatami, M., Morales-Montor, J., Schoeny, R.S., Seed, J.G., Tyagi, R.K., Kirman, C.R., Hays, S.M., 2023. *Weight of evidence evaluation for chemical-induced immunotoxicity for PFOA and PFOS: findings from an independent panel of experts*. Critical Reviews in Toxicology. https://doi.org/10.1080/10408444.2023.2194913

GBD, 2019. Global Burden of Disease Study 2019 (GBD 2019) Data Resources | GHDx [WWW Document]. URL https://ghdx.healthdata.org/gbd-2019 (accessed 6.18.24).

Ge, X., Weis, K., Flaws, J., Raetzman, L., 2022. *Prenatal exposure to the phthalate DEHP impacts reproduction-related gene expression in the pituitary*. Reproductive Toxicology 108, 18–27. https://doi.org/https://doi.org/10.1016/j.reprotox.2021.12.008

Giesy, J.P., Kannan, K., 2001. *Global Distribution of Perfluorooctane Sulfonate in Wildlife*. Environmental Science & Technology 35, 1339–1342. https://doi.org/10.1021/es001834k

Goodrich, J.A., Walker, D., Lin, X., Wang, H., Lim, T., McConnell, R., Conti, D. V, Chatzi, L., Setiawan, V.W., 2022. *Exposure to perfluoroalkyl substances and risk of hepatocellular carcinoma in a multiethnic cohort*. JHEP Reports 4. https://doi.org/10.1016/j.jhepr.2022.100550

Grabiec, K., Majewska, A., Wicik, Z., Milewska, M., Błaszczyk, M., Grzelkowska-Kowalczyk, K., 2016. *The effect of palmitate supplementation on gene expression profile in proliferating myoblasts*. Cell Biology and Toxicology 32, 185–198. https://doi.org/10.1007/s10565-016-9324-2

Grandjean, P., Andersen, E.W., Budtz-Jørgensen, E., Nielsen, F., Mølbak, K., Weihe, P., Heilmann, C., 2012. *Serum Vaccine Antibody Concentrations in Children Exposed to Perfluorinated Compounds*. JAMA 307, 391–397. https://doi.org/10.1001/jama.2011.2034

Grandjean, P., Heilmann, C., Weihe, P., Nielsen, F., Mogensen, U.B., Budtz-Jørgensen, E., 2017. *Serum vaccine antibody concentrations in adolescents exposed to perfluorinated compounds*. Environmental Health Perspectives 125. https://doi.org/10.1289/EHP275

Grindler, N.M., Vanderlinden, L., Karthikraj, R., Kannan, K., Teal, S., Polotsky, A.J., Powell, T.L., Yang, I. V, Jansson, T., 2018. *Exposure to Phthalate, an Endocrine Disrupting Chemical, Alters the First Trimester Placental Methylome and Transcriptome in Women*. Scientific Reports 8, 6086. https://doi.org/10.1038/s41598-018-24505-w

Grishanova, A.Y., Klyushova, L.S., Perepechaeva, M.L., 2023. *AhR and Wnt/β-Catenin Signaling Pathways and Their Interplay*. Current Issues in Molecular Biology 45, 3848–3876. https://doi.org/10.3390/cimb45050248

Hamzé, R., Delangre, E., Tolu, S., Moreau, M., Janel, N., Bailbé, D., Movassat, J., 2022. *Type 2 Diabetes Mellitus and Alzheimer's Disease: Shared Molecular Mechanisms and Potential Common Therapeutic Targets*. International Journal of Molecular Sciences. https://doi.org/10.3390/ijms232315287

Hanahan, D., 2022. *Hallmarks of Cancer: New Dimensions*. Cancer Discovery. https://doi.org/10.1158/2159-8290.CD-21-1059

Hanahan, D., Weinberg, R.A., 2011. *Hallmarks of Cancer: The Next Generation*. Cell 144, 646–674. https://doi.org/10.1016/j.cell.2011.02.013

Hanioka, N., Kinashi, Y., Tanaka-Kagawa, T., Isobe, T., Jinno, H., 2017. *Glucuronidation of mono(2-ethylhexyl) phthalate in humans: roles of hepatic and intestinal UDP-glucuronosyltransferases*. Archives of Toxicology 91, 689–698. https://doi.org/10.1007/s00204-016-1708-9

Hartley, A., Ahmad, I., 2023. *The role of PPARγ in prostate cancer development and progression*. British Journal of Cancer 128, 940–945. https://doi.org/10.1038/s41416-022-02096-8

Hayashi, K., Sasaki, K., Asada, S., Tsuchiya, T., Hayashi, M., Yoshimura, I., Tanaka, N., Umeda, M., 2008. *Technical modification of the Balb/c 3T3 cell transformation assay: the use of serum-reduced medium to optimise the practicability of the protocol.* Alternatives to laboratory animals : ATLA 36, 653–65.

Heidelberger, C., Freeman, A.E., Pienta, R.J., Sivak, A., Bertram, J.S., Casto, B.C., Dunkel, V.C., Francis, M.W., Kakunaga, T., Little, J.B., Schechtman, L.M., 1983. *Cell transformation by chemical agents --a review and analysis of the literature A report of the U.S. Environmental Protection Agency Gene-Tox Program*. Mutation Research 114, 283–385.

Hendriks, G., Adriaens, E., Allemang, A., Clements, J., Cole, G., Derr, R., Engel, M., Hamel, A., Kidd, D., Kellum, S., Kiyota, T., Myhre, A., Naëssens, V., Pfuhler, S., Roy, M., Settivari, R., Schuler, M., Zeller, A., van Benthem, J., Vanparys, P., Kirkland, D., 2024. *Interlaboratory validation of the ToxTracker assay: An in vitro reporter assay for mechanistic genotoxicity assessment*. Environmental and Molecular Mutagenesis 65, 4–24. https://doi.org/https://doi.org/10.1002/em.22592

Hernández, L.G., van Steeg, H., Luijten, M., van Benthem, J., 2009. *Mechanisms of non-genotoxic carcinogens and importance of a weight of evidence approach*. Mutation Research/Reviews in Mutation Research 682, 94–109. https://doi.org/https://doi.org/10.1016/j.mrrev.2009.07.002

Hopf, N.B., Berthet, A., Vernez, D., Langard, E., Spring, P., Gaudin, R., 2014. *Skin permeation and metabolism of di(2-ethylhexyl) phthalate (DEHP)*. Toxicology Letters 224, 47–53. https://doi.org/https://doi.org/10.1016/j.toxlet.2013.10.004

Horling, K., Santos, A.N., Fischer, B., 2011. *The AhR is constitutively activated and affects granulosa cell features in the human cell line KGN*. Molecular Human Reproduction 17, 104–114. https://doi.org/10.1093/molehr/gaq074

Hsieh, T.H., Hsu, C.Y., Yang, P.J., Chiu, C.C., Liang, S.S., Ou-Yang, F., Kan, J.Y., Hou, M.F., Wang, T.N., Tsai, E.M., 2022. *DEHP mediates drug resistance by directly targeting AhR in human breast cancer*. Biomedicine and Pharmacotherapy 145. https://doi.org/10.1016/j.biopha.2021.112400

Hsu, J.-W., Yeh, S.-C., Tsai, F.-Y., Chen, H.-W., Tsou, T.-C., 2019. *Fibroblast growth factor 21 secretion enhances glucose uptake in mono(2-ethylhexyl)phthalate-treated adipocytes*. Toxicology in Vitro 59, 246–254. https://doi.org/https://doi.org/10.1016/j.tiv.2019.04.021

Huang, R., Zhang, Jiaqi, Li, Mingxiao, Yan, P., Yin, H., Zhai, S., Zhu, X., Hu, P., Zhang, Jiaxin, Huang, L., Li, Man, Sun, Z., Meng, T., 2020. *The Role of Peroxisome Proliferator-Activated Receptors (PPARs) in Pan-Cancer* 2020, 19.

Hunt, K.J., Ferguson, P.L., Bloom, M.S., Neelon, B., Pearce, J., Commodore, S., Newman, R.B., Roberts, J.R., Bain, L., Baldwin, W., Grobman, W.A., Sciscione, A.C., Tita, A.T., Nageotte, M.P., Palomares, K., Skupski, D.W., Zhang, C., Wapner, R., Vena, J.E., 2024. *Phthalate and phthalate replacement concentrations in relationship to adiposity in a multi-racial cohort of children*. International Journal of Obesity 48, 1266–1273. https://doi.org/10.1038/s41366-024-01548-w

IARC, 1985. *IARC Monographs on the evaluation of the carcinogenic risk of chemicals to humans. Vol.37*. International Agency for Research on Cancer, Lyon, France.

Ikeda, G.J., Sapienza, P.P., Couvillion, J.L., Farber, T.M., 1980. *Comparative distribution, excretion and metabolism of di-(2-ethylhexyl) phthalate in rats, dogs and miniature pigs*. Food and cosmetics toxicology 18, 637–642. https://doi.org/10.1016/S0015-6264(80)80012-5

Imani, S., Hosseinifard, H., Cheng, J., Wei, C., Fu, J., 2016. *Prognostic Value of EMT-inducing Transcription Factors (EMT-TFs) in Metastatic Breast Cancer: A Systematic Review and Meta-analysis*. Scientific Reports 6, 1–10. https://doi.org/10.1038/srep28587

Isenberg, J.S., Kamendulis, L.M., Ackley, D.C., Smith, J.H., Pugh, G., Lington, A.W., McKee, R.H., Klaunig, J.E., 2001. *Reversibility and persistence of Di-2-ethylhexyl phthalate (DEHP)- and phenobarbital-induced hepatocellular changes in rodents*. Toxicological Sciences 64, 192–199. https://doi.org/10.1093/toxsci/64.2.192

Isenberg, J.S., Kamendulis, L.M., Smith, J.H., Ackley, D.C., Pugh, G., Lington, A.W., Klaunig, J.E., 2000. *Effects of Di-2-ethylhexyl phthalate (DEHP) on gap-junctional intercellular communication (GJIC), DNA synthesis, and peroxisomal beta oxidation (PBOX) in rat, mouse, and hamster liver*. Toxicological Sciences 56, 73–85. https://doi.org/10.1093/toxsci/56.1.73

Ito, Y., Kamijima, M., Nakajima, T., 2019. *Di(2-ethylhexyl) phthalate-induced toxicity and peroxisome proliferator-activated receptor alpha: a review*. Environmental Health and Preventive Medicine 24, 47. https://doi.org/10.1186/s12199-019-0802-z

Ito, Y., Nakajima, T., 2008. *PPARα-and DEHP-induced cancers*. PPAR Research. https://doi.org/10.1155/2008/759716

Ito, Y., Yamanoshita, O., Asaeda, N., Tagawa, Y., Lee, C.-H., Aoyama, T., Ichihara, G., Furuhashi, K., Kamijima, M., Gonzalez, F.J., Nakajima, T., 2007. *Di(2-ethylhexyl)phthalate Induces Hepatic Tumorigenesis through a Peroxisome Proliferator-activated Receptor α-independent Pathway*. Journal of Occupational Health 49, 172–182. https://doi.org/10.1539/joh.49.172

Ito, Y., Yokota, H., Wang, R., Yamanoshita, O., Ichihara, G., Wang, H., Kurata, Y., Takagi, K., Nakajima, T., 2005. *Species differences in the metabolism of di(2-ethylhexyl) phthalate (DEHP) in several organs of mice, rats, and marmosets*. Archives of Toxicology 79, 147–154. https://doi.org/10.1007/s00204-004-0615-7

Iversen, O.H., Iversen, U.M., 1982. *Must initiators come first? Tumorigenic and carcinogenic effects on skin of 3-Methylcholanthrene and TPA in various sequences*. British Journal of Cancer 45.

Jacobs, M.N., Colacci, A., Corvi, R., Vaccari, M., Aguila, M.C., Corvaro, M., Delrue, N., Desaulniers, D., Ertych, N., Jacobs, A., Luijten, M., Madia, F., Nishikawa, A., Ogawa, K., Ohmori, K., Paparella, M., Sharma, A.K., Vasseur, file:///C:/Users/gelso/Dropbox/TESI D. 2023. pdfPaul., 2020. *Chemical carcinogen safety testing: OECD expert group international consensus on the development of an integrated approach for the testing and assessment of chemical non-genotoxic carcinogens*. Archives of Toxicology 94, 2899–2923. https://doi.org/10.1007/s00204-020-02784-5

Jacobs, M.N., Colacci, A., Louekari, K., Luijten, M., Hakkert, B.C., Paparella, M., Vasseur, P., 2016. *International regulatory needs for development of an IATA for non-genotoxic carcinogenic chemical substances*. Altex 33, 359–392. https://doi.org/10.14573/altex.1601201

Jadhao, M., Tsai, E.M., Yang, H.C., Chen, Y.F., Liang, S.S., Wang, T.N., Teng, Y.N., Huang, H.W., Wang, L.F., Chiu, C.C., 2021. *The long-term dehp exposure confers multidrug resistance of triple-negative breast cancer cells through abc transporters and intracellular ros*. Antioxidants 10. https://doi.org/10.3390/antiox10060949

Jeon, S., Kim, K.-T., Choi, K., 2016. *Migration of DEHP and DINP into dust from PVC flooring products at different surface temperature*. Science of The Total Environment 547, 441–446. https://doi.org/https://doi.org/10.1016/j.scitotenv.2015.12.135

Jian, J.-M., Chen, D., Han, F.-J., Guo, Y., Zeng, L., Lu, X., Wang, F., 2018. *A short review on human exposure to and tissue distribution of per- and polyfluoroalkyl substances*

(PFASs). Science of The Total Environment 636, 1058–1069. https://doi.org/https://doi.org/10.1016/j.scitotenv.2018.04.380

Jones, S., Boisvert, A., Francois, S., Zhang, L., Culty, M., 2015. *In Utero Exposure to Di-(2-Ethylhexyl) Phthalate Induces Testicular Effects in Neonatal Rats That Are Antagonized by Genistein Cotreatment1*. Biology of Reproduction 93, 92, 1–14. https://doi.org/10.1095/biolreprod.115.129098

Jones, S.M., Kazlauskas, A., 2001. *Growth Factor-Dependent Signaling and Cell Cycle Progression*. Chemical Reviews 101, 2413–2424. https://doi.org/10.1021/cr000101f

Kakunaga, T., Crow, J.D., 1980. *Cell variants showing differential susceptibility to ultraviolet light--induced transformation.* Science 209, 505–7. https://doi.org/10.1126/SCIENCE.7394516

Kanaujiya, D.K., Sivashanmugam, S., Pakshirajan, K., 2022. *Biodegradation and toxicity removal of phthalate mixture by Gordonia sp. in a continuous stirred tank bioreactor system*. Environmental Technology and Innovation 26. https://doi.org/10.1016/j.eti.2022.102324

Kang, J.H., Asai, D., Toita, R., 2023. *Bisphenol A (BPA) and Cardiovascular or Cardiometabolic Diseases*. Journal of Xenobiotics 13, 775–810. https://doi.org/10.3390/jox13040049

Knerr, S., Schrenk, D., 2006. *Carcinogenicity of 2,3,7,8-tetrachlorodibenzo-p-dioxin in experimental models*. Molecular Nutrition & Food Research 50, 897–907. https://doi.org/https://doi.org/10.1002/mnfr.200600006

Korbecki, J., Bobiński, R., Dutka, M., 2019. *Self-regulation of the inflammatory response by peroxisome proliferator-activated receptors*. Inflammation Research 68, 443–458. https://doi.org/10.1007/s00011-019-01231-1

Krais, A.M., Andersen, C., Eriksson, A.C., Johnsson, E., Nielsen, J., Pagels, J., Gudmundsson, A., Lindh, C.H., Wierzbicka, A., 2018. *Excretion of urinary metabolites of the phthalate esters dep and dehp in 16 volunteers after inhalation and dermal exposure*. International Journal of Environmental Research and Public Health 15. https://doi.org/10.3390/ijerph15112514

Kratochvil, I., Hofmann, T., Rother, S., Schlichting, R., Moretti, R., Scharnweber, D., Hintze, V., Escher, B.I., Meiler, J., Kalkhof, S., von Bergen, M., 2019. *Mono(2-ethylhexyl) phthalate (MEHP) and mono(2-ethyl-5-oxohexyl) phthalate (MEOHP) but not di(2-ethylhexyl) phthalate (DEHP) bind productively to the peroxisome proliferator-activated receptor γ*. Rapid Communications in Mass Spectrometry 33, 75–85. https://doi.org/10.1002/rcm.8258

Krüger, T., Long, M., Bonefeld-Jørgensen, E.C., 2008. *Plastic components affect the activation of the aryl hydrocarbon and the androgen receptor*. Toxicology 246, 112–123. https://doi.org/https://doi.org/10.1016/j.tox.2007.12.028

Landkocz, Y., Poupin, P., Atienzar, F., Vasseur, P., 2011. *Transcriptomic effects of di-(2-ethylhexyl)-phthalate in Syrian hamster embryo cells: An important role of early cytoskeleton disturbances in carcinogenesis?* BMC Genomics 12. https://doi.org/10.1186/1471-2164-12-524

LeBoeuf, R.A., Kerckaert, G.A., Aardema, M.J., Gibson, D.P., Brauninger, R., Isfort, R.J., 1996. The pH 6.7 Syrian hamster embryo cell transformation assay for assessing the carcinogenic potential of chemicals, Mutagenesis Mutation Research.

Lee, C.-Y., Suk, F.-M., Twu, Y.-C., Liao, Y.-J., 2020. *Long-Term Exposure to Low-Dose Di-(2-ethylhexyl) Phthalate Impairs Cholesterol Metabolism in Hepatic Stellate Cells and Exacerbates Liver Fibrosis*. International Journal of Environmental Research and Public Health. https://doi.org/10.3390/ijerph17113802

Lee, J.-E., Ge, K., 2014. *Transcriptional and epigenetic regulation of PPARγ expression during adipogenesis*. Bioscience 4, 1–11. https://doi.org/10.1621/datasets.02001

Li, A., Kang, L., Li, R., Wu, S., Liu, K., Wang, X., 2022. *Modeling di (2-ethylhexyl) Phthalate (DEHP) and Its Metabolism in a Body's Organs and Tissues through Different Intake*

Pathways into Human Body. International Journal of Environmental Research and Public Health 19. https://doi.org/10.3390/ijerph19095742

Li, H., Xu, Yuanzhong, Jiang, Y., Jiang, Z., Otiz-Guzman, J., Morrill, J.C., Cai, J., Mao, Z., Xu, Yong, Arenkiel, B.R., Huang, C., Tong, Q., 2023. *The melanocortin action is biased toward protection from weight loss in mice*. Nature Communications 14, 2200. https://doi.org/10.1038/s41467-023-37912-z

Li, L., Su, Y., Wang, S., Wang, C., Ruan, N., Hu, Z., Cheng, X., Chen, J., Yuan, K., Li, P., Fan, P., 2024. *Neonatal di-(2-ethylhexyl)phthalate exposure induces permanent alterations in secretory CRH neuron characteristics in the hypothalamus paraventricular region of adult male rats*. Experimental Neurology 372, 114616. https://doi.org/https://doi.org/10.1016/j.expneurol.2023.114616

Li, Y., Barregard, L., Xu, Y., Scott, K., Pineda, D., Lindh, C.H., Jakobsson, K., Fletcher, T., 2020. *Associations between perfluoroalkyl substances and serum lipids in a Swedish adult population with contaminated drinking water*. Environmental Health: A Global Access Science Source 19. https://doi.org/10.1186/s12940-020-00588-9

Li, Y., Fletcher, T., Mucs, D., Scott, K., Lindh, C.H., Tallving, P., Jakobsson, K., 2018. *Half-lives of PFOS, PFHxS and PFOA after end of exposure to contaminated drinking water*. Occupational and Environmental Medicine 75, 46. https://doi.org/10.1136/oemed-2017-104651

Liang, G., Li, Y., Lin, Y., Yang, X., Yang, J., Hu, S., Liu, A., 2023. *Nicotinamide N-methyltransferase and liver diseases*. Genes & Diseases 10, 1883–1893. https://doi.org/https://doi.org/10.1016/j.gendis.2022.03.019

Louekari, K., Jacobs, M.N., 2024. *A modular strategy for the testing and assessment of non-genotoxic carcinogens*. Archives of Toxicology 98, 2463–2485. https://doi.org/10.1007/s00204-024-03753-y

Lu, J., Kerns, R.T., Peddada, S.D., Bushel, P.R., 2011. *Principal component analysis-based filtering improves detection for Affymetrix gene expression arrays*. Nucleic Acids Research 39, e86–e86. https://doi.org/10.1093/nar/gkr241

Luijten, M., Corvi, R., Mehta, J., Corvaro, M., Delrue, N., Felter, S., Haas, B., Hewitt, N.J., Hilton, G., Holmes, T., Jacobs, M.N., Jacobs, A., Lamplmair, F., Lewis, D., Madia, F., Manou, I., Melching-Kollmuss, S., Schorsch, F., Schütte, K., Sewell, F., Strupp, C., van der Laan, J.W., Wolf, D.C., Wolterink, G., Woutersen, R., Zvonar, Z., Heusinkveld, H., Braakhuis, H., 2020. *A comprehensive view on mechanistic approaches for cancer risk assessment of non-genotoxic agrochemicals*. Regulatory Toxicology and Pharmacology 118, 104789. https://doi.org/https://doi.org/10.1016/j.yrtph.2020.104789

Lv, D.D., Zhou, L.Y., Tang, H., 2021. *Hepatocyte nuclear factor 4α and cancer-related cell signaling pathways: a promising insight into cancer treatment*. Experimental and Molecular Medicine 53, 8–18. https://doi.org/10.1038/s12276-020-00551-1

Lv, Z., Cheng, J., Huang, S., Zhang, Y., Wu, S., Qiu, Y., Geng, Y., Zhang, Q., Huang, G., Ma, Q., Xie, X., Zhou, S., Wu, T., Ke, Y., 2016. *DEHP induces obesity and hypothyroidism through both central and peripheral pathways in C3H/He mice*. Obesity 24, 368–378. https://doi.org/https://doi.org/10.1002/oby.21359

Mackowiak, B., Wang, H., 2016. *Mechanisms of xenobiotic receptor activation: Direct vs. indirect*. Biochimica et Biophysica Acta (BBA) - Gene Regulatory Mechanisms 1859, 1130–1140. https://doi.org/https://doi.org/10.1016/j.bbagrm.2016.02.006

Madia, F., Corvi, R., Worth, A., Matys, I., Prieto, P., 2020a. *Making Better Use of Toxicity Studies for Human Health by Extrapolating across Endpoints*. Altex 37, 519–531. https://doi.org/10.14573/altex.2005061

Madia, F., Kirkland, D., Morita, T., White, P., Asturiol, D., Corvi, R., 2020b. *EURL ECVAM Genotoxicity and Carcinogenicity Database of Substances Eliciting Negative Results in the Ames Test: Construction of the Database*. Mutation Research - Genetic Toxicology and Environmental Mutagenesis 854–855. https://doi.org/10.1016/j.mrgentox.2020.503199

Madia, F., Pillo, G., Worth, A., Corvi, R., Prieto, P., 2021. *Integration of data across toxicity endpoints for improved safety assessment of chemicals: the example of carcinogenicity assessment.* Archives of toxicology 95. https://doi.org/10.1007/s00204-021-03035-x

Madia, F., Worth, A., Whelan, M., Corvi, R., 2019. *Carcinogenicity assessment: Addressing the challenges of cancer and chemicals in the environment*. Environment International 128, 417–429. https://doi.org/10.1016/j.envint.2019.04.067

Makia, N.L., Goldstein, J.A., 2016. *CYP2C8 Is a Novel Target of Peroxisome Proliferator-Activated Receptor α in Human Liver*. Molecular Pharmacology 89, 154–164. https://doi.org/10.1124/mol.115.100255

Marczyk, M., Jaksik, R., Polanski, A., Polanska, J., 2013. *Adaptive filtering of microarray gene expression data based on Gaussian mixture decomposition*. BMC Bioinformatics 14, 101. https://doi.org/10.1186/1471-2105-14-101

Mariana, M., Cairrao, E., 2023. *The Relationship between Phthalates and Diabetes: A Review*. Metabolites 13. https://doi.org/10.3390/metabo13060746

Mascolo, M.G., Perdichizzi, S., Vaccari, M., Rotondo, F., Zanzi, C., Grilli, S., Paparella, M., Jacobs, M.N., Colacci, A., 2018. *The Transformics Assay: First Steps for the Development of an Integrated Approach to Investigate the Malignant Cell Transformation in vitro*. Carcinogenesis 1–13. https://doi.org/10.1093/carcin/bgy037

Matthews, E.J., Spalding, J.W., Tennant, R.W., 1993. *Transformation of BALB/c-3T3 cells: V - Transformation responses of 168 chemicals compared with mutagenicity in Salmonella and carcinogenicity in rodent bioassays*. Environmental Health Perspectives 101, 347–482. https://doi.org/10.1289/ehp.93101s2347

Mccann, J., Choi, E., Yamasaki, E., Ames, B.N., Jolley, S.B., Streitwieser, D., Jen, G., Donahue, V., Stark, G., Haroun, L., Maron, D., Keng, T., Matsushima, H., Bartsch, E., Weisburger, J., Miller, E., Arcos, J., Tomatis, L., Rosenkranz, H., Poirier, L., 1975. Detection of carcinogens as mutagens in the Salmonella/microsome test: Assay of 300 chemicals* (rapid in vitro screening/environmental carcinogens and mutagens), Medical Sciences.

Meier, M.J., Harrill, J., Johnson, K., Thomas, R.S., Tong, W., Rager, J.E., Yauk, C.L., 2024. *Progress in toxicogenomics to protect human health*. Nature Reviews Genetics. https://doi.org/10.1038/s41576-024-00767-1

Monti, M., Fasano, M., Palandri, L., Righi, E., 2022. *A review of European and international phthalates regulation: focus on daily use products*. European Journal of Public Health 32, ckac131.226. https://doi.org/10.1093/eurpub/ckac131.226

Mu, Y.-M., Yanase, T., Nishi, Y., Waseda, N., Oda, T., Tanaka, A., Takayanagi, R., Nawata, H., 2000. *Insulin Sensitizer, Troglitazone, Directly Inhibits Aromatase Activity in Human Ovarian Granulosa Cells*. Biochemical and Biophysical Research Communications 271, 710–713. https://doi.org/https://doi.org/10.1006/bbrc.2000.2701

Neff, A.M., Inman, Z., Mourikes, V.E., Santacruz-Márquez, R., Gonsioroski, A., Laws, M.J., Flaws, J.A., 2024. *The role of the aryl hydrocarbon receptor in mediating the effects of mono(2-ethylhexyl) phthalate in mouse ovarian antral follicles†*. Biology of Reproduction 110, 632–641. https://doi.org/10.1093/biolre/ioad178

Nigam, S.K., Granados, J.C., 2024. *OAT, OATP, and MRP Drug Transporters and the Remote Sensing and Signaling Theory*. Annual Review of Pharmacology and Toxicology Annu. Rev. Pharmacol. Toxicol. 2023 54, 7. https://doi.org/10.1146/annurev-pharmtox-030322

OECD, 2007. Detailed Review Paper on Cell Transformation Assays for Detection of Chemical Carcinogens . OECD Series on Testing and Assessment, No. 31. Paris.

OECD, 2016a. Users' handbook supplement to the guidance document for developing and assessing AOPs. Series on Testing and Assessment No. 233. Paris.

OECD, 2016b. Guidance document on the in vitro bhas 42 cell transformation assay. Series on Testing and Assessment No. 231. ENV/JM/MONO(2016)1. Paris.

OECD, 2024. *Beating Cancer Inequalities in the EU: Spotlight on Cancer Prevention and Early Detection*, OECD Health Policy Studies. Paris.

Oliveira, P.A., Faustino-Rocha, A.I., 2022. *Chemical Carcinogens*, in: Rezaei, N. (Ed.), Handbook of Cancer and Immunology. Springer International Publishing, Cham, pp. 1–23. https://doi.org/10.1007/978-3-030-80962-1_121-1

Olsen, G.W., Mair, D.C., Church, T.R., Ellefson, M.E., Reagen, W.K., Boyd, T.M., Herron, R.M., Medhdizadehkashi, Z., Nobiletti, J.B., Rios, J.A., Butenhoff, J.L., Zobel, L.R., 2008. *Decline in Perfluorooctanesulfonate and Other Polyfluoroalkyl Chemicals in American Red Cross Adult Blood Donors, 2000−2006*. Environmental Science & Technology 42, 4989–4995. https://doi.org/10.1021/es800071x

Ozaki, H., Sugihara, K., Watanabe, Y., Moriguchi, K., Uramaru, N., Sone, T., Ohta, S., Kitamura, S., 2017. *Comparative study of hydrolytic metabolism of dimethyl phthalate, dibutyl phthalate and di(2-ethylhexyl) phthalate by microsomes of various rat tissues*. Food and Chemical Toxicology 100, 217–224. https://doi.org/https://doi.org/10.1016/j.fct.2016.12.019

Pan, Y., Li, Y., Fan, H., Cui, H., Chen, Z., Wang, Y., Jiang, M., Wang, G., 2024. *Roles of the peroxisome proliferator-activated receptors (PPARs) in the pathogenesis of hepatocellular carcinoma (HCC)*. Biomedicine & Pharmacotherapy 177, 117089. https://doi.org/https://doi.org/10.1016/j.biopha.2024.117089

Paparella, M., Colacci, A., Jacobs, M.N., 2017. *Uncertainties of Testing Methods: What Do We (Want to) Know About Carcinogenicity?* ALTEX 34, 235–252. https://doi.org/10.14573/altex.1608281

Patel, H., Truant, R., Rachubinski, R.A., Capone, J.P., 2005. *Activity and subcellular compartmentalization of peroxisome proliferator-activated receptor α are altered by the centrosome-associated protein CAP350*. Journal of Cell Science 118, 175–186. https://doi.org/10.1242/jcs.01600

Pérez, F., Nadal, M., Navarro-Ortega, A., Fàbrega, F., Domingo, J.L., Barceló, D., Farré, M., 2013. *Accumulation of perfluoroalkyl substances in human tissues*. Environment International 59, 354–362. https://doi.org/https://doi.org/10.1016/j.envint.2013.06.004

Pierozan, P., Jerneren, F., Karlsson, O., 2018. *Perfluorooctanoic acid (PFOA) exposure promotes proliferation, migration and invasion potential in human breast epithelial cells*. Archives of Toxicology 92, 1729–1739. https://doi.org/10.1007/s00204-018-2181-4

Pillo, G., Aldrovandi, F., Mescoli, A., Maffei, G., Mascolo, M.G., Vaccari, M., Colacci, A., 2024. *An insight into carcinogenic activity and molecular mechanisms of Bis(2-ethylhexyl) phthalate*. Frontiers in Toxicology 6.

Pillo, G., Mascolo, M.G., Zanzi, C., Rotondo, F., Serra, S., Bortone, F., Grilli, S., Vaccari, M., Jacobs, M.N., Colacci, A., 2022. *Mechanistic Interrogation of Cell Transformation In Vitro: The Transformics Assay as an Exemplar of Oncotransformation*. International Journal of Molecular Sciences 23. https://doi.org/10.3390/ijms23147603

Pizzurro, D.M., Seeley, M., Kerper, L.E., Beck, B.D., 2019. *Interspecies differences in perfluoroalkyl substances (PFAS)toxicokinetics and application to health-based criteria*. Regulatory Toxicology and Pharmacology. https://doi.org/10.1016/j.yrtph.2019.05.008

Poirier, M.C., 2016. *Linking DNA adduct formation and human cancer risk in chemical carcinogenesis*. Environmental and molecular mutagenesis 57, 499–507. https://doi.org/10.1002/EM.22030

Qazi, M.R., Xia, Z., Bogdanska, J., Chang, S.-C., Ehresman, D.J., Butenhoff, J.L., Nelson, B.D., DePierre, J.W., Abedi-Valugerdi, M., 2009. *The atrophy and changes in the cellular compositions of the thymus and spleen observed in mice subjected to short-term exposure to perfluorooctanesulfonate are high-dose phenomena mediated in part by peroxisome proliferator-activated receptor-alpha (PPARα)*. Toxicology 260, 68–76. https://doi.org/https://doi.org/10.1016/j.tox.2009.03.009

Rajesh, P., Balasubramanian, K., 2014. *Di(2-ethylhexyl)phthalate exposure impairs insulin receptor and glucose transporter 4 gene expression in L6 myotubes*. Human and

Experimental Toxicology 33, 685–700. https://doi.org/10.1177/0960327113506238

Rakateli, L., Huchzermeier, R., van der Vorst, E.P.C., 2023. *AhR, PXR and CAR: From Xenobiotic Receptors to Metabolic Sensors*. Cells. https://doi.org/10.3390/cells12232752

Ranucci, E., 2022. FTALATI: PROPRIETÀ CHIMICO FISICHE E TOSSICITÀ [WWW Document]. Istituto Lombardo - Accademia Di Scienze E Lettere - Incontri di Studio. https://doi.org/https://doi.org/10.4081/incontri.2022.800

Régnier, M., Polizzi, A., Smati, S., Lukowicz, C., Fougerat, A., Lippi, Y., Fouché, E., Lasserre, F., Naylies, C., Bétoulières, C., Barquissau, V., Mouisel, E., Bertrand-Michel, J., Batut, A., Saati, T. Al, Canlet, C., Tremblay-Franco, M., Ellero-Simatos, S., Langin, D., Postic, C., Wahli, W., Loiseau, N., Guillou, H., Montagner, A., 2020. *Hepatocyte-specific deletion of Pparα promotes NAFLD in the context of obesity*. Scientific Reports 10, 6489. https://doi.org/10.1038/s41598-020-63579-3

Rhodes, C., Orton, T.C., Pratt, L.S., Batten, P.L., Bratt, H., Jackson, S.J., Elcombe, C.R., 1986. Comparative Pharmacokinetics and Subacute Toxicity of Di(2-ethylhexyl) Phthalate (DEHP) in Rats and Marmosets: Extrapolation of Effects in Rodents to Man, Environmental Health Perspectives.

Rowdhwal, S.S.S., Chen, J., 2018. *Toxic Effects of Di-2-ethylhexyl Phthalate: An Overview*. BioMed Research International. https://doi.org/10.1155/2018/1750368

Rusyn, I., Corton, J.C., 2012. *Mechanistic considerations for human relevance of cancer hazard of di(2-ethylhexyl) phthalate*. Mutation Research/Reviews in Mutation Research 750, 141–158. https://doi.org/https://doi.org/10.1016/j.mrrev.2011.12.004

Sakai, A., 2007. *BALB/c 3T3 cell transformation assays for the assessment of chemical carcinogenicity*. AATEX 14, 367–373.

Salvalaglio, M., Muscionico, I., Cavallotti, C., 2010. *Determination of Energies and Sites of Binding of PFOA and PFOS to Human Serum Albumin*. The Journal of Physical Chemistry B 114, 14860–14874. https://doi.org/10.1021/jp106584b

Sancar, G., Liu, S., Gasser, E., Alvarez, J.G., Moutos, C., Kim, K., van Zutphen, T., Wang, Y., Huddy, T.F., Ross, B., Dai, Y., Zepeda, D., Collins, B., Tilley, E., Kolar, M.J., Yu, R.T., Atkins, A.R., van Dijk, T.H., Saghatelian, A., Jonker, J.W., Downes, M., Evans, R.M., 2022. *FGF1 and insulin control lipolysis by convergent pathways*. Cell Metabolism 34, 171-183.e6. https://doi.org/10.1016/j.cmet.2021.12.004

Sasaki, K., Bohnenberger, S., Hayashi, K., Kunkelmann, T., Muramatsu, D., Phrakonkham, P., Poth, A., Sakai, A., Salovaara, S., Tanaka, N., Thomas, B.C., Umeda, M., 2012a. *Recommended protocol for the BALB/c 3T3 cell transformation assay*. Mutation Research - Genetic Toxicology and Environmental Mutagenesis 744, 30–35. https://doi.org/10.1016/j.mrgentox.2011.12.014

Sasaki, K., Bohnenberger, S., Hayashi, K., Kunkelmann, T., Muramatsu, D., Poth, A., Sakai, A., Salovaara, S., Tanaka, N., Thomas, B.C., Umeda, M., 2012b. *Photo catalogue for the classification of foci in the BALB/c 3T3 cell transformation assay*. Mutation Research - Genetic Toxicology and Environmental Mutagenesis 744, 42–53. https://doi.org/10.1016/j.mrgentox.2012.01.009

SCENIHR, 2016. Scientific Opinion on the safety of medical devices containing DEHP-plasticized PVC or other plasticizers on neonates and other groups possibly at risk. 2015. https://doi.org/10.1016/j.yrtph.2016.01.013

Schaedlich, K., Gebauer, S., Hunger, L., Beier, L.S., Koch, H.M., Wabitsch, M., Fischer, B., Ernst, J., 2018. *DEHP deregulates adipokine levels and impairs fatty acid storage in human SGBS-adipocytes*. Scientific Reports 8. https://doi.org/10.1038/s41598-018-21800-4

SCHEER, 2024. Update of the guidelines on the benefit-risk assessment of the presence of CMR/ED phthalates in certain medical devices covering phthalates which are carcinogenic, mutagenic, toxic to reproduction (CMR) or have endocrine-disrupting (ED) properties.

Schrenk, D., 2019. *What is the meaning of "A compound is carcinogenic"?* Toxicology

Reports 5, 504–511. https://doi.org/10.1016/j.toxrep.2018.04.002

Senga, S.S., Bisson, W.H., Colacci, A., 2024. *Key characteristics of carcinogens meet hallmarks for prevention-cutting the Gordian knot*. Frontiers in Oncology 14. https://doi.org/10.3389/fonc.2024.1420687

Sérée, E., Villard, P.-H., Pascussi, J.-M., Pineau, T., Maurel, P., Nguyen, Q.B., Fallone, F., Martin, P.-M., Champion, S., Lacarelle, B., Savouret, J.-F., Barra, Y., 2004. *Evidence for a new human CYP1A1 regulation pathway involving PPAR-α and 2 PPRE sites*. Gastroenterology 127, 1436–1445. https://doi.org/https://doi.org/10.1053/j.gastro.2004.08.023

Shan, N., Yuexin, C., Ruiwen, C., Megha, B., P, S.A., Alan, D., Carla, N., 2024. *A State-of-the-Science Review of Interactions of Per- and Polyfluoroalkyl Substances (PFAS) with Renal Transporters in Health and Disease: Implications for Population Variability in PFAS Toxicokinetics*. Environmental Health Perspectives 131, 076002. https://doi.org/10.1289/EHP11885

Shao, P., Wang, Y., Zhang, M., Wen, X., Zhang, J., Xu, Z., Hu, M., Jiang, J., Liu, T., 2019. *The interference of DEHP in precocious puberty of females mediated by the hypothalamic IGF-1/PI3K/Akt/mTOR signaling pathway*. Ecotoxicology and Environmental Safety 181, 362–369. https://doi.org/https://doi.org/10.1016/j.ecoenv.2019.06.017

She, Y., Jiang, Liping, Zheng, L., Zuo, H., Chen, M., Sun, X., Li, Q., Geng, C., Yang, G., Jiang, Lijie, Liu, X., 2017. *The role of oxidative stress in DNA damage in pancreatic β cells induced by di-(2-ethylhexyl) phthalate*. Chemico-Biological Interactions 265, 8–15. https://doi.org/https://doi.org/10.1016/j.cbi.2017.01.015

Shizu, R., Ezaki, K., Sato, T., Sugawara, A., Hosaka, T., Sasaki, T., Yoshinari, K., 2021. *PxR suppresses PPARα-dependent HMGCS2 gene transcription by inhibiting the interaction between PPARα and PGC1α*. Cells 10. https://doi.org/10.3390/cells10123550

Silano, V., Barat Baviera, J.M., Bolognesi, C., Chesson, A., Cocconcelli, P.S., Crebelli, R., Gott, D.M., Grob, K., Lampi, E., Mortensen, A., Rivière, G., Steffensen, I.L., Tlustos, C., Van Loveren, H., Vernis, L., Zorn, H., Cravedi, J.P., Fortes, C., Tavares Poças, M. de F., Waalkens-Berendsen, I., Wölfle, D., Arcella, D., Cascio, C., Castoldi, A.F., Volk, K., Castle, L., 2019. *Update of the risk assessment of di-butylphthalate (DBP), butyl-benzyl-phthalate (BBP), bis(2-ethylhexyl)phthalate (DEHP), di-isononylphthalate (DINP) and di-isodecylphthalate (DIDP) for use in food contact materials*. EFSA Journal 17. https://doi.org/10.2903/J.EFSA.2019.5838

Silva, M.J., Barr, D.B., Reidy, J.A., Kato, K., Malek, N.A., Hodge, C.C., Hurtz, D., Calafat, A.M., Needham, L.L., Brock, J.W., 2003. *Glucuronidation patterns of common urinary and serum monoester phthalate metabolites*. Archives of Toxicology 77, 561–567. https://doi.org/10.1007/s00204-003-0486-3

Smith, M.T., Guyton, K.Z., Kleinstreuer, N., Borrel, A., Cardenas, A., Chiu, W.A., Felsher, D.W., Gibbons, C.F., Goodson, W.H., Houck, K.A., Kane, A.B., La Merrill, M.A., Lebrec, H., Lowe, L., McHale, C.M., Minocherhomji, S., Rieswijk, L., Sandy, M.S., Sone, H., Wang, A., Zhang, L., Zeise, L., Fielden, M., 2020. *The key characteristics of carcinogens: Relationship to the hallmarks of cancer, relevant biomarkers, and assays to measure them*. Cancer Epidemiology Biomarkers and Prevention. https://doi.org/10.1158/1055-9965.EPI-19-1346

Sonich-Mullin, C., Fielder, R., Wiltse, J., Baetcke, K., Dempsey, J., Fenner-Crisp, P., Grant, D., Hartley, M., Knaap, A., Kroese, D., Mangelsdorf, I., Meek, E., Rice, J.M., Younes, M., 2001. *IPCS Conceptual Framework for Evaluating a Mode of Action for Chemical Carcinogenesis*. Regulatory Toxicology and Pharmacology 34, 146–152. https://doi.org/10.1006/RTPH.2001.1493

Steenland, K., Tinker, S., Frisbee, S., Ducatman, A., Vaccarino, V., 2009. *Association of Perfluorooctanoic Acid and Perfluorooctane Sulfonate With Serum Lipids Among Adults Living Near a Chemical Plant*. American Journal of Epidemiology 170, 1268–1278. https://doi.org/10.1093/aje/kwp279

Steenland, K., Winquist, A., 2021. *PFAS and cancer, a scoping review of the epidemiologic evidence*. Environmental Research 194, 110690. https://doi.org/10.1016/j.envres.2020.110690

Steinberg, P., 2016. *In Vitro–In Vivo Carcinogenicity*, in: Reifferscheid, G., Buchinger, S. (Eds.), In Vitro Environmental Toxicology - Concepts, Application and Assessment. Advances in Biochemical Engineering/Biotechnology. Vol 157. Springer International Publishing, pp. 81–96. https://doi.org/https://doi.org/10.1007/10_2015_5013

Stewart, B.W., 2019. *Mechanisms of carcinogenesis: from initiation and promotion to the hallmarks*, in: Baan, R.A., Stewart, B.W., Straif, K. (Eds.), Tumour Site Concordance and Mechanisms of Carcinogenesis Lyon (FR): International Agency for Research on Cancer. pp. 93–106.

Sugizaki, T., Watanabe, M., Horai, Y., Kaneko-Iwasaki, N., Arita, E., Miyazaki, T., Morimoto, K., Honda, A., Irie, J., Itoh, H., 2014. *The Niemann-Pick C1 Like 1 (NPC1L1) Inhibitor Ezetimibe Improves Metabolic Disease Via Decreased Liver X Receptor (LXR) Activity in Liver of Obese Male Mice*. Endocrinology 155, 2810–2819. https://doi.org/10.1210/en.2013-2143

Sui, Y., Meng, Z., Chen, J., Liu, J., Hernandez, R., Gonzales, M.B., Gwag, T., Morris, A.J., Zhou, C., 2021. *Effects of dicyclohexyl phthalate exposure on PXR activation and lipid homeostasis in mice*. Environmental Health Perspectives 129. https://doi.org/10.1289/EHP9262

Tait, S., Carli, F., Busani, L., Buzzigoli, E., Della Latta, V., Deodati, A., Fabbrizi, E., Gaggini, M., Maranghi, F., Tassinari, R., Toffol, G., Cianfarani, S., Gastaldelli, A., La Rocca, C., 2020. *Biomonitoring of Bis(2-ethylhexyl)phthalate (DEHP) in Italian children and adolescents: Data from LIFE PERSUADED project*. Environmental Research 185, 109428. https://doi.org/https://doi.org/10.1016/j.envres.2020.109428

Takada, I., Makishima, M., 2020. *Peroxisome proliferator-activated receptor agonists and antagonists: a patent review (2014-present)*. Expert Opinion on Therapeutic Patents 30, 1–13. https://doi.org/10.1080/13543776.2020.1703952

Takeshita, A., Inagaki, K., Igarashi-Migitaka, J., Ozawa, Y., Koibuchi, N., 2006. *The endocrine disrupting chemical, diethylhexyl phthalate, activates MDR1 gene expression in human colon cancer LS174T cells*. Journal of Endocrinology 190, 897–902. https://doi.org/10.1677/joe.1.06664

Tan, F., Jin, Y., Liu, W., Quan, X., Chen, J., Liang, Z., 2012. *Global Liver Proteome Analysis Using iTRAQ Labeling Quantitative Proteomic Technology to Reveal Biomarkers in Mice Exposed to Perfluorooctane Sulfonate (PFOS)*. Environmental Science & Technology 46, 12170–12177. https://doi.org/10.1021/es3027715

Tanaka, A., Adachi, T., Takahashi, T., Yamaha, T., 1975. *Biochemical studies on phthalic esters I. Elimination, distribution and metabolism of di-(2-ethylhexyl)phthalate in rats*. Toxicology. 4, 253–264. https://doi.org/10.1016/0300-483X(75)90105-5

Tanaka, N., Bohnenberger, S., Kunkelmann, T., Munaro, B., Ponti, J., Poth, A., Sabbioni, E., Sakai, A., Salovaara, S., Sasaki, K., Thomas, B.C., Umeda, M., 2012. *Prevalidation study of the BALB/c 3T3 cell transformation assay for assessment of carcinogenic potential of chemicals*. Mutation Research - Genetic Toxicology and Environmental Mutagenesis 744, 20–29. https://doi.org/10.1016/j.mrgentox.2011.12.008

Thapa, B. Sen, Pandit, S., Mishra, R.K., Joshi, S., Idris, A.M., Tusher, T.R., 2024. *Emergence of per- and poly-fluoroalkyl substances (PFAS) and advances in the remediation strategies*. Science of The Total Environment 916, 170142. https://doi.org/https://doi.org/10.1016/j.scitotenv.2024.170142

Thiebaut, C., Vlaeminck-Guillem, V., Trédan, O., Poulard, C., Le Romancer, M., 2021. *Non-genomic signaling of steroid receptors in cancer*. Molecular and Cellular Endocrinology 538, 111453. https://doi.org/https://doi.org/10.1016/j.mce.2021.111453

Tickner, J.A., Schettler, T., Guidotti, T., McCally, M., Rossi, M., 2001. *Health risks posed by use of Di-2-ethylhexyl phthalate (DEHP) in PVC medical devices: A critical review*. American Journal of Industrial Medicine 39, 100–111.

https://doi.org/https://doi.org/10.1002/1097-0274(200101)39:1<100::AID-AJIM10>3.0.CO;2-Q

Toyoda, Y., Takada, T., Umezawa, M., Tomura, F., Yamanashi, Y., Takeda, K., Suzuki, H., 2019. *Identification of hepatic NPC1L1 as an NAFLD risk factor evidenced by ezetimibe-mediated steatosis prevention and recovery*. FASEB BioAdvances 1, 283–295. https://doi.org/https://doi.org/10.1096/fba.2018-00044

Tsutsui, T., Watanabe, E., Barrett, J.C., 1993. *Ability of peroxisome proliferators to induce cell transformation, chromosome aberrations and peroxisome proliferation in cultured Syrian hamster embryo cells*. Carcinogenesis 14, 611–618. https://doi.org/10.1093/carcin/14.4.611

Tu, T., Zhang, H., Xu, H., 2023. *Targeting sterol-O-acyltransferase 1 to disrupt cholesterol metabolism for cancer therapy*. Frontiers in Oncology 13, 1–7. https://doi.org/10.3389/fonc.2023.1197502

U.S. EPA, 2024. Human Health Toxicity Assessment for Perfluorooctane Sulfonic Acid (PFOS) and Related Salts. Washington, D.C.

Uchio-Yamada, K., Kasai, F., Ozawa, M., Kohara, A., 2017. *Incorrect strain information for mouse cell lines: sequential influence of misidentification on sublines*. In Vitro Cellular and Developmental Biology - Animal 53, 225–230. https://doi.org/10.1007/s11626-016-0104-3

Uhl, M., Schoeters, G., Govarts, E., Bil, W., Fletcher, T., Haug, L.S., Hoogenboom, R., Gundacker, C., Trier, X., Fernandez, M.F., Calvo, A.C., López, M.E., Coertjens, D., Santonen, T., Murínová, Ľ.P., Richterová, D., Brouwere, K. De, Hauzenberger, I., Kolossa-Gehring, M., Halldórsson, Þ.I., 2023. *PFASs: What can we learn from the European Human Biomonitoring Initiative HBM4EU*. International Journal of Hygiene and Environmental Health. https://doi.org/10.1016/j.ijheh.2023.114168

Umemoto, T., Fujiki, Y., 2012. *Ligand-dependent nucleo-cytoplasmic shuttling of peroxisome proliferator-activated receptors, PPARα and PPARγ*. Genes to Cells 17, 576–596. https://doi.org/10.1111/j.1365-2443.2012.01607.x

Useini, A., Engelberger, F., Künze, G., Sträter, N., 2023. *Structural basis of the activation of PPARγ by the plasticizer metabolites MEHP and MINCH*. Environment International 173. https://doi.org/10.1016/j.envint.2023.107822

Vaccari, M., Serra, S., Ranzi, A., Aldrovandi, F., Maffei, G., Mascolo, M.G., Mescoli, A., Montanari, E., Pillo, G., Rotondo, F., Scaroni, I., Vaccari, L., Zanzi, C., Fletcher, T., Paparella, M., Colacci, A., 2024. *In vitro evaluation of the carcinogenic potential of perfluorinated chemicals*. ALTEX - Alternatives to animal experimentation 41, 439–456. https://doi.org/10.14573/altex.2310281

Veltman, C.H.J., Pennings, J.L.A., van de Water, B., Luijten, M., 2023. *An Adverse Outcome Pathway Network for Chemically Induced Oxidative Stress Leading to (Non)genotoxic Carcinogenesis*. Chemical Research in Toxicology 36, 805–817. https://doi.org/10.1021/acs.chemrestox.2c00396

Villard, P.H., Caverni, S., Baanannou, A., Khalil, A., Martin, P.G., Penel, C., Pineau, T., Seree, E., Barra, Y., 2007. *PPARα transcriptionally induces AhR expression in Caco-2, but represses AhR pro-inflammatory effects*. Biochemical and Biophysical Research Communications 364, 896–901. https://doi.org/https://doi.org/10.1016/j.bbrc.2007.10.084

Wahli, W., Michalik, L., 2012. *PPARs at the crossroads of lipid signaling and inflammation*. Trends in Endocrinology & Metabolism 23, 351–363. https://doi.org/10.1016/j.tem.2012.05.001

Wang, J., Xiao, Q., Wang, L., Wang, Y., Wang, D., Ding, H., 2022. *Role of ABCA1 in Cardiovascular Disease*. Journal of Personalized Medicine. https://doi.org/10.3390/jpm12061010

Wang, S., Cao, S., Arhatte, M., Li, D., Shi, Y., Kurz, S., Hu, J., Wang, L., Shao, J., Atzberger, A., Wang, Z., Wang, C., Zang, W., Fleming, I., Wettschureck, N., Honoré,

E., Offermanns, S., 2020. *Adipocyte Piezo1 mediates obesogenic adipogenesis through the FGF1/FGFR1 signaling pathway in mice*. Nature Communications 11, 2303. https://doi.org/10.1038/s41467-020-16026-w

Wang, W., Mutka, A.-L., Zmrzljak, U.P., Rozman, D., Tanila, H., Gylling, H., Remes, A.M., Huttunen, H.J., Ikonen, E., 2014. *Amyloid precursor protein α- and β-cleaved ectodomains exert opposing control of cholesterol homeostasis via SREBP2*. The FASEB Journal 28, 849–860. https://doi.org/https://doi.org/10.1096/fj.13-239301

Wang, Y., Zhu, H., Kannan, K., 2019. *A review of biomonitoring of phthalate exposures*. Toxics. https://doi.org/10.3390/TOXICS7020021

Wang, Z., Chen, S., Guo, Y., Zhang, R., Zhang, Q., Jiang, X., Li, M., Jiang, Y., Ye, L., Guo, X., Li, C., Zhang, G., Li, D., Chen, L., Chen, W., 2024. *Intestinal carcinogenicity screening of environmental pollutants using organoid-based cell transformation assay*. Archives of Toxicology 98, 1937–1951. https://doi.org/10.1007/s00204-024-03729-y

Wee, S.Y., Aris, A.Z., 2023. *Revisiting the "forever chemicals", PFOA and PFOS exposure in drinking water*. npj Clean Water. https://doi.org/10.1038/s41545-023-00274-6

Wiklund, L., Pípal, M., Weiss, J., Beronius, A., 2024. *Exploring a mechanism-based approach for the identification of endocrine disruptors using Adverse Outcome Pathways (AOPs) and New Approach Methodologies (NAMs) : A perfluorooctane sulfonic acid case study*. Toxicology 504. https://doi.org/10.1016/j.tox.2024.153794

Wójtowicz, A.K., Sitarz-Głownia, A.M., Szczęsna, M., Szychowski, K.A., 2019. *The Action of Di-(2-Ethylhexyl) Phthalate (DEHP) in Mouse Cerebral Cells Involves an Impairment in Aryl Hydrocarbon Receptor (AhR) Signaling*. Neurotoxicity Research 35, 183–195. https://doi.org/10.1007/s12640-018-9946-7

Wolf, C.J., Schmid, J.E., Lau, C., Abbott, B.D., 2012. *Activation of mouse and human peroxisome proliferator-activated receptor-alpha (PPARα) by perfluoroalkyl acids (PFAAs): Further investigation of C4–C12 compounds*. Reproductive Toxicology 33, 546–551. https://doi.org/https://doi.org/10.1016/j.reprotox.2011.09.009

Wu, H., Zhang, W., Zhang, Y., Kang, Z., Miao, X., Na, X., 2021. *Novel insights into di-(2-ethylhexyl)phthalate activation: Implications for the hypothalamus-pituitary-thyroid axis*. Molecular Medicine Reports 23. https://doi.org/10.3892/MMR.2021.11930

Xie, W., Ludewig, G., Wang, K., Lehmler, H.-J., 2010. *Model and cell membrane partitioning of perfluorooctanesulfonate is independent of the lipid chain length*. Colloids and Surfaces B: Biointerfaces 76, 128–136. https://doi.org/https://doi.org/10.1016/j.colsurfb.2009.10.025

Xu, H.E., Stanley, T.B., Montana, V.G., Lambert, M.H., Shearer, B.G., Cobb, J.E., McKee, D.D., Galardi, C.M., Plunket, K.D., Nolte, R.T., Parks, D.J., Moore, J.T., Kliewer, S.A., Willson, T.M., Stimmel, J.B., 2002. *Structural basis for antagonist-mediated recruitment of nuclear co-repressors by PPARα*. Nature 415, 813–817. https://doi.org/10.1038/415813a

Xu, Q., Zhou, L., Ri, H., Li, X., Zhang, X., Qi, W., Ye, L., 2022. *Role of estrogen receptors in thyroid toxicity induced by mono (2-ethylhexyl) phthalate via endoplasmic reticulum stress: An in vitro mechanistic investigation*. Environmental Toxicology and Pharmacology 96, 104007. https://doi.org/https://doi.org/10.1016/j.etap.2022.104007

Xu, X., Otsuki, M., Saito, H., Sumitani, S., Yamamoto, H., Asanuma, N., Kouhara, H., Kasayama, S., 2001. *PPARα and GR Differentially Down-Regulate the Expression of Nuclear Factor-κB-Responsive Genes in Vascular Endothelial Cells*. Endocrinology 142, 3332–3339. https://doi.org/10.1210/endo.142.8.8340

Yamaguchi, M., Hankinson, O., 2018. *2,3,7,8-Tetrachlorodibenzo-p-dioxin suppresses the growth of human liver cancer HepG2 cells in vitro: Involvement of cell signaling factors*. Int J Oncol 53, 1657–1666. https://doi.org/10.3892/ijo.2018.4507

Yanase, T., Mu, Y.-M., Nishi, Y., Goto, K., Nomura, M., Okabe, T., Takayanagi, R., Nawata, H., 2001. *Regulation of aromatase by nuclear receptors*. The Journal of Steroid Biochemistry and Molecular Biology 79, 187–192.

https://doi.org/https://doi.org/10.1016/S0960-0760(01)00161-3

Yang, J., Antin, P., Berx, G., Blanpain, C., Brabletz, T., Bronner, M., Campbell, K., Cano, A., Casanova, J., Christofori, G., Dedhar, S., Derynck, R., Ford, H.L., Fuxe, J., García de Herreros, A., Goodall, G.J., Hadjantonakis, A.K., Huang, R.J.Y., Kalcheim, C., Kalluri, R., Kang, Y., Khew-Goodall, Y., Levine, H., Liu, J., Longmore, G.D., Mani, S.A., Massagué, J., Mayor, R., McClay, D., Mostov, K.E., Newgreen, D.F., Nieto, M.A., Puisieux, A., Runyan, R., Savagner, P., Stanger, B., Stemmler, M.P., Takahashi, Y., Takeichi, M., Theveneau, E., Thiery, J.P., Thompson, E.W., Weinberg, R.A., Williams, E.D., Xing, J., Zhou, B.P., Sheng, G., 2020. *Guidelines and definitions for research on epithelial–mesenchymal transition*. Nature Reviews Molecular Cell Biology. https://doi.org/10.1038/s41580-020-0237-9

Yaşar, P., Ayaz, G., User, S.D., Güpür, G., Muyan, M., 2017. *Molecular mechanism of estrogen–estrogen receptor signaling*. Reproductive Medicine and Biology 16, 4–20. https://doi.org/https://doi.org/10.1002/rmb2.12006

Yen, P.-L., How, C.M., Hsiu-Chuan Liao, V., 2021. *Early-life and chronic exposure to di(2-ethylhexyl) phthalate enhances amyloid-β toxicity associated with an autophagy-related gene in Caenorhabditis elegans Alzheimer's disease models*. Chemosphere 273, 128594. https://doi.org/https://doi.org/10.1016/j.chemosphere.2020.128594

Yu, N., Wei, S., Li, M., Yang, J., Li, K., Jin, L., Xie, Y., Giesy, J.P., Zhang, X., Yu, H., 2016. *Effects of Perfluorooctanoic Acid on Metabolic Profiles in Brain and Liver of Mouse Revealed by a High-throughput Targeted Metabolomics Approach*. Scientific Reports 6, 23963. https://doi.org/10.1038/srep23963

Zahm, S., Bonde, J.P., Chiu, W.A., Hoppin, J., Kanno, J., Abdallah, M., Blystone, C.R., Calkins, M.M., Dong, G.H., Dorman, D.C., Fry, R., Guo, H., Haug, L.S., Hofmann, J.N., Iwasaki, M., Machala, M., Mancini, F.R., Maria-Engler, S.S., Møller, P., Ng, J.C., Pallardy, M., Post, G.B., Salihovic, S., Schlezinger, J., Soshilov, A., Steenland, K., Steffensen, I.L., Tryndyak, V., White, A., Woskie, S., Fletcher, T., Ahmadi, A., Ahmadi, N., Benbrahim-Tallaa, L., Bijoux, W., Chittiboyina, S., de Conti, A., Facchin, C., Madia, F., Mattock, H., Merdas, M., Pasqual, E., Suonio, E., Viegas, S., Zupunski, L., Wedekind, R., Schubauer-Berigan, M.K., 2024. *Carcinogenicity of perfluorooctanoic acid and perfluorooctanesulfonic acid*. The Lancet. Oncology 25, 16–17. https://doi.org/10.1016/S1470-2045(23)00622-8

Zhang, C., Zhang, B., Zhang, X., Sun, G., Sun, X., 2020. *Targeting Orphan Nuclear Receptors NR4As for Energy Homeostasis and Diabetes*. Frontiers in Pharmacology. https://doi.org/10.3389/fphar.2020.587457

Zhang, P., Guan, X., Yang, M., Zeng, L., Liu, C., 2018. *Roles and potential mechanisms of selenium in countering thyrotoxicity of DEHP*. Science of the Total Environment 619–620, 732–739. https://doi.org/10.1016/j.scitotenv.2017.11.169

Zhang, S., Xiao, X., Yi, Y., Wang, X., Zhu, L., Shen, Y., Lin, D., Wu, C., 2024. *Tumor initiation and early tumorigenesis: molecular mechanisms and interventional targets*. Signal Transduction and Targeted Therapy 9, 149. https://doi.org/10.1038/s41392-024-01848-7

Zhang, X., Chen, L., Fei, X.-C., Ma, Y.-S., Gao, H.-W., 2009. *Binding of PFOS to serum albumin and DNA: insight into the molecular toxicity of perfluorochemicals*. BMC Molecular Biology 10, 16. https://doi.org/10.1186/1471-2199-10-16

Zhang, X., Qi, W., Xu, Q., Li, X., Zhou, L., Ye, L., 2022. *Di(2-ethylhexyl) phthalate (DEHP) and thyroid: biological mechanisms of interference and possible clinical implications*. Environmental Science and Pollution Research. https://doi.org/10.1007/s11356-021-17027-y

Zhang, Y., Feng, H., Tian, A., Zhang, C., Song, F., Zeng, T., Zhao, X., 2023. *Long-term exposure to low-dose Di(2-ethylhexyl) phthalate aggravated high fat diet-induced obesity in female mice*. Ecotoxicology and Environmental Safety 253, 114679. https://doi.org/https://doi.org/10.1016/j.ecoenv.2023.114679

Zhao, A., Wang, L., Pang, X., Liu, F., 2022. *Phthalates in skin wipes: Distribution, sources,*

and exposure via dermal absorption. Environmental Research 204, 112041. https://doi.org/https://doi.org/10.1016/j.envres.2021.112041

Zhao, J., Ren, S., Liu, C., Huo, L., Liu, Z., Zhai, L., 2018. *Di-(2-ethylhexyl) phthalate increases obesity-induced damage to the male reproductive system in mice*. Oxidative Medicine and Cellular Longevity 2018. https://doi.org/10.1155/2018/1861984

Zheng, X., Su, H., Huang, S., Su, W., Zheng, R., Shang, Y., Su, Q., Zhou, L., Yao, Y., Su, Z., 2023. *Secondary oxidized di-2-ethylhexyl phthalate metabolites may be associated with progression from isolated premature thelarche to central precocious or early puberty*. Scientific Reports 13, 1–9. https://doi.org/10.1038/s41598-023-32768-1

Zhu, X., Liu, Q., Patterson, A.D., Sharma, A.K., Amin, S.G., Cohen, S.M., Gonzalez, F.J., Peters, J.M., 2023. *Accumulation of Linoleic Acid by Altered Peroxisome Proliferator-Activated Receptor-α Signaling Is Associated with Age-Dependent Hepatocarcinogenesis in Ppara Transgenic Mice*. Metabolites. https://doi.org/10.3390/metabo13080936

Zou, Q.-Y., Hong, S.-L., Kang, H.-Y., Ke, X., Wang, X.-Q., Li, J., Shen, Y., 2020. *Effect of di-(2-ethylhexyl) phthalate (DEHP) on allergic rhinitis*. Scientific Reports 10, 14625. https://doi.org/10.1038/s41598-020-71517-6

Zuang, V., Worth, A., Corvi, R., Munn, S., Deceuninck, P., 2024. *Non-animal methods in Science and Regulation – EURL ECVAM Status Report 2023*. Publications Office of the European Union, Luxembourg. https://doi.org/doi:10.2760/44273